NASA CONTRACTOR REPORT

NASA CR-1152

NASA CR-1152

NEW METHODS IN ADAPTIVE FLIGHT CONTROL

by Lee Gregor Hofmann and John J. Best

Prepared by
SYSTEMS TECHNOLOGY, INC.
Princeton, N. J.
for Langley Research Center

NATIONAL AERONAUTICS AND SPACE ADMINISTRATION • WASHINGTON, D. C. • SEPTEMBER 1968

NASA CR-1152

NEW METHODS IN ADAPTIVE FLIGHT CONTROL

By Lee Gregor Hofmann and John J. Best

Prepared under Contract No. NAS 1-6813 by
SYSTEMS TECHNOLOGY, INC.
Princeton, N.J.

for Langley Research Center

NATIONAL AERONAUTICS AND SPACE ADMINISTRATION

For sale by the Clearinghouse for Federal Scientific and Technical Information
Springfield, Virginia 22151 - CFSTI price $3.00

ABSTRACT

A new approach to the design of adaptive control systems has been developed. It is called the "adaptive control function approach," and the systems so designed are called "adaptive control function systems." This terminology is descriptive of the basic operating principle for these systems.

The basic operating principle is that sums of properly modulated, conventional linear feedback and feedforward signals provide the control inputs needed to obtain specified responses in a number of output variables of a linear controlled element. The theoretical development in this report deals with linear, constant coefficient controlled elements only. With this restriction, the number of linearly independent controlled element responses which can be arbitrarily specified is equal to the number of independent control points. These specified responses then determine what the (ideal) control inputs should be.

Adaptive control function systems are mechanized so that the actual input at each control point approaches the ideal input because of a steepest descent feedback mechanism. The difference between the ideal and actual control inputs can be made arbitrarily close to zero, in principle, by increasing the rate of descent in the steepest descent procedure. Increasing this rate is accomplished by increasing adaptive loop gains. This increases the rate at which the gains modulating the feedback and feedforward signals can be changed. Selection of the adaptive loop gains is at the choice of the designer. In principle, adaptive gains may be set arbitrarily high, but when practical devices are used to realize the system, there is actually a finite upper limit.

The adaptive control function approach is applied here to the design of an adaptive, lateral stability augmentation system for a hypothetical, manned, lifting-body, entry vehicle. The objective of the application is to effect considerable improvement in the fickle and sometimes rapidly changing lateral-directional handling qualities of this vehicle. Data from a simulation of the system demonstrate its effectiveness in meeting the objective. Practical modifications, necessary for reducing adaptive control function theory to practice, are given careful attention in the example application.

CONTENTS

FIGURES

FIGURES (Concluded)

TABLES

SYMBOLS

The standard symbology used in describing aircraft dynamics is given in Ref. 11. All other symbols not explicitly defined where they are used in the text are defined below.

a_c	lead compensated lateral accelerometer output
a_{c_c}	commanded value of a_c
a_y	lateral acceleration of the vehicle c.g.
a_y'	lateral acceleration of the vehicle measured at a point 3.88 feet forward of the c.g.
a_y''	lateral acceleration of the vehicle measured at a point 3.38 feet forward of the c.g.
a_{y_p}	lateral acceleration of the vehicle measured at the pilots head, estimated to be 5.88 feet forward of the c.g.
$A_{\dot{\phi}}$	gain for adaptive adjustment of roll rate SAS gain, $K_{\dot{\phi}}$
A_y	gain for adaptive adjustment of lateral acceleration SAS gain, K_y
d	disturbance input to the vehicle
e_a	error signal for the adaptive roll rate gain loop
e_r	error signal for the adaptive lateral acceleration gain loop
f_a	roll rate component of the criterion for the digital adjustment scheme
f_r	lateral acceleration component of the criterion for the digital adjustment scheme
$f_{\dot{\phi}}$	forcing function in the roll rate gain differential equation
f_y	forcing function in the lateral acceleration gain differential equation
G_ϕ	roll feedback transfer function
$G_{a_y''}$	lateral acceleration feedback transfer function
J	criterion function

$K_{\dot{\phi}}$	gain of the roll rate SAS loop
K_y, $K_{a_y''}$	gain of the lateral acceleration SAS loop
K_p	gain of the pilot describing function
l_{x_o}	location of the rudder center of percussion
m	subscript designating model variable
$N_{\delta_1}^{q_2}$	numerator of the transfer function between δ_1 and q_2
$N_{\delta_1\delta_2}^{q_3 q_4}$	coupling numerator for δ_1, δ_2, q_3 and q_4
q	unspecified motion quantity
r	yaw rate
s	Laplace operator
T	time constant of the filter, F(s)
Y_{as}	aileron servo transfer function
Y_{rs}	rudder servo transfer function
$Y_{a_y''}$	lateral acceleration feedback compensation
$Y_{\dot{\phi}}$	roll rate feedback compensation
Y_p	pilot describing function
Y_{cf}	crossfeed transfer function
β_g	sideslip gust disturbance
δ_a	aileron deflection
δ_r	rudder deflection
Δ	characteristic polynomial
ϕ	roll angle
$\lvert\phi/\beta\rvert$	magnitude of the ratio of roll to sideslip evaluated at the dutch roll frequency, ω_d
τ_e	effective time delay in the pilot describing function
ω_ϕ	natural frequency of the dutch roll zeros for aileron inputs
ω_d	natural frequency of the dutch roll poles

NEW METHODS IN ADAPTIVE FLIGHT CONTROL

By Lee Gregor Hofmann and John J. Best
Systems Technology, Inc.

SECTION I

INTRODUCTION

Self-adaptive control systems have been fashionable subjects for controls research, now, for somewhat longer than a decade. As engineers and scientists, we have tackled this subject using techniques ranging from experimental synthesis in the laboratory to elegant mathematical analysis. More often than not, these research efforts have been quite successful in terms of producing practical solutions for particular problems. In terms of producing generally applicable techniques capable of serving the needs of system designers, however, success has been considerably less.

The self-adaptive control system developed in this report provides a system design technique, which in our opinion, considerably lessens (but does not eliminate) the limitations mentioned above. Like almost all "new" techniques, this is the product of continued reflection upon the literature of this field, and a closely related field, system identification. The main links of this research with past efforts are conceptual in nature. For example, the basic idea of employing a model of the desired system and/or response is very often attributed to Lang and Ham (Ref. 1). The model was used as an (explicit) part of the conditional feedback system in Ref. 1. Later the model or model-reference concept was utilized by Whitaker, Yamron and Kezer (Ref. 2) in the first version of the model-reference adaptive control system. New theoretical developments gave rise to a second version of the model-reference adaptive control system (Ref. 3). It is worthwhile to note that just about the only feature of the first version to appear in the second was the model. Models also were employed in an implicit sense for system identification. Here the work of Graupe (Ref. 4), and of Potts, Ornstein and Clymer (Ref. 5) should be mentioned because

the equation error technique used by these investigators results in an implicit manifestation of a model.

Models are involved in the present work in an implicit way. Their involvement is in the spirit of the model-reference technique although their precise role is distinctly different.

Many adaptive control systems and system identification schemes depend upon minimization of a non-negative criterion function of some convenient error. This is also true in the present work. This approach, however, is often limited by slow convergence and/or stability problems. A number of research efforts have been helpful in minimizing the effects of this limitation. First, one essential requirement is to choose errors which contain some direct algebraic dependency upon the adjustable gains or parameters in addition to whatever other functional dependencies might exist. This was pointed out by Graupe (Ref. 4) and Potts, Ornstein and Clymer (Ref. 5). Stability of identification systems using such errors was proved by Miller (Ref. 6). Lion (Ref. 7) later extended the Miller proof to show these systems are asymptotically stable for two broad (and useful) classes of forcing functions. Lion also found that the key to obtaining rapid convergence lay with using a sufficient number of linearly independent errors. This enables one to construct a positive definite criterion function (in terms of the adjustable gains or parameters) of the errors. The need for additional errors can be fulfilled making use of Rucker's state variable decomposition filters (Ref. 8).

The multiloop analysis technique developed by McRuer, Ashkenas, and Pass (Ref. 9) is used to guide selection of quantities for feedback and to expose simplifying identities in the filter portion of adaptive control function systems.

All of the above concepts and innovations play a role in our "new" technique. The significance of "new" lies in their unique combination which results in the adaptive control function system. This is the

first adaptive technique, not requiring explicit identification of the controlled element, which is also applicable to multi-control point problems.†

GOALS OF THE RESEARCH

The primary goal in this research program was to develop an adaptive control system capable of compensating for very rapid variations in controlled element dynamic characteristics. The resulting technology was to be applied to a significant flight control problem. Stability augmentation of the lateral-directional dynamics of a manned, lifting-body entry vehicle was selected because this problem requires very rapid compensation for varying vehicle characteristics and because it is a multi-point control problem of general importance.

Secondary goals were to arrive at a basic configuration for the lateral SAS which would be consistent with present conventional design techniques and which would considerably improve the handling qualities over those for the unaugmented vehicle. The range of vehicle dynamics considered is implicitly specified by a single entry trajectory. The trajectory was specifically chosen to emphasize the dynamical problems in terms of handling qualities. The limitation to a single trajectory, however, was necessary in order to prevent the handling qualities aspect of the research from overwhelming the primary goal. For this reason, the feedback quantities and the adaptive gains used herein should not be accepted without question for use in a broader context. This is not to say the chosen configuration is inappropriate for other trajectories, but rather that the configuration is most appropriate for the handling qualities problems fixable with the given feedbacks. If other trajectories give rise to other handling qualities

†Shipley, Engel and Hung (Ref. 10) have developed an adaptive lateral stability augmentation system for aircraft. However, their system employs explicit identification of the control element, and the adjustment of the control system gain is open-loop.

problems for which the chosen feedbacks are inappropriate, new choices are in order.

The techniques applied here to a flight control system, apply in general for adaptive control of any controlled element which can be modelled by a linear constant coefficient differential equations with reasonable accuracy for a period approximately equal to the controlled element response time.

ORGANIZATION OF THE REPORT

The body of the report consists of four main Sections. The material presented in these Sections pertains directly to the design of an adaptive lateral stability augmentation system (SAS) for a hypothetical, manned, lifting-body, entry vehicle (MLEV). By first developing the theory within the context of an application, and later generalizing the development in an Appendix, we hope to spare the readers' consideration, at the outset, of many details of secondary importance.

Section II explains the key concepts for designing adaptive control function systems. These are then applied to design the adaptive lateral SAS for the MLEV. The stability of the resulting system is analyzed. Then, the "paper design" is modified to take non-ideal effects such as flight control servo dynamics into account, and to eliminate physically impractical operations such as signal differentiation.

Readers who are most concerned with the adaptive lateral SAS configuration and system performance may prefer to skip Section II which deals with the theoretical development, and proceed directly to Section III.

In Section III, the system configuration is summarized, and performance of the adaptive lateral SAS is demonstrated. The data presented are the result of an extensive analog simulation program.

The simulated vehicle equations of motion are time-varying and represent entry along a trajectory which produces several different handling qualities problems when the vehicle is unaugmented.

The effects of further system simplication are explored in Section IV. The objective is to reduce system complexity to minimal levels from the point of view flight hardware. One simplication in the mechanization of the adapti ng gains replaces multipliers with logic elements. In this case, the s'stem is not only made less complex, but the adaptive action of the system also is made independent of forcing function level. Simulation data is presented to illustrate the performance of the modified system.

Concluding remarks form a very brief Section V.

Appendix A summarizes the dynamic characteristics and systems surveys for the MLEV. The systems surveys lead to a choice of lateral acceleration feedback to rudder and roll rate feedback to aileron for the basic SAS configuration.

Appendix B presents a more general and compact derivation of the adaptive control function system equations.

Diagrams documenting the simulation of the adaptive lateral SAS and the MLEV form the bulk of Appendix C.

SECTION II

ANALYSIS

In the first portion of this Section, we present a description of the lateral dynamics of the hypothetical manned, lifting-body, entry vehicle (MLEV). This is the controlled element used for the application of the adaptive control theory. Next, we proceed through the steps for synthesizing an adaptive control function system which will perform the lateral stability augmentation (SAS) function for the MLEV. The selection of the motion quantities for feedback is accomplished in Appendix A using the competing systems technique. While it is the case that the selection is based on calculations which assume the SAS consists of linear, constant coefficient feedbacks of motion quantities, we hold that such a selection process is best for our purposes here for reasons of flight safety. That is, the closed-loop system should be capable of delivering at least marginal performance, with the adaptive system turned off and SAS gains set manually to suitable values for emergency operation.

Once the SAS feedback quantities have been selected, we then proceed to define the errors for adaptive system operation, choose an adaptive gain adjustment law and then examine the stability of the adaptive gain adjustments under certain ideal circumstances. The final and perhaps most important step of all is that of making modifications to the resulting theoretical design that will allow us to accomodate the non-ideal effects which are a part of any system with real components. The practical modification techniques presented are for coping with the lags inherent in the flight control servos, replacing pure differentiations with pseudo-differentiators and for adding additional low pass filtering to combat noise.

CONTROLLED ELEMENT AND FEEDBACK QUANTITIES

The lateral MLEV dynamics are characterized by transfer functions for the theoretical portion of this study. In actual fact, the differential equations describing the vehicle are time-varying. However, the time-varying effects are negligible for engineering purposes over all of the given flight profile except for the 10 sec or less during which the vehicle is in the transonic flight regime. In that regime, adaptive system performance is a matter of surpassing importance and great interest. However, analysis which takes time-varying environmental parameters into account is beyond the capability of the theoretical tools available. Therefore, we shall have to rely upon simulation to indicate system performance in this regime.

The feedbacks selected as most appropriate for improving the handling qualities of the MLEV are:

- Lateral acceleration measured 3.38 ft forward of the vehicle center of gravity, a_y'', compensated by a lead/lag network, $(s + 1.5)/(s + 15.0)$, and fed to rudder
- Roll rate feedback to aileron

Figure 1 is a block diagram of this system. A capsule summary of the systems survey analyses leading to selection of these feedbacks is contained in Appendix A. Clearly, the variables to be controlled are $\dot{\phi}$ and a_c. A working notation, K_y, is used here for the gain, $K_{a_y''}$, of Appendix A.

The notation for describing aircraft dynamic characteristics involved in handling qualities is given in Ref. 11. In-depth analyses for explaining and predicting handling qualities for aircraft on the basis of closed-loop pilot-vehicle system considerations is given in Ref. 12.

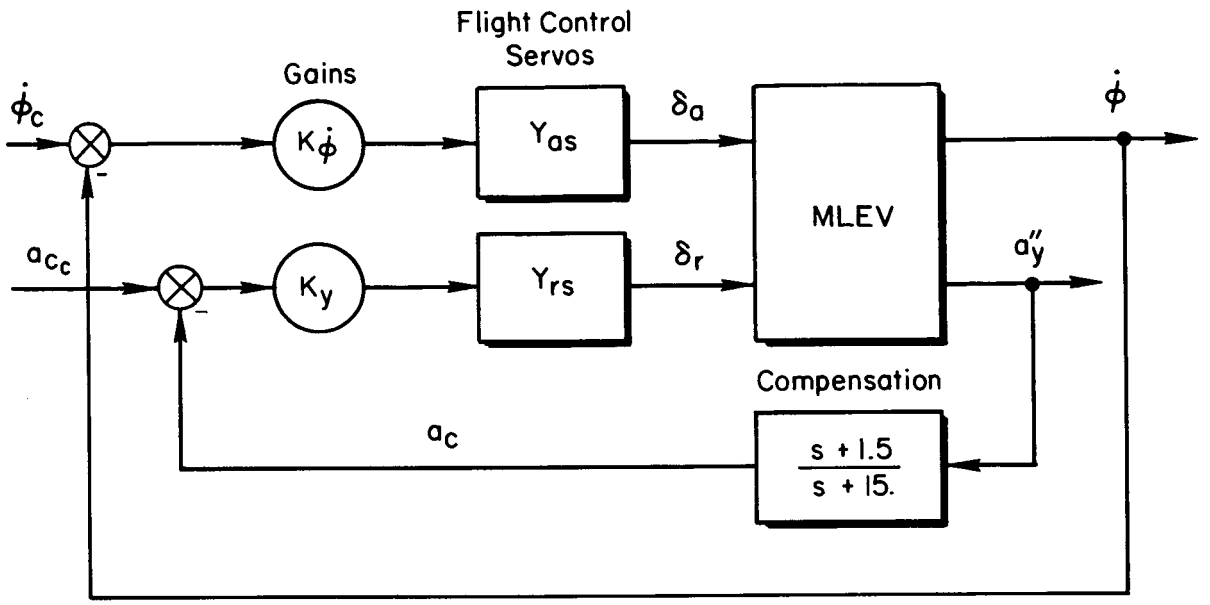

Figure 1. Block Diagram of MLEV Lateral SAS

Handling qualities problems specific to the unaugmented MLEV are reviewed in Appendix A. They may be summarized as follows:

- Very low roll damping at all flight conditions requires considerable lead from the pilot for control of roll angle with aileron
- Dutch roll damping is very low at all flight conditions
- Roll reversal (ω_ϕ^2 is negative) accompanied by low dutch roll stiffness at flight condition 810 requires unconventional piloting technique which is marginal at best.

- Too large a frequency separation between ω_φ and ω_d early in the flight (at 630 and 725 sec) when rudder control effectiveness is virtually non-existent leads to roll rate reversals in response to aileron

- Too small a frequency separation between ω_φ and ω_d late in the flight (at 865 sec) leads to inability to damp the dutch roll to any appreciable degree for roll control with aileron only.

The lateral acceleration-to-rudder feedback fixes the roll reversal (negative ω_φ^2) problem and stiffens the dutch roll at flight condition 810. It also is used to increase the separation between ω_φ and ω_d at flight condition 865. By including lead-lag compensation, the dutch roll damping can be increased at all flight conditions where there is rudder control effectiveness.

The roll rate-to-aileron feedback fixes the low roll damping problem. It also augments the dutch roll damping and suppresses the $|\varphi/\beta|$ ratio in the dutch roll mode.

The systems surveys in Appendix A show that reasonable choices for adjustable gains are $K_{\dot\varphi}$ and K_y. $K_{\dot\varphi}$ should be adjustable to compensate for the large magnitude changes in the control effectiveness derivatives. K_y should be adjustable because there is no constant value of this gain which would not produce instability at some flight conditions. On the other hand, there is no alternative to lateral acceleration-to-rudder capable of coping with the special problems at flight conditions 810 and 865 and capable of supplying some modest amount of dutch roll damping. In particular, yaw rate feedback to rudder cannot accomplish all these objectives simultaneously.

When the preferred feedbacks are used, the MLEV transfer functions of interest are those involving aileron and rudder inputs and roll rate, $\dot\varphi$†, and lateral acceleration, a_y'', outputs. The transfer functions

†We have assumed here that $\dot\varphi$ is a derived rate obtained from a vertical gyro operating as a free gyro during the entry.

are expressed in terms of ratios of numerator polynomials, $N_{(\ )}^{(\ )}$, to the characteristic polynomial, Δ. Thus, for example, the unaugmented aileron-to-roll angle rate transfer function is $N_{\delta_a}^{\dot{\phi}}/\Delta$. The subscript on N indicates the input for the transfer function while the superscript indicates the output.

The MLEV equations can be expressed in matrix form and in terms of transfer functions as

$$\begin{Bmatrix} \dot{\phi} \\ a_y'' \end{Bmatrix} = \frac{1}{\Delta}\begin{bmatrix} N_{\delta_a}^{\dot{\phi}} & N_{\delta_r}^{\dot{\phi}} \\ N_{\delta_a}^{a_y''} & N_{\delta_r}^{a_y''} \end{bmatrix} \begin{Bmatrix} \delta_a \\ \delta_r \end{Bmatrix} \tag{1}$$

and the control law as:

$$\begin{Bmatrix} \delta_a \\ \delta_r \end{Bmatrix} = \begin{bmatrix} K_{\dot{\phi}} & 0 \\ 0 & K_y \end{bmatrix} \left(\begin{Bmatrix} \dot{\phi}_c \\ a_{c_c} \end{Bmatrix} - \begin{bmatrix} 1 & 0 \\ 0 & \frac{s + 1.5}{s + 15.0} \end{bmatrix} \begin{Bmatrix} \dot{\phi} \\ a_y'' \end{Bmatrix} \right) \tag{2}$$

The problem at hand is a multi-control point problem. Because of this, we will make use of the so-called coupling numerators of the multiloop analysis technique developed in Ref. 9. A synopsis of the multiloop analysis technique is given in Appendix A. It provides the analytical tools necessary here.

The coupling numerator is convenient because it expresses in a simplified and compact way a combination of numerators and the characteristic polynomials which occurs frequently in multi-control point problems. Here we are concerned with the aileron-to-roll, rudder-to-lateral acceleration coupling numerator, $N_{\delta_a\delta_r}^{\dot{\phi}\ a_y''}$:

$$N_{\delta_a\delta_r}^{\dot{\phi}\ a_y''} = \frac{N_{\delta_a}^{\dot{\phi}} N_{\delta_r}^{a_y''} - N_{\delta_r}^{\dot{\phi}} N_{\delta_a}^{a_y''}}{\Delta} \tag{3}$$

The characteristic polynomial, Δ, is always an exact factor of the numerator on the RHS of Eq 3. This suggests that easier means than direct evaluation of Eq 3 can be found to calculate $N^{\dot{\phi}}_{\delta_a} a''_{y_{\delta_r}}$. Indeed, this is the case.

One of the really useful features of the coupling numerator is that it can be calculated by a method analogous to Cramer's rule. That is, $N^{\dot{\phi}}_{\delta_a} a''_{y_{\delta_r}}$ can be obtained from the Laplace transformed aircraft equations of motion by substituting the δ_a control effectiveness column into the $\dot{\phi}$ column of the characteristic matrix and the δ_r control effectiveness column into the a''_y column of the characteristic matrix and then computing the determinant of the result. The coupling numerator notation is suggestive of this operation.

Numerical evaluations of the characteristics, numerator, and coupling numerator polynomial in terms of exact factors are tabulated in Table A-4 at six flight conditions.

The transfer functions for the closed-loop system shown in Fig. 1 are given by Eq 4 through 7. These assume $K_{\dot{\phi}}$ and K_y are constants.

$$\frac{\dot{\phi}}{\dot{\phi}_c} = \frac{K_{\dot{\phi}} Y_{as} N^{\dot{\phi}}_{\delta_a}}{\Delta''} \tag{4}$$

$$\frac{a''_y}{\dot{\phi}_c} = \frac{K_{\dot{\phi}} Y_{as} N^{a''_y}_{\delta_a}}{\Delta''} \tag{5}$$

$$\frac{a''_y}{a_{c_c}} = \frac{K_y Y_{rs} N^{a''_y}_{\delta_r}}{\Delta''} \tag{6}$$

$$\frac{\dot{\phi}}{a_{c_c}} = \frac{K_y Y_{rs} N^{\dot{\phi}}_{\delta_r}}{\Delta''} \tag{7}$$

where $$N_{\delta_a}^{\dot{\phi}''} = N_{\delta_a}^{\dot{\phi}} + K_y Y_{rs} \frac{(s + 1.5)}{(s + 15.0)} N_{\delta_a \delta_r}^{\dot{\phi}\, a_y''} \tag{8}$$

$$N_{\delta_r}^{a_y''''} = N_{\delta_r}^{a_y''} + K_{\dot{\phi}} Y_{as} N_{\delta_a \delta_r}^{\dot{\phi}\, a_y''} \tag{9}$$

$$\Delta'' = \Delta + K_{\dot{\phi}} Y_{as} N_{\delta_a}^{\dot{\phi}} + K_y Y_{rs} \frac{(s + 1.5)}{(s + 15.0)} N_{\delta_r}^{a_y''}$$

$$+ K_{\dot{\phi}} K_y Y_{as} Y_{rs} \frac{(s + 1.5)}{(s + 15.0)} N_{\delta_a \delta_r}^{\dot{\phi}\, a_y''}$$

$$= \Delta + K_y Y_{rs} \frac{(s + 1.5)}{(s + 15.0)} N_{\delta_r}^{a_y''} + K_{\dot{\phi}} Y_{as} N_{\delta_a}^{\dot{\phi}''} \tag{10}$$

The transfer functions which of course, concern us most are those for the commanded variables, Eq 4 and 6.

We have at this point established and justified the basic loop configuration for the MLEV lateral SAS. (The study is actually presented in detail in Appendix A.) We have also justified the need for adjusting the $K_{\dot{\phi}}$ and K_y gains. The case for <u>adaptive</u> adjustment of these gains can be made based upon the rich variety of reasonable entry trajectories possible, and the large ranges in angle of attack, Mach number and air density which can be encountered. The first factor eliminates time-scheduled gain changes as impractical. The second factor together with some uncertainty in vehicle aerodynamic characteristics tends to make air-data scheduled gain changes unattractive. Manual adjustment of the gains is precluded by the rapidity of the adjustment required in the transonic regime.

Next we shall proceed with development of the adaptive system.

CLOSED-LOOP SYSTEM MODEL

An implicit model of the closed-loop system is used in the adaptive control function scheme. Choice of a model may be somewhat arbitrary. For compelling reasons, however, we make a rather specific choice here.

The model used has the same configuration as the system in Fig. 1. What is more, we take the transfer functions for the MLEV model to be approximately those for the actual MLEV at one flight condition. Since the system feedbacks have been chosen because they can provide a good SAS at any flight condition we are assured that this choice of closed-loop model will be a good one. The settings for the SAS model gains are, of course, those calculated in the systems surveys for that particular flight condition. Another reason for choosing the model to closely approximate the system at one flight condition is that we intuitively expect this will tend to require smaller control surface deflections than will a model less closely related to the characteristics of the actual system. The transfer functions developed in Eq 4 through 10 apply as well to this model if it is understood that the subscript m added to the characteristic, numerator, and coupling numerator polynomials and the gain symbols, designates model values.

The system model transfer functions themselves are not explicitly used. Instead, we take the mathematical inverse of these transfer functions. The result is another set of transfer functions which is capable of generating model values of the command inputs, $\dot{\Phi}_{c_m}$ and $a_{c_{c_m}}$ from given $\dot{\Phi}$ and a''_y signals.

The mathematical inverse of the system model transfer functions can be obtained most efficiently using the constituents of the system transfer functions in matrix form. The MLEV model transfer functions are:

$$\begin{Bmatrix} \dot{\Phi} \\ a''_y \end{Bmatrix} = \frac{1}{\Delta_m} \begin{bmatrix} N^{\dot{\Phi}}_{\delta_a} & N^{\dot{\Phi}}_{\delta_r} \\ N^{a''_y}_{\delta_a} & N^{a''_y}_{\delta_r} \end{bmatrix}_m \begin{Bmatrix} \delta_a \\ \delta_r \end{Bmatrix}_m \qquad (11)$$

The model control law (neglecting flight control servo dynamics in the model) is:

$$\begin{Bmatrix} \delta_a \\ \delta_r \end{Bmatrix}_m = \begin{bmatrix} K_{\dot{\phi}} & 0 \\ 0 & K_y \end{bmatrix}_m \left(\begin{Bmatrix} \dot{\phi}_c \\ a_{c_c} \end{Bmatrix}_m - \begin{bmatrix} 1 & 0 \\ 0 & \frac{s + 1.5}{s + 15.0} \end{bmatrix} \begin{Bmatrix} \dot{\phi} \\ a''_y \end{Bmatrix} \right) \quad (12)$$

Solving for $\text{col}\{\delta_a, \delta_r\}_m$ in Eq 11 gives,

$$\begin{Bmatrix} \delta_a \\ \delta_r \end{Bmatrix}_m = \frac{1}{\left(N^{\dot{\phi}}_{\delta_a} N^{a''_y}_{\delta_r}\right)_m} \begin{bmatrix} N^{a''_y}_{\delta_r} & -N^{\dot{\phi}}_{\delta_r} \\ -N^{a''_y}_{\delta_a} & N^{\dot{\phi}}_{\delta_a} \end{bmatrix}_m \begin{Bmatrix} \dot{\phi} \\ a''_y \end{Bmatrix} \quad (13)$$

where the coupling numerator $N^{\dot{\phi}}_{\delta_a} N^{a''_y}_{\delta_r}$ arises from the determinant of the matrix of numerators when calculating the inverse of that matrix. We can then solve for $\text{col}\{\dot{\phi}_c, a_{c_c}\}_m$ using Eq 12 and 13.

$$\begin{Bmatrix} \dot{\phi}_c \\ a_{c_c} \end{Bmatrix}_m = \left(\begin{bmatrix} 1 & 0 \\ 0 & \frac{s + 1.5}{s + 15.0} \end{bmatrix} + \frac{1}{\left(N^{\dot{\phi}}_{\delta_a} N^{a''_y}_{\delta_r}\right)_m} \begin{bmatrix} 1/K_{\dot{\phi}} & 0 \\ 0 & 1/K_y \end{bmatrix}_m \begin{bmatrix} N^{a''_y}_{\delta_r} & -N^{\dot{\phi}}_{\delta_r} \\ -N^{a''_y}_{\delta_a} & N^{\dot{\phi}}_{\delta_a} \end{bmatrix}_m \right) \begin{Bmatrix} \dot{\phi} \\ a''_y \end{Bmatrix} \quad (14)$$

CHOOSING APPROPRIATE ERRORS

The error signals are defined to be proportional to the differences between the actual commands and the model representations of the commands. Thus,

$$\begin{aligned} e_a &= (\dot{\phi}_c - \dot{\phi}_{c_m}) K_{\dot{\phi}_m} \\ e_r &= (a_c - a_{c_{c_m}}) K_{y_m} \end{aligned} \quad (15)$$

The signal e_a represents error in the aileron control channel: the subscript a standing for aileron. The signal e_r represents error in the lateral acceleration rudder control channel: the subscript r

standing for rudder. Each error will be used to adjust the loop gain in its corresponding channel.

More convenient expressions for the errors are in terms of the system servo errors, $(\dot{\phi}_c - \dot{\phi})$ and $(a_{c_c} - a_c)$, and the model control deflections, δ_{a_m} and δ_{r_m}. These are obtained by eliminating $K_{\dot{\phi}_m}\dot{\phi}_{cm}$ and $K_{y_m}a_{c_{cm}}$ between Eq 12 and 15. Notice that $a_c = \left[(s + 1.5)/(s + 15.)\right]a''_y$. The result is:

$$\begin{aligned} e_a &= (\dot{\phi}_c - \dot{\phi})\, K_{\dot{\phi}m} - \delta_{a_m} \\ e_r &= (a_{c_c} - a_c)\, K_{y_m} - \delta_{r_m} \end{aligned} \tag{16}$$

These equations are the mechanizational basis for the system and we shall return to them later.

STABILITY CHARACTERISTICS AND GAIN ADJUSTMENT LAW

Always vitally important as a performance indicator is the stability of a system. The crucial underlying design principle in our effort is to seek a system which is stable under reasonably defined ideal conditions. This has been accomplished. Notice that from the synthesis point of view, system stability rather than satisfaction of some criterion function is the prime objective. After a stable design is obtained we shall then seek the criterion function implied as a matter of curiosity. We shall defer elaborating upon "reasonably defined ideal conditions" until the equations are set down.

The first step is to develop expressions for the errors in terms of parameters differences. Subtracting from Eq 16 the system feedback equations (see Fig. 1):

$$\begin{aligned} 0 &= K_{\dot{\phi}}\, (\dot{\phi}_c - \dot{\phi}) - \delta_a \\ 0 &= K_y\, (a_{c_c} - a_c) - \delta_r \end{aligned} \tag{17}$$

and defining the gain-differences,

$$\begin{aligned} \Delta K_{\dot{\phi}} &= K_{\dot{\phi}_m} - K_{\dot{\phi}} \\ \Delta K_y &= K_{y_m} - K_y \end{aligned} \tag{18}$$

results in the following error equations:

$$\begin{aligned} e_a &= (\dot{\phi}_c - \dot{\phi})\ \Delta K_{\dot{\phi}} - (\delta_{a_m} - \delta_a) \\ e_r &= (a_{c_c} - a_c)\ \Delta K_y - (\delta_{r_m} - \delta_r) \end{aligned} \tag{19}$$

The next step is to define the rules by which gain changes will be made. The gain adjustment laws are defined as:

$$\begin{aligned} \dot{K}_{\dot{\phi}} &= A_{\dot{\phi}}\ (\dot{\phi}_c - \dot{\phi})\ e_a \\ \dot{K}_y &= A_y\ (a_{c_c} - a_c)\ e_r \end{aligned} \tag{20}$$

where $A_{\dot{\phi}}$ and A_y are positive constants. They are the adaptive loop gains. In terms of the gain-differences defined by Eq 18 the adjustment laws are,

$$\begin{aligned} \dot{\Delta K}_{\dot{\phi}} &= -A_{\dot{\phi}}\ (\dot{\phi}_c - \dot{\phi})\ e_a \\ \dot{\Delta K}_y &= -A_y\ (a_{c_c} - a_c)\ e_r \end{aligned} \tag{21}$$

since $K_{\dot{\phi}_m}$ and K_{y_m} are constants.

By substituting Eq 19 into Eq 21 we obtain

$$\begin{aligned} \dot{\Delta K}_{\dot{\phi}} &= -A_{\dot{\phi}}\ (\dot{\phi}_c - \dot{\phi})^2\ \Delta K_{\dot{\phi}} + f_{\dot{\phi}} \\ \dot{\Delta K}_y &= -A_y\ (a_{c_c} - a_c)^2\ \Delta K_y + f_y \end{aligned} \tag{22}$$

where:

$$f_{\dot{\phi}} = A_{\dot{\phi}} (\dot{\phi}_c - \dot{\phi})(\delta_{a_m} - \delta_a)$$
$$f_y = A_y (a_{c_c} - a_c)(\delta_{r_m} - \delta_r) \qquad (23)$$

Equations 22 are first order differential equations with time varying gains and forcing functions given by Eq 23. They describe the dynamic response of the adaptive loops.

Equations 22 indicate that the adaptive system is stable in the sense that for $f_{\dot{\phi}}$ and f_y equal to zero, $\Delta K_{\dot{\phi}}$ and ΔK_y as functions of time approach zero monotonically. This follows from the fact that the time varying gains in the homogeneous equations are always non-positive. That is, for example in the $\Delta K_{\dot{\phi}}$ equation, the term $\left[-A_{\dot{\phi}}(\dot{\phi}_c - \dot{\phi})^2\right]$ is either a negative number or, at worst, zero. Thus when $f_{\dot{\phi}}$ and f_y are identically zero, $\Delta K_{\dot{\phi}}$ and ΔK_y cannot diverge.

In addition to these favorable stability features, there is another important attribute of the system. The adjustable gains are uncoupled. An offset in one gain will not result in a transient disturbance of the other gain when $f_{\dot{\phi}}$ and f_y are zero. Traditional multi-parameter adaptive systems have often suffered from coupling which, with increasing adjustment gain, generally tends to cause oscillatory behavior.

Now we must examine what conditions are implied by $f_{\dot{\phi}}$ and f_y equal to zero. These conditions will in fact be those "reasonably defined ideal conditions" mentioned at the beginning of the subsection. Hence the conditions are actually requirements for validity of our conclusions on stability. Notice that $f_{\dot{\phi}}$ and f_y are zero over all time if and only if $(\dot{\phi}_c - \dot{\phi})$ or $(\delta_{a_m} - \delta_a)$ and $(a_{c_c} - a_c)$ or $(\delta_{r_m} - \delta_r)$ respectively are zero over all time. When a servo error, $(\dot{\phi}_c - \dot{\phi})$ and/or $(a_{c_c} - a_c)$, is zero, the following observations hold:

- The system output quantity related to the servo error which is zero is exactly equal to the commanded quantity

- When a servo error is zero the rate of change of the corresponding adaptive gain is zero. See Eq 20.

The first observation above leads to the conclusion that if a servo error is zero for all time there is no need for adaptive action in that channel. The second observation leads to the conclusion that if a servo error is zero for all time, indeed, there will be no adaptive action in that channel. This then constitutes a trivial case. The alternative way for $f_{\dot{\phi}}$ or f_y to be zero is for $(\delta_{a_m} - \delta_a)$ or $(\delta_{r_m} - \delta_r)$ respectively to be zero. If $f_{\dot{\phi}}$ and f_y are to be zero over all time in the non-trivial case, $(\delta_{a_m} - \delta_a)$ and $(\delta_{r_m} - \delta_r)$ must be zero over all time except at isolated instants when a servo error is zero. Conditions for $(\delta_{a_m} - \delta_a)$ and $(\delta_{r_m} - \delta_r)$ to be zero for all time are:

- No vehicle-vehicle model mismatch. Stated another way the vehicle and the vehicle model must have precisely the same transfer functions and
- The initial conditions on the corresponding vehicle and vehicle model variables must be the same and
- No disturbance inputs may act on the vehicle.

While these restrictive assumptions are severe, the stability for this special case of Eq 22 is a most gratifying and important characteristic. This special case of Eq 22 provides a firm and attractive theoretical basis for adaptive system operation.

Let us consider the stability of the errors e_a and e_r under the same restrictive assumptions. Equations 19 become

$$\begin{aligned} e_a &= (\dot{\phi}_c - \dot{\phi})\ \Delta K_{\dot{\phi}} \\ e_r &= (a_{c_c} - a_c)\ \Delta K_y \end{aligned} \tag{24}$$

Clearly these errors are always asymptotically stable to zero since either

- $\Delta K_{(\ )}$ goes to zero by virtue of Eq 22, or
- $\Delta K_{(\ )}$ goes to a constant value by virtue of Eq 22. This implies that the servo error is zero since otherwise $\Delta K_{(\ )}$ would approach zero.

Under these assumptions, if the gain adjustment law given by Eq 20 is a steepest descent law, the criterion being satisfied (to within an arbitrary, multiplicative, positive constant) is:

$$J = 1/2\ (A_{\dot{\phi}}\ e_a^{\,2} + A_y\ e_r^{\,2}) \tag{25}$$

That this is so can be verified by computing $\partial J/\partial \Delta K_{\dot{\phi}}$ and $\partial J/\partial \Delta K_y$ using Eq 24 and noting that:

$$\begin{aligned} \Delta\dot{K}_{\dot{\phi}} &= -\frac{\partial J}{\partial \Delta K_{\dot{\phi}}} = -A_{\dot{\phi}}(\dot{\phi}_c - \dot{\phi})e_a \\ \Delta\dot{K}_y &= -\frac{\partial J}{\partial \Delta K_y} = -A_y(a_{c_c} - a_c)e_r \end{aligned} \tag{26}$$

Certain observations can now be made about stability for the more general case of Eq 22 when the forcing terms are not zero. First of all, for a well chosen model; one which is a reasonably close approximation to the vehicle in the regime of flight being considered, the forcing terms will be small in the absence of disturbance inputs. This conclusion follows from the fact that each forcing term contains a factor $\left(\delta_{(\ )_m} - \delta_{(\ )}\right)$ which becomes vanishingly small as the model and the plant become the same. Nevertheless, there will actually be some small amount of forcing due to this mismatch, and the adjusting gains will accordingly be perturbed. As a matter of fact, this same effect will also cause a small amount of cross-coupling between gains through the forcing terms. Neither of these non-ideal effects is expected to be troublesome.

Next we shall write some equations to express these qualitative observations. The approach will be to express $(\delta_{a_m} - \delta_a)$ and $(\delta_{r_m} - \delta_r)$ in Eq 22 in terms of the servo errors, disturbance input and transfer functions for the vehicle and vehicle model. From Eq 1, 2, 13 and 18:

$$\delta_{a_m} - \delta_a = \left[\frac{N_{\delta_a}^{\dot{\Phi}} N_{\delta_{r_m}}^{a''_y} - N_{\delta_a}^{a''_y} N_{\delta_{r_m}}^{\dot{\Phi}}}{\left(N_{\delta_a}^{\dot{\Phi}} {}^{a''_y}_{\delta_r} \right)_m} - 1 \right] \left[(\dot{\phi}_c - \dot{\phi})(K_{\dot{\phi}_m} - \Delta K_{\dot{\phi}}) \right]_{\mathcal{L}} \dagger$$

$$+ \frac{N_{\delta_r}^{\dot{\Phi}} N_{\delta_{r_m}}^{a''_y} - N_{\delta_r}^{a''_y} N_{\delta_{r_m}}^{\dot{\Phi}}}{\Delta \left(N_{\delta_a}^{\dot{\Phi}} {}^{a''_y}_{\delta_r} \right)_m} \left[(a_{c_c} - a_c)(K_{y_m} - \Delta K_y) \right]_{\mathcal{L}}$$

$$+ \frac{N_d^{\dot{\Phi}} N_{\delta_{r_m}}^{a''_y} - N_d^{a''_y} N_{\delta_{r_m}}^{\dot{\Phi}}}{\Delta \left(N_{\delta_a}^{\dot{\Phi}} {}^{a''_y}_{\delta_r} \right)_m} d$$

$$\delta_{r_m} - \delta_r = \frac{N_{\delta_a}^{a''_y} N_{\delta_{a_m}}^{\dot{\Phi}} - N_{\delta_a}^{\dot{\Phi}} N_{\delta_{a_m}}^{a''_y}}{\Delta \left(N_{\delta_a}^{\dot{\Phi}} {}^{a''_y}_{\delta_r} \right)_m} \left[(\dot{\phi}_c - \dot{\phi})(K_{\dot{\phi}_m} - \Delta K_{\dot{\phi}}) \right]_{\mathcal{L}}$$

$$+ \left[\frac{N_{\delta_r}^{a''_y} N_{\delta_{a_m}}^{\dot{\Phi}} - N_{\delta_r}^{\dot{\Phi}} N_{\delta_{a_m}}^{a''_y}}{\Delta \left(N_{\delta_a}^{\dot{\Phi}} {}^{a''_y}_{\delta_r} \right)_m} - 1 \right] \left[(a_{c_c} - a_c)(K_{y_m} - \Delta K_y) \right]_{\mathcal{L}}$$

$$+ \frac{N_d^{a''_y} N_{\delta_{a_m}}^{\dot{\Phi}} \quad N_d^{\dot{\Phi}} N_{\delta_{a_m}}^{a''_y}}{\Delta \left(N_{\delta_a}^{\dot{\Phi}} {}^{a''_y}_{\delta_r} \right)_m} d \qquad (27)$$

---

† $\left[\cdot \right]_{\mathcal{L}}$ denotes the Laplace transform of the time domain quantity, $\left[\cdot \right]$.

Substitution of Eq 23 and 27 into Eq 22 gives:

①

$$\Delta\dot{K}_{\dot{\Phi}} = -A_{\dot{\Phi}}(\dot{\Phi}_c - \dot{\Phi})\left[\frac{N^{\dot{\Phi}}_{\delta_a} N^{a''_y}_{\delta_{r_m}} - N^{\dot{\Phi}}_{\delta_{r_m}} N^{a''_y}_{\delta_a}}{\Delta\left(N^{\dot{\Phi}\ a''_y}_{\delta_a \delta_{r_m}}\right)} \left\{(\dot{\Phi}_c - \dot{\Phi})\ \Delta\dot{K}_{\dot{\Phi}}\right\}_{\mathcal{L}}\right]_{\mathcal{L}^{-1}}$$

②

$$-A_{\dot{\Phi}}(\dot{\Phi}_c - \dot{\Phi})\left[\frac{N^{\dot{\Phi}}_{\delta_r} N^{a''_y}_{\delta_{r_m}} - N^{\dot{\Phi}}_{\delta_{r_m}} N^{a''_y}_{\delta_r}}{\Delta\left(N^{\dot{\Phi}\ a''_y}_{\delta_a \delta_{r_m}}\right)} \left\{(a_{c_c} - a_c)\ \Delta K_y\right\}_{\mathcal{L}}\right]_{\mathcal{L}^{-1}}$$

③

$$-A_{\dot{\Phi}}K_{\dot{\Phi}_m}(\dot{\Phi}_c - \dot{\Phi})\left[\left(1 - \frac{N^{\dot{\Phi}}_{\delta_a} N^{a''_y}_{\delta_{r_m}} - N^{\dot{\Phi}}_{\delta_{r_m}} N^{a''_y}_{\delta_a}}{\Delta\left(N^{\dot{\Phi}\ a''_y}_{\delta_a \delta_{r_m}}\right)}\right)(\dot{\Phi}_c - \dot{\Phi})\right]_{\mathcal{L}^{-1}}$$

④

$$+A_{\dot{\Phi}}K_{y_m}(\dot{\Phi}_c - \dot{\Phi})\left[\frac{N^{\dot{\Phi}}_{\delta_r} N^{a''_y}_{\delta_{r_m}} - N^{\dot{\Phi}}_{\delta_{r_m}} N^{a''_y}_{\delta_r}}{\Delta\left(N^{\dot{\Phi}\ a''_y}_{\delta_a \delta_{r_m}}\right)}(a_{c_c} - a_c)\right]_{\mathcal{L}^{-1}}$$

⑤

$$+A_{\dot{\Phi}}(\dot{\Phi}_c - \dot{\Phi})\left[\frac{N^{\dot{\Phi}}_{d} N^{a''_y}_{\delta_{r_m}} - N^{\dot{\Phi}}_{\delta_{r_m}} N^{a''_y}_{d}}{\Delta\left(N^{\dot{\Phi}\ a''_y}_{\delta_a \delta_{r_m}}\right)}\ d\right]_{\mathcal{L}^{-1}}$$

$$\dot{\Delta K}_y = \text{①} - A_y(a_{c_c} - a_c)\left[\frac{N^{\dot{\Phi}}_{\delta_{a_m}} N^{a''_y}_{\delta_r} - N^{\dot{\Phi}}_{\delta_r} N^{a''_y}_{\delta_{a_m}}}{\Delta\left(N^{\dot{\Phi}\ a''_y}_{\delta_a \delta_{r_m}}\right)} \left\{(a_{c_c} - a_c)\ \Delta K_y\right\}_{\mathcal{L}}\right]_{\mathcal{L}^{-1}}$$

$$\text{②} - A_y(a_{c_c} - a_c)\left[\frac{N^{a''_y}_{\delta_a} N^{\dot{\Phi}}_{\delta_{a_m}} - N^{a''_y}_{\delta_{a_m}} N^{\dot{\Phi}}_{\delta_a}}{\Delta\left(N^{\dot{\Phi}\ a''_y}_{\delta_a \delta_{r_m}}\right)} \left\{(\dot{\phi}_c - \dot{\phi})\ \Delta K_{\dot{\phi}}\right\}_{\mathcal{L}}\right]_{\mathcal{L}^{-1}}$$

$$\text{③} - A_y K_{y_m}(a_{c_c} - a_c)\left[\left(1 - \frac{N^{\dot{\Phi}}_{\delta_{a_m}} N^{a''_y}_{\delta_r} - N^{\dot{\Phi}}_{\delta_r} N^{a''_y}_{\delta_{a_m}}}{\Delta\left(N^{\dot{\Phi}\ a''_y}_{\delta_a \delta_{r_m}}\right)}\right)(a_{c_c} - a_c)\right]_{\mathcal{L}^{-1}}$$

$$\text{④} + A_y K_{y_m}(a_{c_c} - a_c)\left[\frac{N^{a''_y}_{\delta_a} N^{\dot{\Phi}}_{\delta_{a_m}} - N^{a''_y}_{\delta_{a_m}} N^{\dot{\Phi}}_{\delta_a}}{\Delta\left(N^{\dot{\Phi}\ a''_y}_{\delta_a \delta_r}\right)_m} (\dot{\phi}_c - \dot{\phi})\right]_{\mathcal{L}^{-1}}$$

$$\text{⑤} + A_y(a_{c_c} - a_c)\left[\frac{N^{\dot{\Phi}}_{\delta_{a_m}} N^{a''_y}_{d} - N^{\dot{\Phi}}_{d} N^{a''_y}_{\delta_{a_m}}}{\Delta\left(N^{\dot{\Phi}\ a''_y}_{\delta_a \delta_r}\right)_m}\ d\right]_{\mathcal{L}^{-1}} \qquad (28)\dagger$$

†Notice that Eq 28 are time domain equations. $\left[\cdot\right]_{\mathcal{L}^{-1}}$ denotes the inverse Laplace transform of the frequency domain quantity, $\left|\cdot\right|$.

Next we shall discuss the significance of the terms on the RHS of Eq 28. The significance of like numbered terms in each equation is the same.

Term (1) is the principal term. When no controlled element mismatch exists, the factor contained by the vinculum is unity, and the coefficient of $\Delta K_{(\ )}$ is non-positive. When mismatch is "small", this factor tends to consist of pole-zero dipoles.

Term (2) is a gain-difference cross-coupling term. When no controlled element mismatch exists, the factor contained by the vinculum is zero, and the cross-coupling vanishes. When mismatch is "small", the numerator polynomial coefficients of this factor tend to be "small". This term represents a controlled element mismatch cross-coupling effect.

Terms (3) and (4) are controlled element mismatch forcing effects. When no controlled element mismatch exists, these forcing terms vanish by virtue of the values assumed by the factors contained by vincula as discussed in connection with terms (1) and (2).

Term (5) is a disturbance input forcing effect. When no controlled element mismatch exists, the factor contained by the vinculum becomes the ratio of coupling numerators, $N_{d\delta_r}^{\dot{\Phi} a''_y} / N_{\delta_a \delta_r}^{\dot{\Phi}\ a''_y}$ for the $\Delta\dot{K}_{\dot{\Phi}}$ equation, and $N_{\delta_a d}^{\dot{\Phi}\ a''_y} / N_{\delta_a \delta_r}^{\dot{\Phi}\ a''_y}$ for the $\Delta\dot{K}_{\dot{y}}$ equation.

The above observations lead to the qualitative conclusions that controlled element mismatch and disturbance inputs can each be expected to provide both steady and transient forcing of the $\Delta K_{(\ )}$ responses. The question of stability of the $\Delta K_{(\ )}$ responses remains open for the most general case.

MECHANIZING THE SYSTEM

With the theoretical development of the adaptive system accomplished, we are faced with the task of identifying ways for realizing the system within the limitations of physical devices. The mechanizational basis

for the adaptive system is given by the equations below.

$$\begin{aligned} e_a^* &= (\dot{\phi}_c - \dot{\phi})^* K_{\dot{\phi}_m} - \delta^*_{a_m} = F(s)e_a \\ e_r^* &= (a_{c_c} - a_c)^* K_{y_m} - \delta^*_{r_m} = F(s)e_r \end{aligned} \tag{29}$$

$$\begin{aligned} \dot{K}_{\dot{\phi}} &= A_{\dot{\phi}}(\dot{\phi}_c - \dot{\phi})^* e_a^* \\ \dot{K}_y &= A_y(a_{c_c} - a_c)^* e_r^* \end{aligned} \tag{30}$$

These equations are quite similar to Eq 16 and 20. The exception is that starred quantities are used in Eq 29 and 30. The starred quantities are obtained by passing the corresponding unstarred quantities through high frequency cut-off filters with transfer functions, F(s). Subsequent discussion will make the need for this filtering in practical mechanization apparent.

Examination of Eq 29 and 30 shows that aside from the signals available in the system, $(\dot{\phi}_c - \dot{\phi})$ and $(a_{c_c} - a_c)$, we will also require δ_{a_m} and δ_{r_m}. These are generated by filtering the outputs of the vehicle sensors, φ and a_y'' with transfer functions representing the mathematical inverse of the vehicle model. Refer to Eq 13. The problem here is to realize these transfer functions.

Below, we will show how this may be accomplished with a single filter. Consider the vehicle equations of motion, Eq A-1, A-2, A-4 and A-5 presented in Appendix A. Here we will be discussing these equations as they pertain to the vehicle model. Certain approximations can be made in the model for the sake of simplicity. Namely, θ_o $(l_x + Y_{\delta_r}/N'_{\delta_r})$, L'_r, L'_p, N'_p and N'_r can be set to zero. Y_{δ_r} can be set to zero in the sideslip equation but <u>not</u> in the lateral acceleration equation.† The term $(g/V_{T_o})\cos\theta_o\varphi$ is set to zero in the sideslip

†Y_v could also be set to zero insofar as the accuracy of the approximations is concerned. We retain it here so that the roots of $\left(N^{\dot{\phi}}_{\delta_a} a''_y\right)_m$ will have a positive damping ratio.

equation. For simplicity in the model equations, approximate l_x by $l_{x_o} = -Y_{\delta_r}/N'_{\delta_r}$. The effects of all these approximations are negligible. In fact, if we make similar approximations in the vehicle equations, the short term time responses are imperceptably changed. This is also true for the long term responses with the exception of $\left(g/V_{T_o}\right)\cos\theta_o\varphi$ approximation effect. All these considerations can be combined to write the equations of motion for the model as

$$\begin{bmatrix} (s - Y_v) & -W_o/V_{T_o} & U_o/V_{T_o} & 0 \\ -L'_\beta & s & 0 & 0 \\ -N'_\beta & 0 & s & 0 \\ -V_{T_o}Y_v & 0 & s\,Y_{\delta_r}/N'_{\delta_r} & 1 \end{bmatrix}_m \begin{Bmatrix} \beta \\ \dot{\varphi} \\ r \\ a''_y \end{Bmatrix} =$$

$$\begin{bmatrix} 0 & 0 \\ L'_{\delta_a} & L'_{\delta_r} \\ N'_{\delta_a} & N'_{\delta_r} \\ 0 & Y_{\delta_r} \end{bmatrix}_m \begin{Bmatrix} \delta_a \\ \delta_r \end{Bmatrix}_m \qquad (31)$$

The polynomials which form the transfer functions in Eq 13 are related to Eq 31 in following ways. Using Cramer's rule and its counterpart for the coupling numerator we find:

$$N^{a''_y}_{\delta_{r_m}} = \begin{vmatrix} (s - Y_v) & -W_o/V_{T_o} & U_o/V_{T_o} & 0 \\ -L'_\beta & s & 0 & L'_{\delta_r} \\ -N'_\beta & 0 & s & N'_{\delta_r} \\ -V_{T_o}Y_v & 0 & s\,Y_{\delta_r}/N'_{\delta_r} & Y_{\delta_r} \end{vmatrix}_m \qquad (32)$$

$$-N^{\dot{\Phi}}_{\delta_{r_m}} = \begin{vmatrix} (s - Y_v) & 0 & U_o/V_{T_o} & 0 \\ -L'_\beta & -L'_{\delta_r} & 0 & 0 \\ -N'_\beta & -N'_{\delta_r} & s & 0 \\ -V_{T_o}Y_v & -Y_{\delta_r} & s\, Y_{\delta_r}/N'_{\delta_r} & 1 \end{vmatrix}_m \tag{33}$$

$$-N^{a''_y}_{\delta_{a_m}} = \begin{vmatrix} (s - Y_v) & -W_o/V_{T_o} & U_o/V_{T_o} & 0 \\ -L'_\beta & s & 0 & -L'_{\delta_a} \\ -N'_\beta & 0 & s & -N'_{\delta_a} \\ -V_{T_o}Y_v & 0 & s\, Y_{\delta_r}/N'_{\delta_r} & 0 \end{vmatrix}_m \tag{34}$$

$$N^{\dot{\Phi}}_{\delta_{a_m}} = \begin{vmatrix} (s - Y_v) & 0 & U_o/V_{T_o} & 0 \\ -L'_\beta & L'_{\delta_a} & 0 & 0 \\ -N'_\beta & N'_{\delta_a} & s & 0 \\ -V_{T_o}Y_v & 0 & s\, Y_{\delta_r}/N'_{\delta_r} & 1 \end{vmatrix}_m \tag{35}$$

$$N^{\dot{\Phi}\ a''_y}_{\delta_a\delta_r} = \begin{vmatrix} (s - Y_v) & 0 & U_o/V_{T_o} & 0 \\ -L'_\beta & L'_{\delta_a} & 0 & L'_{\delta_r} \\ -N'_\beta & N'_{\delta_a} & s & N'_{\delta_r} \\ -V_{T_o}Y_v & 0 & s\, Y_{\delta_r}/N'_{\delta_r} & Y_{\delta_r} \end{vmatrix}_m \tag{36}$$

Considered together with Eq 13 these determinants imply the equations for mechanizing the filter for generating δ_{a_m} and δ_{r_m} from $\dot{\Phi}$ and a''_y. We can write down a set of equations having the same transfer functions as Eq 13 by inspection of the above determinants. In actual fact, we are applying Cramer's rule in reverse in this "inspection" process.

$$\begin{bmatrix} (s - Y_v) & 0 & U_o/V_{T_o} & 0 \\ -L'_\beta & L'_{\delta_a} & 0 & L'_{\delta_r} \\ -N'_\beta & N'_{\delta_a} & s & N'_{\delta_r} \\ -V_{T_o}Y_v & 0 & s\, Y_{\delta_r}/N'_{\delta_r} & Y_{\delta_r} \end{bmatrix}_m \begin{Bmatrix} x_1 \\ \delta_a \\ x_3 \\ \delta_r \end{Bmatrix}_m =$$

$$\begin{bmatrix} -W_o/V_{T_o} & 0 \\ s & 0 \\ 0 & 0 \\ 0 & 1 \end{bmatrix}_m \begin{Bmatrix} \dot{\phi} \\ a''_y \end{Bmatrix} \qquad (37)$$

This filter is only second order and may be mechanized quite simply using operational elements. The mechanization resulting after the algebraic loops in Eq 37 are eliminated is shown in Fig. 2. The values of the coefficients for Fig. 2 are given in Table I. Notice in Fig. 2 that there is an implied requirement that we either measure $\ddot{\phi}$ or calculate $\ddot{\phi}$ by differentiating $\dot{\phi}$. Neither alternative is really acceptable. We can get around this point by using a pseudo-differentiator to obtain $\ddot{\phi}^*$ from $\dot{\phi}$ and insert a cut-off filter in all the other input paths to compensate for the characteristics of the differentiating filter. This amounts to specifying part of the filter, F(s). That is, if the pseudo-differentiator has a transfer function $(s/T)/(s + 1/T)$ then F(s) will contain the factor $(1/T)/(s + 1/T)$. To this point, we have neglected the flight control servo dynamics. It is clear that the servo dynamics will interpose between the gains, $K_{\dot{\phi}}$ and K_y, and the control surface deflections δ_a and δ_r respectively. Refer to Fig. 1. We could include the flight control servo dynamics with the vehicle

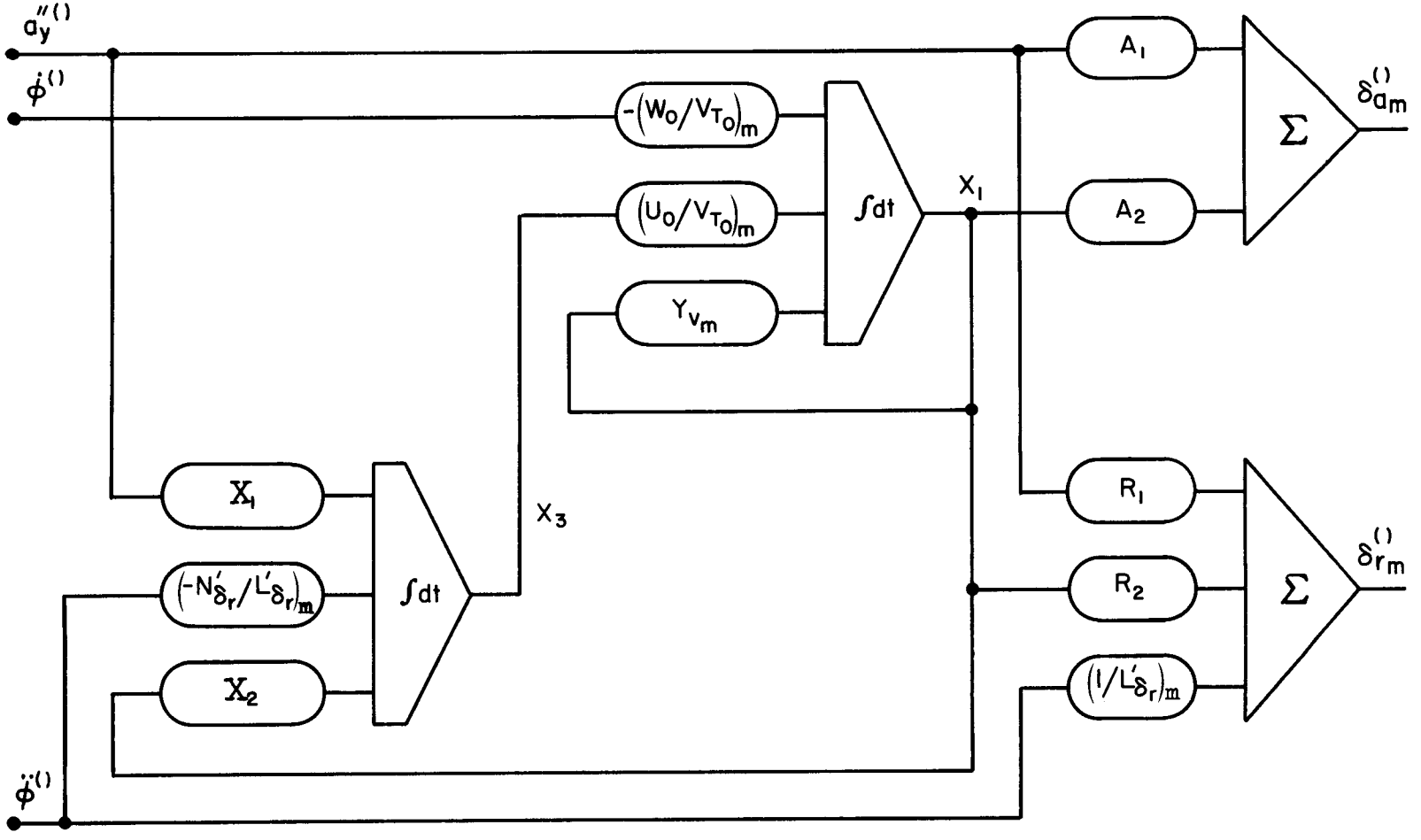

NOTE: Symbols are defined in Table I (next page)

Figure 2. Mechanization of Filter

TABLE I

FILTER COEFFICIENTS

COEFFICIENT	LITERAL EXPRESSION
A_1	$\left[-N'_{\delta_r}/(N'_{\delta_a}Y_{\delta_r})\right]_m$
A_2	$\left[N'_{\delta_r}(N'_\beta/N'_{\delta_r} - Y_v/Y^*_{\delta_r})/N'_{\delta_a}\right]_m$
R_1	$\left[N'_{\delta_r}L'_{\delta_a}/(Y_{\delta_r}N'_{\delta_a}L'_{\delta_r})\right]_m$
R_2	$\left[L'_\beta/L'_{\delta_r} - N'_\beta L'_{\delta_a}/(N'_{\delta_a}L'_{\delta_r}) + Y_v N'_{\delta_r}L'_{\delta_a}/(Y^*_{\delta_r}N'_{\delta_a}L'_{\delta_r})\right]_m$
X_1	$\left[-N'_{\delta_r}L'_{\delta_a}(N'_{\delta_r} - N'_{\delta_a}L'_{\delta_r}/L'_{\delta_a})/(Y_{\delta_r}N'_{\delta_a}L'_{\delta_r})\right]_m$
X_2	$\left[N'_{\delta_r}\left\{L'_{\delta_a}(N'_\beta - N'_{\delta_r}Y_v/Y^*_{\delta_r})/N'_{\delta_a} - (L'_\beta - L'_{\delta_r}Y_v/Y^*_{\delta_r})\right\}/L'_{\delta_r}\right]_m$

equations of motion by calling the servo commands δ_a and δ_r instead of servo outputs. We could then proceed in a routine fashion to calculate the filter equations etc. We would find, however, that more differentiations would be required to generate inputs for the filter. Ultimately pseudo-differentiations would be employed for practical reasons. Therefore, it is useful to short-circuit this process by noting that the flight control servos act in the same manner as factors of F(s) operating upon $\dot{\phi}$ and a''_y. By merely placing similar factors in the F(s) operating upon $(\dot{\phi}_c - \dot{\phi})$ and $(a_{c_c} - a_c)$ we can preserve the relationship of Eq 29. If we assume that both flight control servos have the same transfer function, $25/(s + 25)$, and if we take $1/T$ in the pseudo-differentiator to be 15.0/sec., the following

equations will hold:

$$(\dot{\phi}_c - \dot{\phi})^* = \frac{15.}{s + 15.} \frac{25.}{s + 25.} (\dot{\phi}_c - \dot{\phi}) \tag{38}$$

$$(a_{c_c} - a_c)^* = \frac{15.}{s + 15.} \frac{25.}{s + 25.} (a_{c_c} - a_c) \tag{39}$$

$$\ddot{\phi}^* = \frac{15.s}{s + 15.} \dot{\phi} \tag{40}$$

$$\dot{\phi}^* = \left\{ \frac{15.}{s + 15.} \dot{\phi} \right\} \tag{41}$$

$$a_y''^* = \left\{ \frac{15.}{s + 15.} a_y'' \right\} \tag{42}$$

The braces on the RHS of Eq 41 and 42 are to call attention to the fact that these signals are generated in the filters for obtaining $\ddot{\phi}^*$ from $\dot{\phi}$, and a_c from a_y'' respectively. In the latter case, we can now see a very modest simplification was afforded by choosing the time constant of the pseudo-differentiator equal to that for the feedback compensation pole.

If it is necessary to include sensor dynamic effects or additional signal conditioning filters, these may be included in a manner similar to that for including the flight control servo dynamics. A word of caution is in order, however. The theoretical treatment of system stability given earlier assumes throughout that $F(s) \equiv 1$. Any deviations from this, particularly those which will introduce appreciable lag within the bandwidth of the augmented vehicle, might cause instability of the adapting gains when the adaptive loop gains, $A_{\dot{\phi}}$ and A_y, are at very high values.

At this point, we shall summarize the adaptive system mechanization to set the stage for discussion of the system simulation in Section III. The adaptive system is mechanization shown in Fig. 3. It is worthwhile

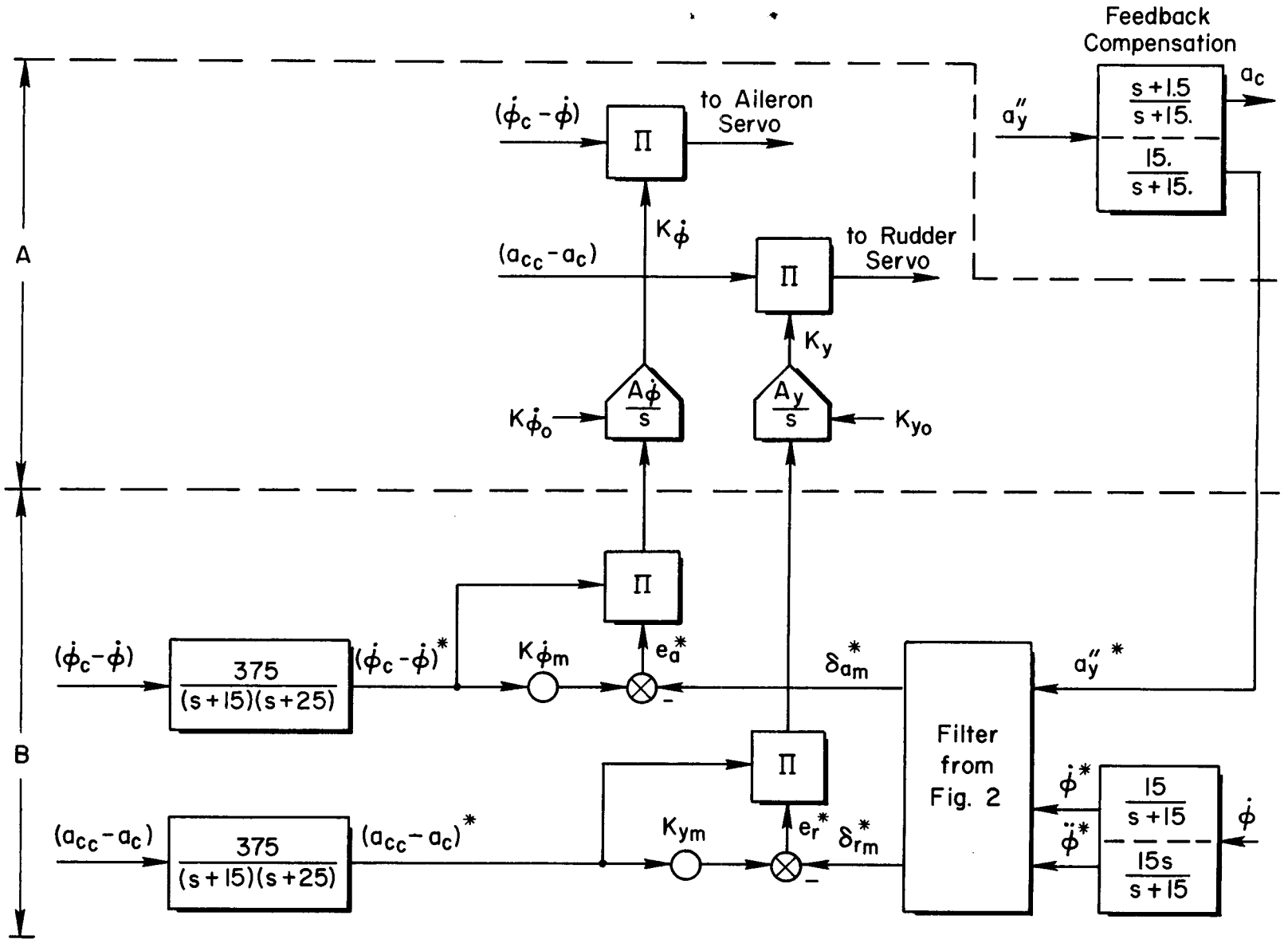

Figure 3. Adaptive System Mechanization

to remark here that the amount of equipment required to mechanize this adaptive system is indeed modest. Consider that the equipment spanned by arrow A in Fig. 3 is required for any system in which gains are adjusted, as for example, in an air data scheduled system. The equipment spanned by arrow B in Fig. 3 is specifically for the adaptive control function mechanization. Required are two electronic multiplications, two second order filters with real poles and one third order filter. These relatively modest equipment requirements for the adaptive control function mechanization are remarkable considering the breadth of capabilities for which the system is designed, and in contrast to the amount of equipment required for some earlier adaptive system designs. (See for example, Ref. 3, 10 and 13 through 15, each of which must be regarded as a competent and successful effort.)

SECTION III

SIMULATION RESULTS

We present here the results of a simulation effort to demonstrate the performance of the adaptive control function system described in Section II. The nature of the gain adjustment, that is, speed and stability (tendency toward oscillation), as well as sensitivity to various disturbances, such as mismatch and gusts, are the items of most general interest. But, realistically, and ultimately, performance assessment must deal with the ability of the adaptive system to cope with the problems for which its use is specifically intended.

Our viewpoint in this study is to demonstrate a new adaptive method in the context of a particular control task. That task is the time varying augmentation of the lateral motions of a manned, lifting-body, entry vehicle during a critical segment of its mission. The vehicle is a hypothetical one which exhibits a variety of handling quality problems. Some of the difficulties do not specifically depend on adaptive augmentation for their correction. For instance, the roll damping deficiency of the bare airframe may be remedied with a fixed gain roll damper. The overall handling quality problem cannot, however, be solved without resorting to time varying gains in the multiloop augmenter as has already been demonstrated. We show in this Section, not merely that the gains can be changed automatically, but also, and more importantly, that the rationale for constructing the system is legitimate.

In attempting to validate the adaptive control function concept we face a certain difficulty: the system is non-linear. Analysis presented in Section II goes a long way toward solving the non-linear equations but, not surprisingly, a general solution evades us. The simulation effort is, therefore, more than a means to communicate the results in a widely appreciated format. It also serves to extend and strengthen the analytical results where exact mathematical solutions

not unavailable. Specifically in the important case when mismatch (vehicle model not equal to vehicle) is present, simulation is needed to support the analytical results.

Figures 1 and 3 in Section II have shown block diagrams of the system and have defined symbols. The text describes both the features of the adaptive system and the handling qualities problems with which we are dealing. Appendix A describes the vehicle and the results of SAS configuration surveys. Reference 16 also provides this information. Appendix C gives the details of the simulation. Some readers may prefer to review that Appendix before reading this Section. Figure 4, presented here, summarizes the adaptive lateral SAS configuration which is evolved in the other Sections of this report cited above.

ADAPTIVE SYSTEM OPERATION

Attention will be focused, for the moment, on fixed flight conditions. Flight condition 810 is especially important because the model of the vehicle has been selected to be very nearly the same as the vehicle itself at this time of flight. Some obviously accurate simplifying assumptions: L_p', L_r', N_p' and $N_r' = 0$, have been made in implementing the model and, in addition, an artifically large side force due to sideslip, Y_β, has been employed to improve the model† characteristics. Y_β provides damping of the coupling numerator $(N^{\dot{\phi}}_{\delta_a} a''_{y_{\delta_r}})$ singularities. These are the poles of the model as it is implemented.

At flight condition 810, the analysis proves asymptotic stability when only command inputs exist. If the adaptive system failed to achieve the "ideal" performance predicted by the theory in this no-mismatch situation, one would hold little hope that satisfactory operation could be obtained in the presence of mismatch.

---

†"Model" in Section III will be used to mean "inverse of the MLEV model" for sake of brevity.

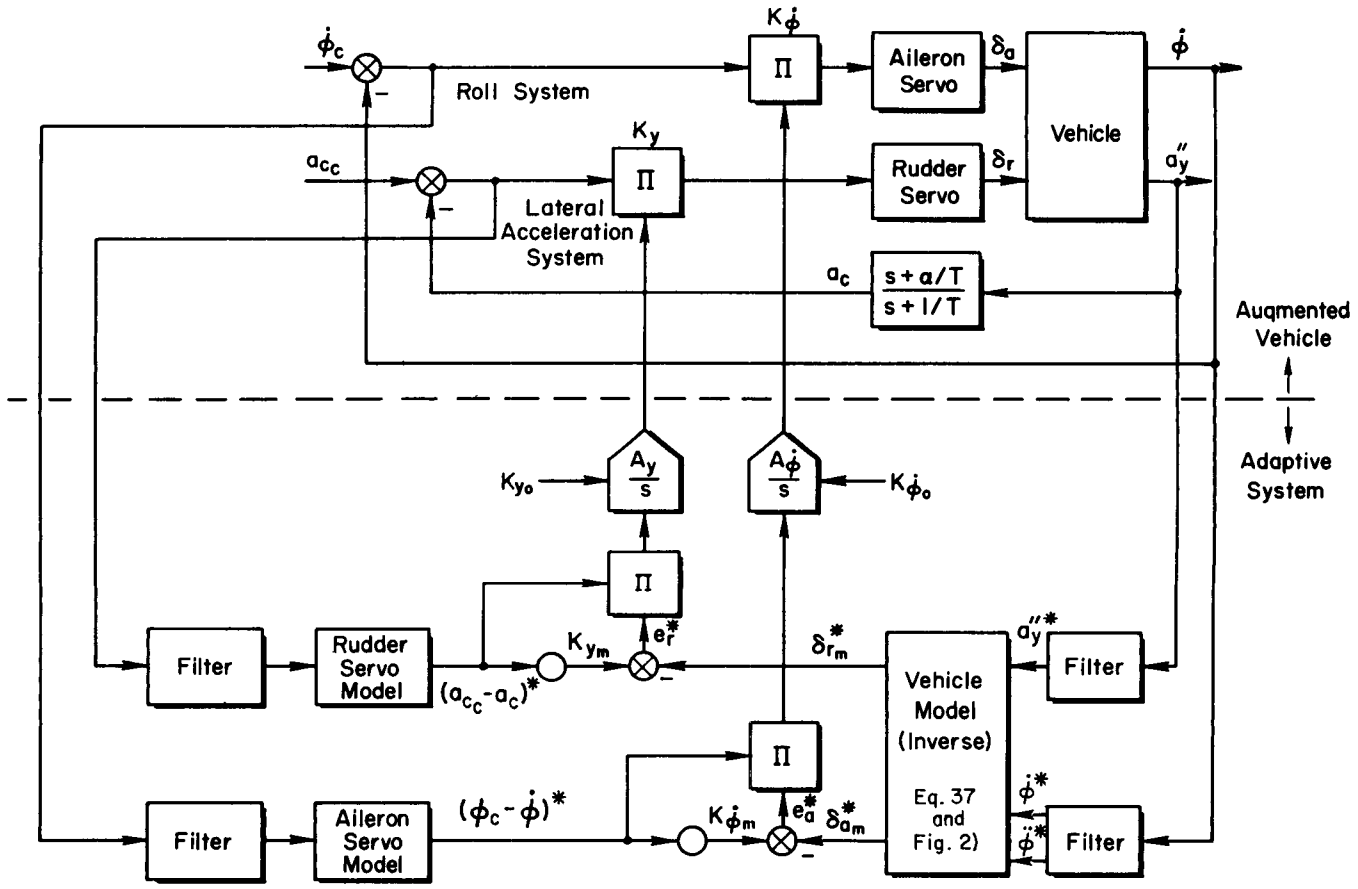

Figure 4. Adaptive Lateral SAS Configuration

Part a of Fig. 5 shows the responses of the system to a square wave roll rate command for the no-mismatch case. The roll rate response is excellent. The adaptive stability augmentation system gains, $K_{\dot{\phi}}$ and K_y, are initially set at the same value chosen for the model. It is observed that (adaptively) the gains prefer a slightly higher value. This is because of the small differences between the model and the vehicle. (See above.) While the offset correction is small it is worth noting that the adaptive system provides a valuable function here, that is, it might compensate for unknown deviations from the mathematical model of the system.

One of the first questions resolved by the simulation was the effect of including the primary lateral piloting task, control of bank angle with aileron. Recall that the system design (Section II) did not account for the presence of this outer loop. An analysis showed that the pilot loop did introduce additional terms into the adaptive system stability equations but that these were not expected to have a deleterious effect. This is the case, as is shown by comparing Parts a and b of Fig. 5. The gain responses for the two cases are very nearly identical. No situations were encountered where the presence or absence of the pilot loop closure made more than a minor difference in adaptation. In all the cases which follow, the pilot closure is included.

We have already reached the conclusion that when the gains are initially very near their optimum or desired values the adaptive process is well behaved. Figure 6 shows the gain responses for all combinations of large, high and low, initial offsets. The offset magnitudes are roughly 50% of the correct values for each gain. In each case the gains change toward their desired values. The adaptive process performs the function we desire. More than that can be said. It is particularly noteworthy that the gain adjustments are uncoupled. That is to say, an error in the initial value of only one gain does not result in a

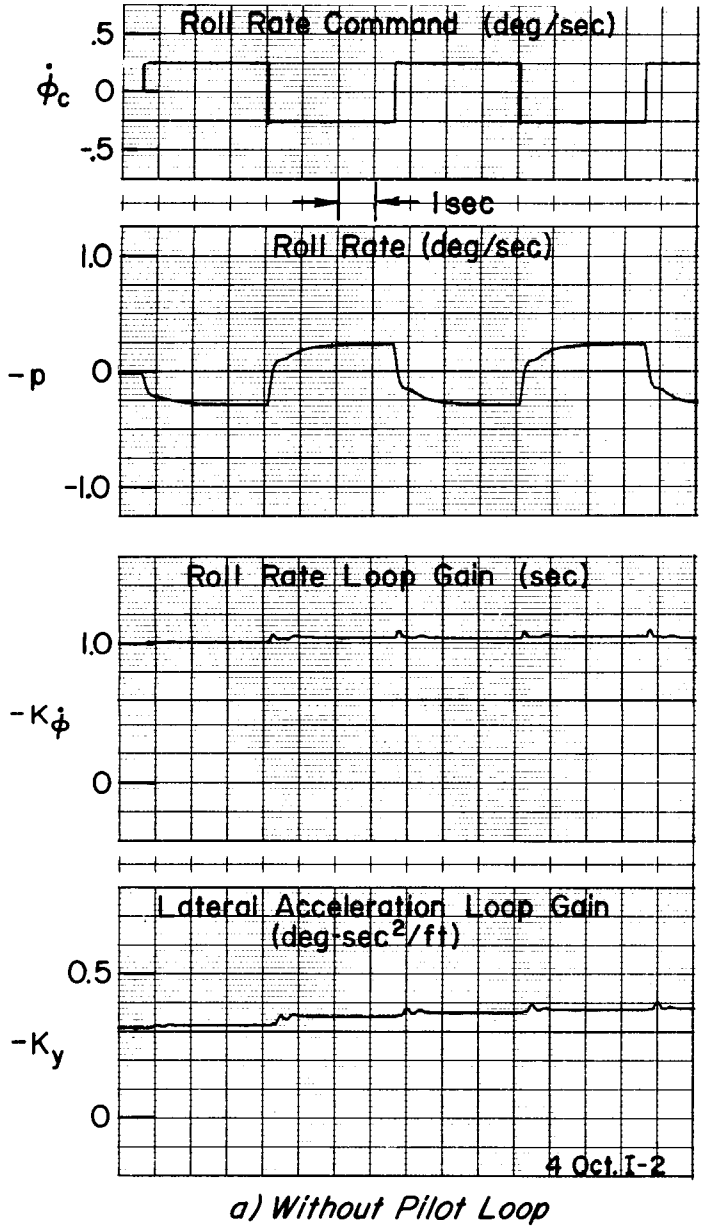

a) Without Pilot Loop

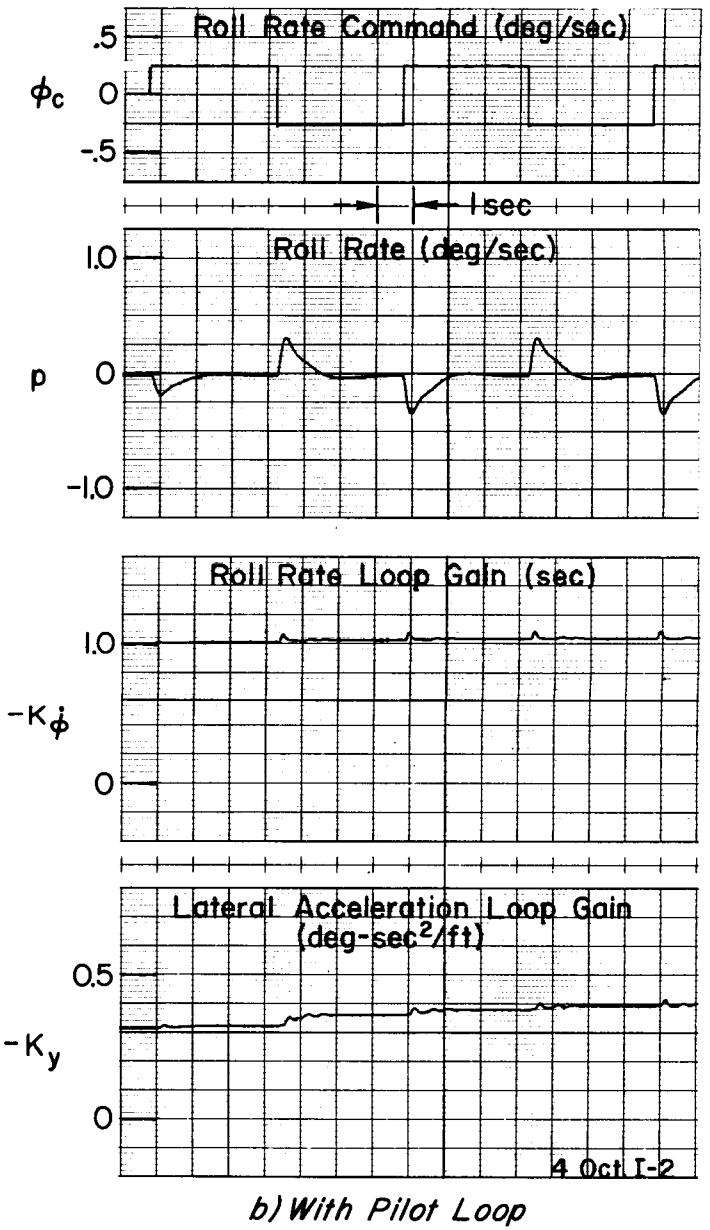

b) With Pilot Loop

Figure 5. Roll Characteristics at Flight Condition 810

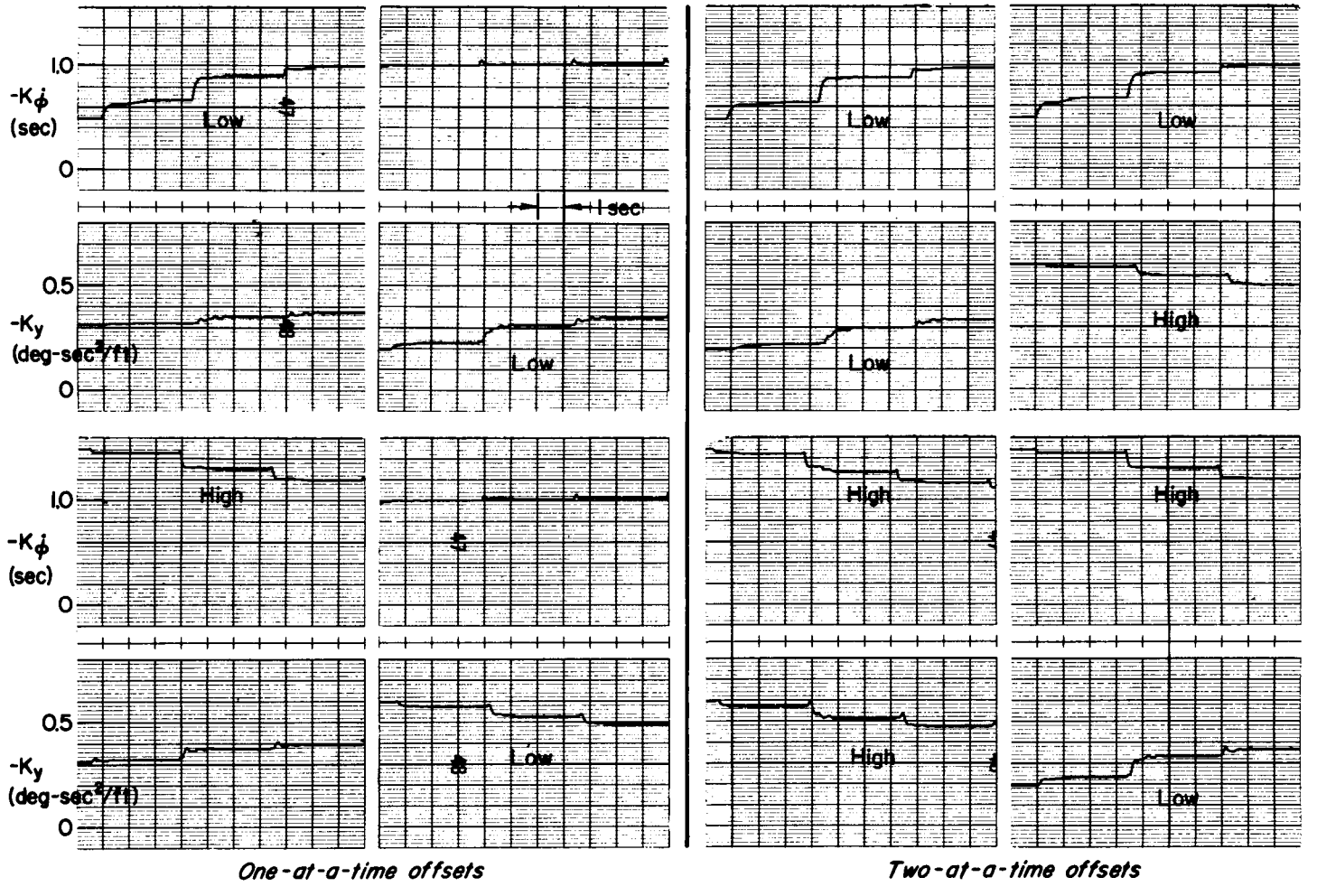

Figure 6. Gain Responses for High and Low Initial Offsets

readjustment of the other, correctly set, gain. See the portion of Figure 6 labeled, "One-at-a-time offsets." This is indeed a most desirable situation since the possibility of "ping-pong" adaptation is circumvented. This phenomenon has been responsible, at least in part, for disqualifying certain adaptive schemes as candidates for actual application in aerospace vehicles.

The adaptive loop gains used to generate the SAS gain responses shown in Fig. 6 are those which optimize the real flight time situation. They can, however, as the analysis predicts, be made much larger for this particular input and flight condition. But at other flight conditions, where there is substantial mismatch between the vehicle and the vehicle model, only slightly higher gains may be employed. Figure 7 shows one of the adaptive gains, $K_{\dot{\phi}}$, responding from a low initial value when the same square wave roll angle command used previously is impressed upon the system. Two flight conditions are shown, 810 and 790. In each case the responses for two adaptive loop gains are shown, the nominal gain and ten times the nominal gain. For the nominal adaptive loop gain the responses are quite satisfactory, converging nicely to the optimum value in each case. When, however, the adaptive loop gain is increased by a factor of ten (20 dB), an oscillatory response occurs. At the 810 flight condition the oscillation is small and reasonably well damped. (The oscillation here must be attributed to non-ideal effects in the simulation.)

At condition 790 the oscillation is much more severe. It would not be unfair to characterize the adaptive system as marginally stable in this case since the gain $K_{\dot{\phi}}$ appears to limit cycle between two levels. As it happens, however, the system responses are entirely satisfactory, and, in fact, are hardly distinquishable from those which occur at condition 810. Further it must be pointed out that a more realistic input, one with greater frequency content, was observed to produce a smooth, monotonic gain function which converged, in time, to the

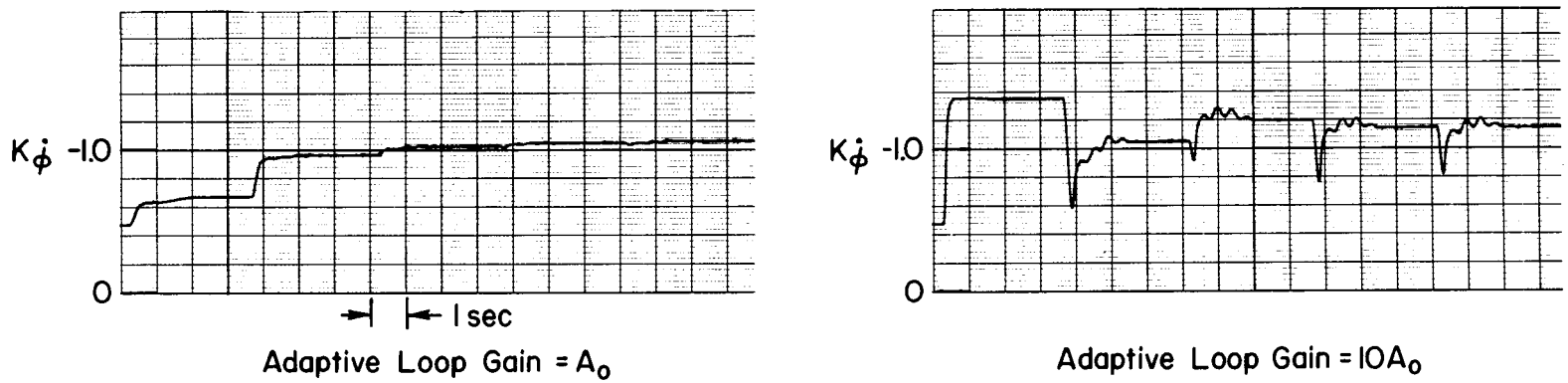

a) Flight Condition 810 - No Mismatch

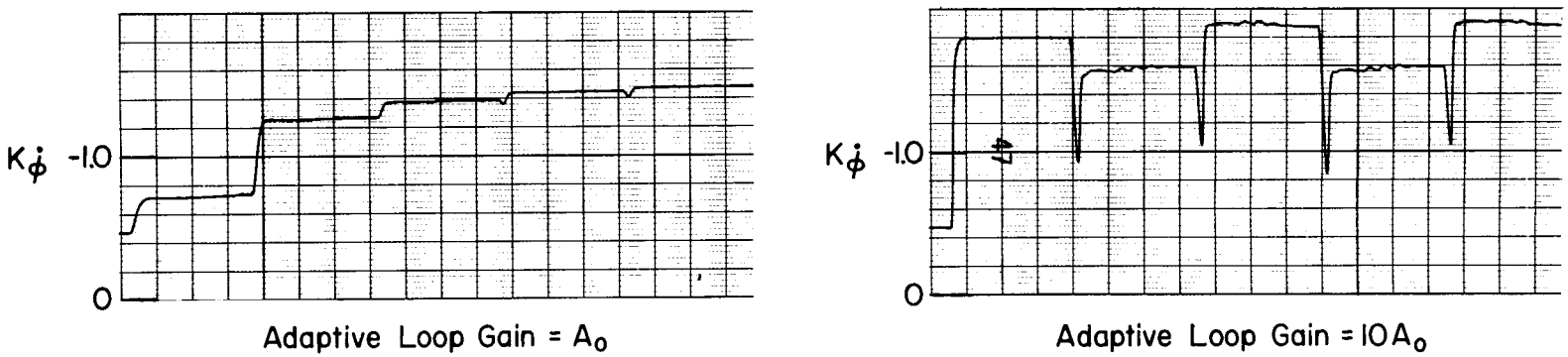

b) Flight Condition 790 - Mismatch

Figure 7. Mismatch and High Gain Effects

optimum value. Also a smaller initial gain offset markedly improved the form of the gain response. Thus, in more ways than one, the situation at flight condition 790, depicted in Fig. 7 is a bit contrived. Our intent is to show, as the reader must suspect, that there are combinations of flight condition,input spectrum,initial gain offset and adaptive loop gain for which adaptive system performance may not be entirely satisfactory. It is comforting to find out that the conditions under which the adaptive system begins to misbehave are very,very far from those under which it will, in a real situation, be likely to encounter.

HANDLING QUALITY ENHANCEMENT

At the outset of this program the critical segment of the mission was determined to be between 620 and 870 seconds. During this 250 second interval which includes high supersonic through subsonic flight regimes, the vehicle dynamics vary very markedly. Among the handling quality deficiencies which arise, either individually or simultaneously, are, as we have seen, low roll damping, low rudder and aileron control effectiveness, the possibility of roll rate reversals in response to aileron steps, roll reversal($\omega_\varphi^2 < 0$), adverse rudder induced roll, high $|\varphi/\beta|$ ratio in the dutch roll mode and unfavorable ω_φ/ω_q ratios. These problems are not all mutually exclusive. The stability augmentation system must improve many vehicle deficiencies in addition to compensating for control effectiveness variations.

Six flight conditions were selected from the 250 second mission segment so that surveys could be made to determine the best stability augmentation system configuration (Ref. 16 and Appendix A of this document). The flight conditions as designated by the corresponding flight times are: 630, 725, 810, 840, 850 and 865. (We have already dealt with flight condition 810, the case where the model of the vehicle and the vehicle are very nearly identical.) The flight conditions are more closely spaced in the transonic region where the

stability derivatives experience large and rapid variations. Mach 1.0 flight occurs between 840 and 850 sec.

Prior to 725 sec the control effectivenesses are extremely low. Thus augmenter effectiveness will be limited. Rate and position limiting of the control surfaces will occur nullifying the attempt to compensate for the low control effectivenesses with high augmenter gains. In practice, reaction controls would be imperative during the early, near zero dynamic pressure, portion of flight. The adaptive technique might be used to blend the reaction and aerodynamic surface control modes during the transition from one to the other.

In addition to the low control effectiveness of both the rudder and the ailerons, the unaugmented vehicle possesses troublesome dutch roll characteristics in the early portion of the reentry. Specifically the ratio ω_{ϕ}/ω_{d} is lower than 0.7, the value often used as the lower bound on an acceptable ω_{ϕ}/ω_{d}. Only partial correction of this difficulty is possible because of the absence of rudder control. Thus, incipient roll rate reversals will be apparent in the real time data shortly to be presented.

In consequence of the low control effectiveness and the exclusion of reaction controls from consideration in this study, the adaptive gains would, if unconstrained, seek unrealistically high levels during the early segment of the flight. To avoid this situation, limits are imposed on each of the adaptive gains. (Limits, of course, would always be included in practice.) The limiting is implemented in a simple manner. It employs a servo motor with tachometer feedback to make it act as an integrator, a clutch and a pot whose arm, driven from the clutch, has stops to restrain its motion. This scheme is shown in the sketch below along with the corresponding electrical analog which was actually used in the simulation.

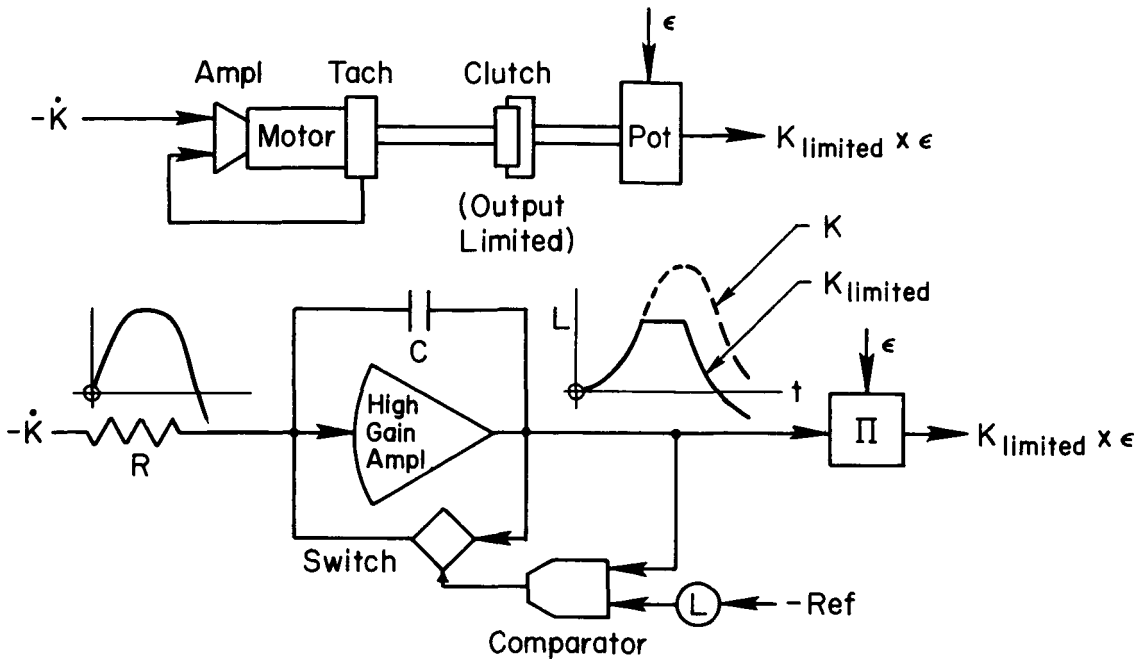

Subsequent to 725 sec the control effectivenesses go through a large excursion. Their rates of change are particularly large during the transonic flight regime, 840 to 850 sec. While the pilot can adapt his gain to compensate for large control effectiveness variations, say by a factor of 100, he prefers not to. He will downgrade his rating of the system as his gain changes even though he can maintain good closed-loop control. Presently it will be shown that, in consequence of the particular system configuration which was selected, the pilot's gain adaptation is minimized by the action of the adaptive SAS gains.

With this background, the real time behavior of the adaptively augmented MLEV can be discussed. Figure 8 shows a 250 sec run which encompasses the entire mission segment of interest. The time scale is necessarily severely compressed so that only a gross view of system response and parameter adjustment can be discerned.

The input for this run, shown in the top trace, is a square wave bank angle command. No gust disturbances are present. The pilot's

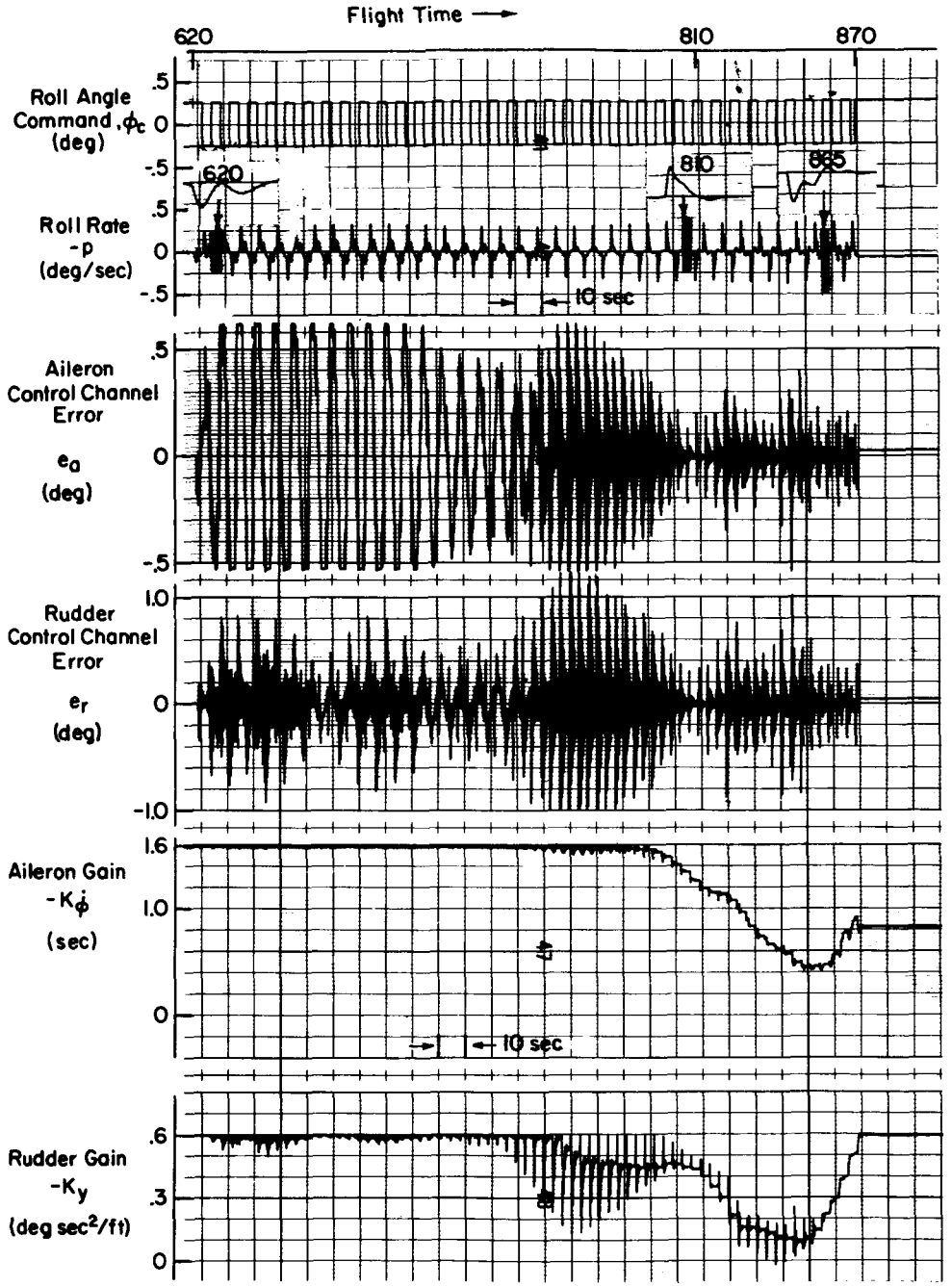

Figure 8. Real Time with Square Wave Roll Angle Command

loop is closed at constant gain. The dominant frequency (fundamental) of the input is approximately one rad/sec. The second trace shows the roll rate response. Three expanded excerpts from this trace are presented to show system characteristics at flight conditions 630, 810 and 865. Notice the incipient roll rate reversal at 630, the very well behaved response at the no-mismatch condition, 810, and the presumably acceptable response at 865.

The third, fourth, fifth and sixth traces are: aileron control channel error, e_a, rudder control channel error, e_r, aileron gain, $K\dot{\phi}$, and rudder gain, K_y. The errors are initially large because of the need for higher gains to compensate for low control effectiveness. At flight condition 810 the errors are small and the gains have decreased from their limits and lie near the gains specified by the model; $K\dot{\phi} = -1.0$ and $K_y = -.316$. The gains then continue to decrease and finally increase again during the final 20 sec of flight.

The time histories of the gains are not smooth in this case because of the step nature of the command. The rudder path gain, K_y, in particular, has large spikes superimposed on a fairly smooth average characteristic. It should be recognized, however, that the square wave input, although it conveniently provides roll responses which can be easily judged by eye, is obviously not a realistic one.

In Fig. 9 the input command is a quasi-random time function having an approximately Gaussian amplitude distribution. (See Appendix C for details.) Otherwise the situation duplicates the one shown in Fig. 8. Again, the errors are initially large, very small at flight condition 810 (no mismatch) and then increase somewhat by the end of the flight segment of interest. The gain time histories have approximately the same characteristics also, being initially high, dropping down as the control effectivenesses increase and, finally, increasing at the end of the flight segment.

It is interesting to compare the actual gain time histories during the final minute of flight with the desired ones inferred from the

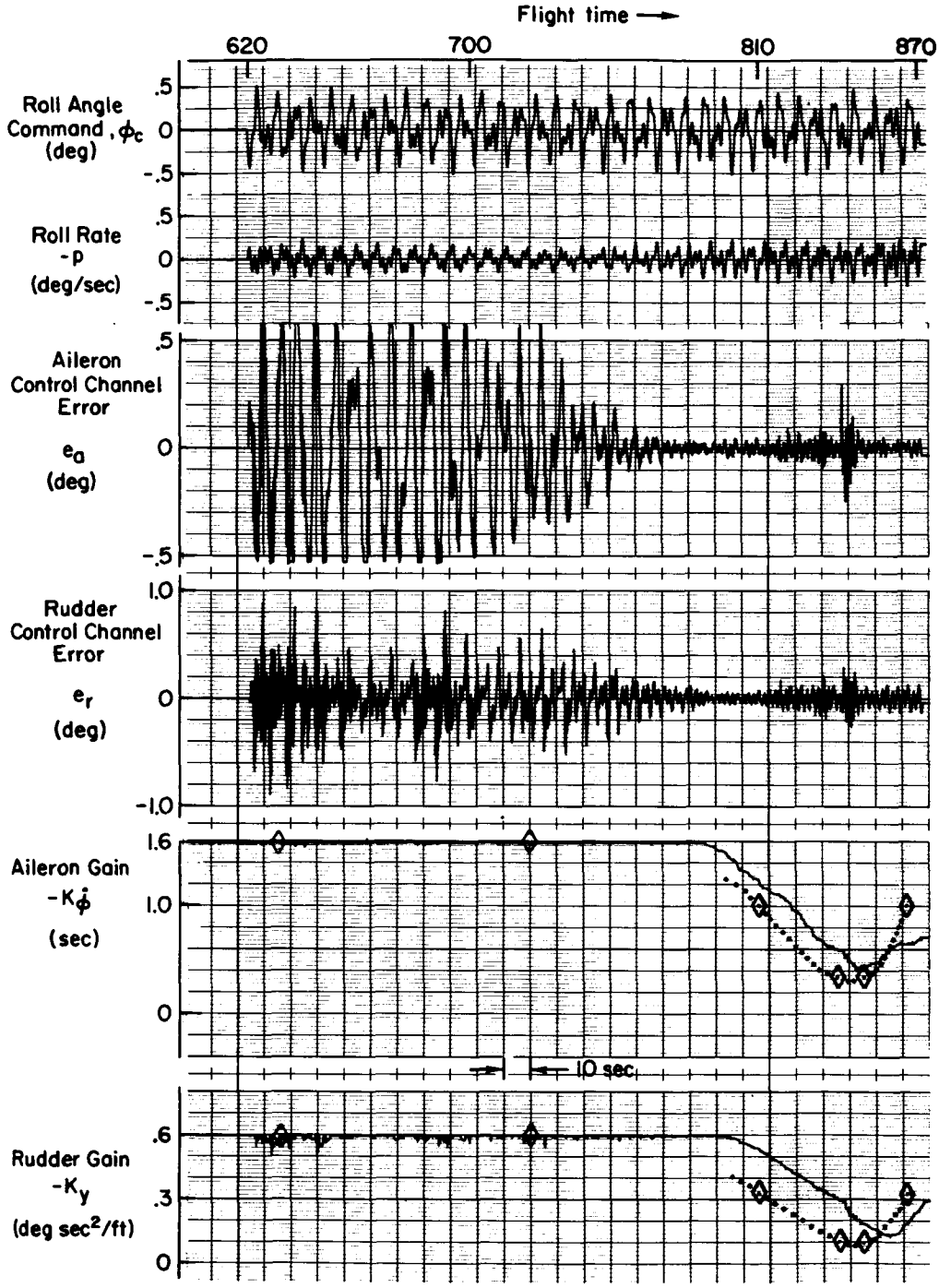

Figure 9. Real Time with Gaussian Roll Angle Command

surveys. Again referring to Fig. 9 we see overplotted on the gain traces, dotted curves which pass through the survey gain values indicated by the diamond symbol. These values, however, were based on a handling quality assessment and should not necessarily be taken to be the anticipated action of the adaptive system. Nevertheless the correspondence between the simulation result and the results of the surveys is remarkably good. Assuming that the surveys produced "optimum" gain schedules from a handling quality viewpoint (which was the desired objective, but was admittedly only approximately accomplished), it follows that the adaptive system tends to provide optimum handling qualities. The system performance objective has, therefore, been achieved.

Returning for a moment to the important matter of control effectiveness, it may be shown that the adaptive system provides a valuable function in this regard also. It has been pointed out that, while pilots can adapt their gains to compensate for gain variations of the controlled element, they prefer not to. Figure 10 shows comparisons between $|L'_{\delta_a}|$ and $|K_\phi L'_{\delta_a}|$ and between $|N'_{\delta_r}|$ and $|K_y N'_{\delta_r}|$. The objective here is to indicate that the range of gain variation of the unaugmented vehicle is considerably larger than the range of gain variation of the vehicle with adaptive augmentation. L'_{δ_a} and N'_{δ_r} are taken as measures of bare airframe gains and $K_\phi L'_{\delta_a}$ and $K_y N'_{\delta_r}$ are, of course, the corresponding gains when the augmenter is present and the pilot's inputs are used as augmenter commands. The aileron gain range is 10:1 without augmentation and about 3:1 with augmentation. In the (less important) case of the rudder path, the ranges are about 3.5:1 without augmentation and 1.3:1 with augmentation. Hence, the suppression of gain variation effects is helpfully great, about 3:1 in each case.

The last remaining item of concern is the effect on performance of including disturbance inputs. In this regard, certain limitations were imposed on the effort. A very simple gust model was used because only a limited amount of equipment was available for its implementation.

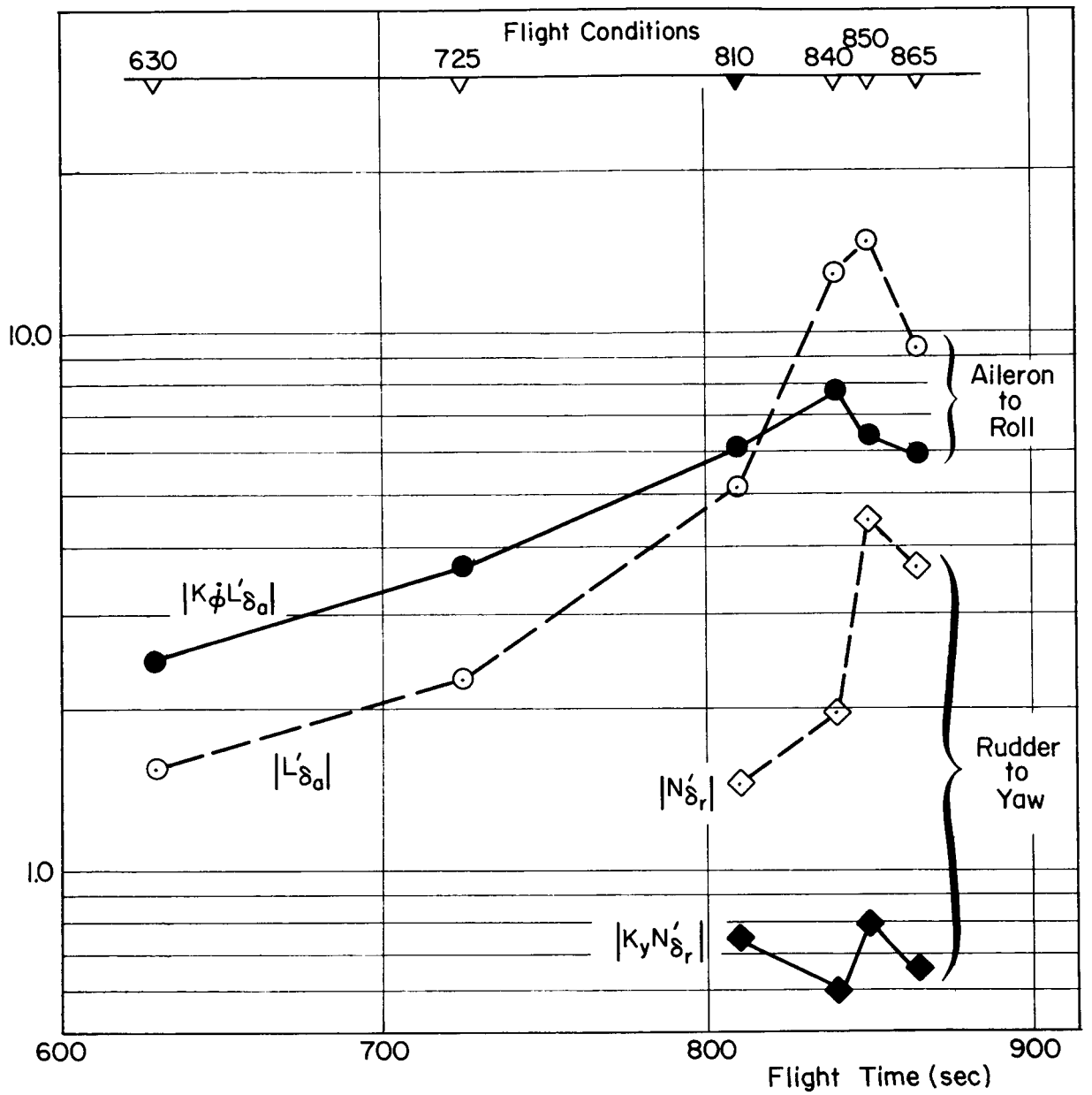

Figure 10. Reduction of Variation of Effective Controlled Element Gain

The gust characteristics were assumed invariant throughout the flight segment considered. This assumption is admittedly unrealistic because of the speed and altitude range through which the vehicle flies. Nevertheless, the assumption is not necessarily unconservative, and therefore does not place the results in question.

The second limitation imposed by practical considerations was that the disturbance input had to be correlated with the command input. The same input signal generator was used to produce the fundamental component of both forcing functions. Ideally, it would have been desirable to generate an independent gust disturbance, one which corresponded to known atmospheric turbulence models.

Figure 11 shows the effect on the $K_{\dot{\phi}}$ gain response of including the gust input. The system is forced by a square wave bank angle command and a quasi-random side gust, β_g. Both these time functions were used previously. The time segment is from 700 to 870 sec. The first 80 sec have been dropped from the record since no interesting information is lost by doing so and also so that the time scale may be expanded. Only the aileron gain $K_{\dot{\phi}}$ is shown in Fig. 10 although the K_y gain is also being adjusted adaptively.

For the purpose of comparison a second $K_{\dot{\phi}}$ trace is shown in Fig. 11 and is labeled "without gust present." This gain time history results in response to the application of the same bank angle command but without the gust disturbance input. There is little difference in the gain functions. Thus, for the disturbance used here, nearly optimum handling qualities, as previously defined, are still maintained.

As the level of disturbance is increased in relation to the command, the gains tend toward higher values. This is entirely proper from the viewpoint of minimizing the aileron and rudder control channel errors as they are defined. The model does not include disturbance effects so that the system attempts, with high gain, to suppress gust induced output motions. This is not at all undesirable and, in fact, can be

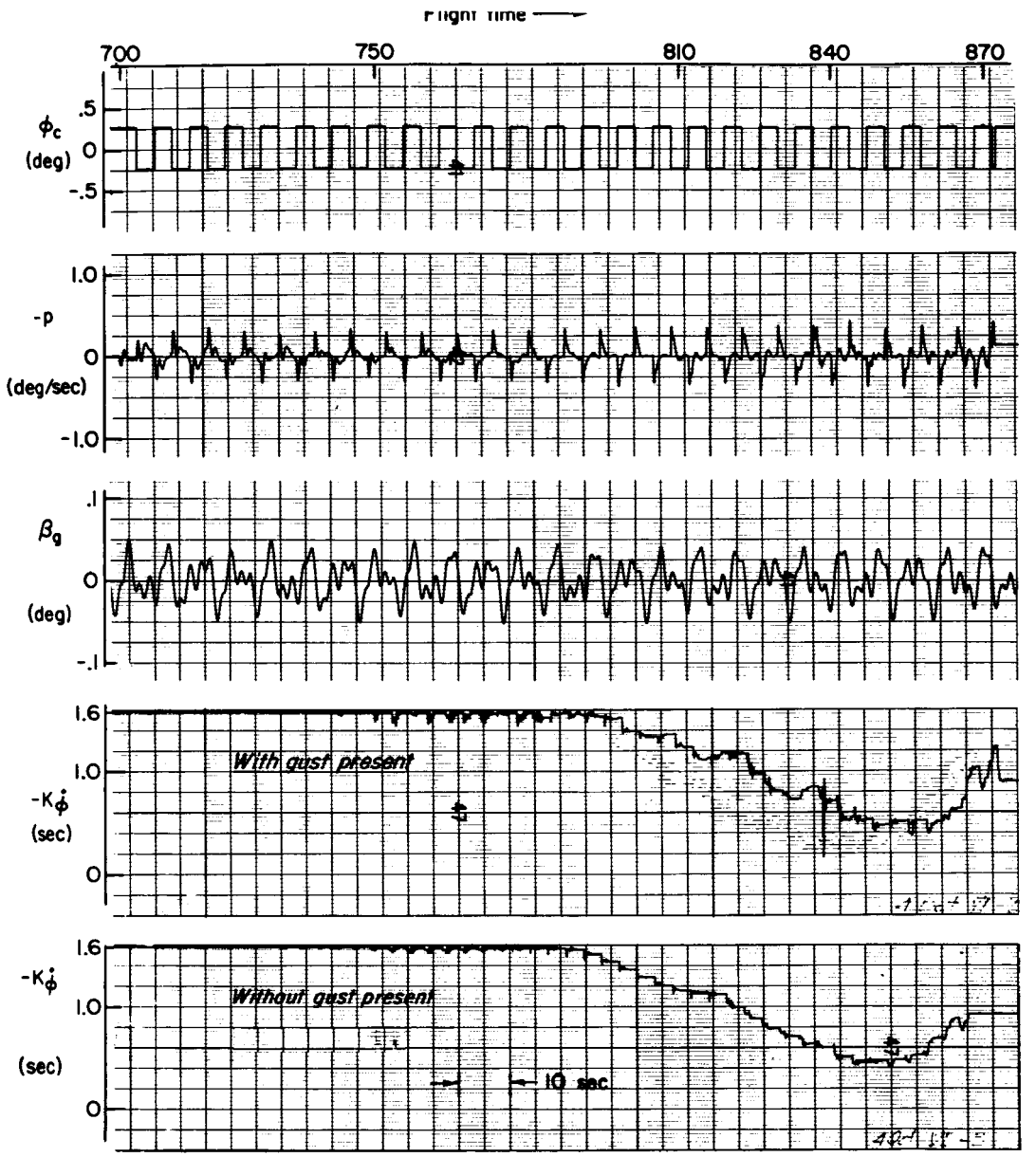

Figure 11. Real Time with φ_c and β_g Inputs

thought of as motivating, in part at least, the use of adaptive stability augmentation. That is, when and if a gusty environment is encountered, the adaptive system provides a means for increasing the gust suppressing function of the SAS by raising the gain. When the turbulence subsides the command-response transfer function characteristics are automatically reoptimized with lower gains. In a fixed or preprogrammed SAS configuration, the trade off between gust suppression and command-response characteristics must be made ab initio. When, as might occur, the two requirements lead to opposing controller specifications, the optimization is accomplished over the ensemble of anticipated gust environments and leads to the best average performance. An adaptive system, on the other hand, might be said to optimize performance for each particular flight environment.

The important points which have been made in this Section are:

- The gains will adjust rapidly and in an uncoupled fashion and when the vehicle and the vehicle model are nearly identical.
- Mismatch, while somewhat bothersome for very high adaptive gains, is easily accomodated for gains appropriate to the real-time adaptive problem.
- The adaptive system provides near optimum handling qualities as they were defined by the surveys.
- Disturbance inputs do not degrade operation of the adaptive system.

SECTION IV

SIMPLIFICATION OF THE SYSTEM

DIGITAL ADJUSTMENT LOGIC

A charge frequently leveled at adaptive systems is that they are overly complex. This seems to be especially true when no pressing need for the adaptive feature exists. Stability augmentation systems have, for some years, been designed for all kinds of aircraft, and have operated successfully, without the benefit of self-adjustment. Reference 17 perhaps provides the only imperative justification for the adaptive feature in flight control. Where the need does exist, and it may be that the manned lifting-body problem is one such application, the complexity of the proposed scheme actually seems modest in relation to the resulting benefits. Nevertheless, simplifications are always worth seeking. One simplification might be digital gain adjustment logic as an alternative to the more complex analog gain adjustment logic which exactly implements the theory described analytically in Section II. The all-analog system was, of course, the one investigated experimentally with the results presented in Section III.

The multiplier which weights the error signal for each adaptive gain provides the function specified by "×" in the general gain adjustment equation,

$$\dot{K} = A(\epsilon \times \frac{\partial e}{\partial K}) \tag{43}$$

where

$A \triangleq$ adaptive loop gain

$e \triangleq$ an error signal

$\partial e/\partial K \triangleq$ the error weighting signal for the gain K.

Equation 43 will be referred to as implementing the analog adjustment logic in distinction to the digital adjustment logic to be discussed next.

A gain adjustment law of the form

$$\dot{K} = A \operatorname{sgn}\left(e \frac{\partial e}{\partial K}\right) \tag{44}$$

suggests itself as an alternative to the analog adjustment law given by Eq 43. The symbol "sgn" indicates the signum function which is defined by

$$\operatorname{sgn}(x) = \begin{cases} -1 & x < 0 \\ 0 & x = 0 \\ +1 & x > 0 \end{cases} \tag{45}$$

Equation (44) is referred to as the digital adjustment logic. The gain rate, $\dot{K}$, will be plus or minus A depending on the sign of the product, $e \times \partial e/\partial K$ and zero when $e \times \partial e/\partial K$ is zero. Thus, for one thing, the dependency of the gain rate on input magnitude is removed. This itself might be a substantial advantage of the scheme. But a marked mechanizational simplification also results because of the identity

$$\operatorname{sgn}(xy) = \operatorname{sgn}(x)\operatorname{sgn}(y) \tag{46}$$

Thus it is not necessary to multiply e and $\partial e/\partial K$ since Eq 44 may now be written

$$\dot{K} = A \operatorname{sgn}(e)\operatorname{sgn}(\partial e/\partial K) \tag{47}$$

Now, the "sgn" operator represents an ideal relay so that this adjustment rule can be mechanized with electronic switches (fast relays) and AND gates. Figure 12 shows both the analog and the digital gain adjustment schemes. A typical electronic (quarter-square) multiplier

is shown since high bandwidth requirements dictate its use. The digital adjustment logic employs comparators to provide A/D conversion, AND gates to provide logic operations, and electronic switches to provide D/A conversion. Three summations and two inversions are required in the analog system while only one summation is required in the digital scheme. The hardware needed for the digital adjustment logic is considerably simpler and therefore probably more reliable than that needed for the analog adjustment logic.

In both mechanizational schemes some additional logic may be required for practical reasons. First, threshold is needed to washout low level d.c. signals which might otherwise tend to bias the gain in one direction or the other. It is also even likely, as we have seen, that, for very high adaptive gains a limit cycle will occur because of the closed loop nature of the adaptive scheme. In order to circumvent both these possibilities, threshold may be added to each scheme with two additional comparators.

The second additional logic function dictated by practical considerations is for limits on the range through which the adaptively set gains can vary. (The necessity for an upper limit was discussed in Section III.)

MODIFICATION TO STABILITY ANALYSIS

The fact is clear that the gain adjustment law given by Eq 47 results in a simpler system to mechanize. The important remaining question is, "How does such simplification affect the stability of the adapting gains and the errors?" We shall examine this point here. The simplified gain adjustment laws for our particular example are:

$$\begin{aligned} \dot{\Delta K}_{\dot{\phi}} &= -A_{\dot{\phi}} \operatorname{sgn}(\dot{\phi}_c - \dot{\phi}) \operatorname{sgn}(e_a) \\ \dot{K}_y &= -A_y \operatorname{sgn}(a_{c_c} - a_c) \operatorname{sgn}(e_r) \end{aligned} \tag{48}$$

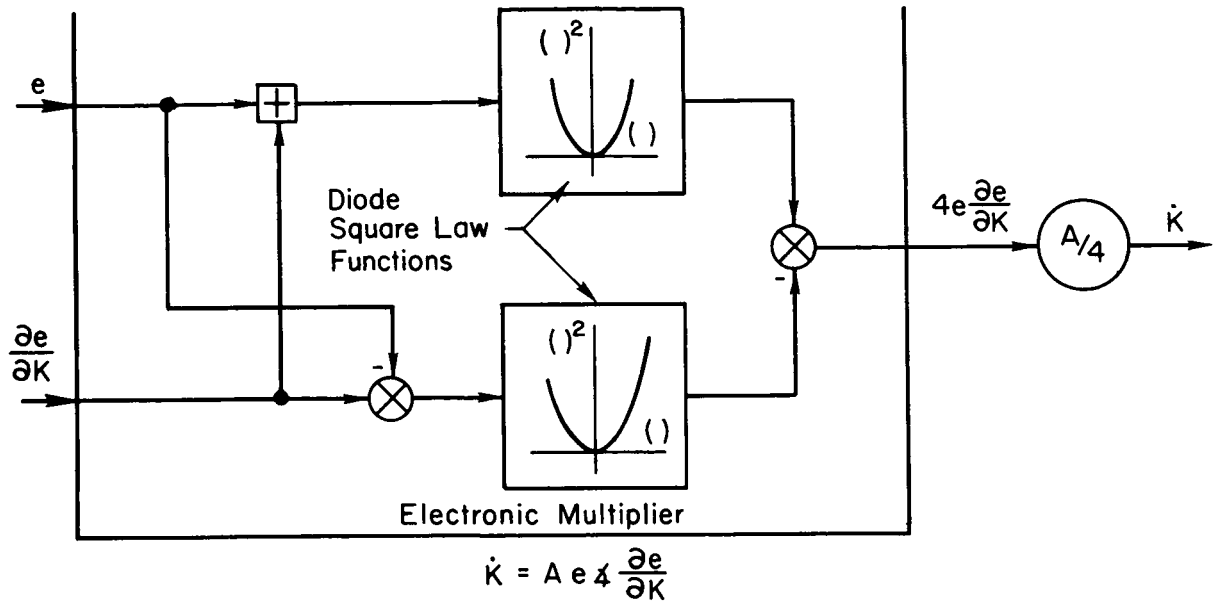

Analog Adjustment Logic

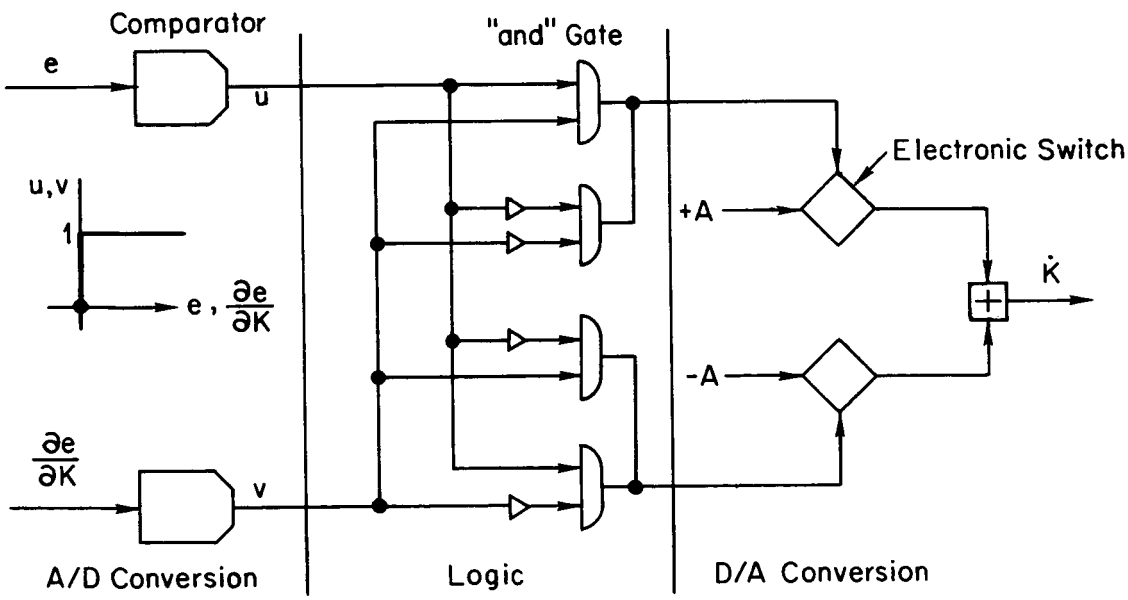

Digital Adjustment Logic

Figure 12. Comparison of Adjustment Schemes

Stability analysis here, as before in Section II, can be carried out only under the restrictions that there is no controlled element mismatch and that no disturbance inputs are acting. Equation 48 then reduces to

$$\begin{aligned} \dot{\Delta K}_{\dot{\phi}} &= -A_{\dot{\phi}} \operatorname{sgn} \Delta K_{\dot{\phi}} \operatorname{sgn}(\dot{\phi}_c - \dot{\phi})^2 \\ \dot{\Delta K}_y &= -A_y \operatorname{sgn} \Delta K_y \operatorname{sgn}(a_{c_c} - a_c)^2 \end{aligned} \tag{49}$$

The above equations each are stable, but not asymptotically stable. That is, $\Delta K_{\dot{\phi}}$ and ΔK_y do not diverge because the rate of change of each ΔK is either in the direction of the origin or is zero.

This describes system stability in terms of the gain deviations. While this is one interesting aspect of the problem, there is another which concerns us equally. We are interested in system stability in terms of the errors. In addition, we would like to know what criterion is implied. It is easy to verify that the criterion implied, assuming that Eq 49 represents a steepest descent law, is:

$$J = A_{\dot{\phi}} \left|\Delta K_{\dot{\phi}}\right| \operatorname{sgn}(\dot{\phi}_c - \dot{\phi})^2 + A_y \left|\Delta K_y\right| \operatorname{sgn}(a_{c_c} - a_c)^2 \tag{50}$$

This criterion is a positive definite function of f_a and f_r where

$$\begin{aligned} f_a &= \Delta K_{\dot{\phi}} \operatorname{sgn}(\dot{\phi}_c - \dot{\phi})^2 \\ f_r &= \Delta K_y \operatorname{sgn}(a_{c_c} - a_c)^2 \end{aligned} \tag{51}$$

since

$$\begin{aligned} e_a &= (\dot{\phi}_c - \dot{\phi})\Delta K_{\dot{\phi}} \\ e_r &= (a_{c_c} - a_c)\Delta K_y \end{aligned} \tag{52}$$

f_a and f_r have the property that they vanish if and only if the errors e_a and e_r, respectively, vanish. Thus the criterion is still one which

is implicitly a positive definite function of the errors. Stated in other words, the goal for system performance remains unchanged from the case where $J=(1/2)(A_{\dot{\phi}}\, e_a^2 + A_y\, e_r^2)$ was the criterion as in Section II. The shape of the criterion surface (as a function of f_a and f_r) is a time invariant inverted pyramid. See the sketch below.

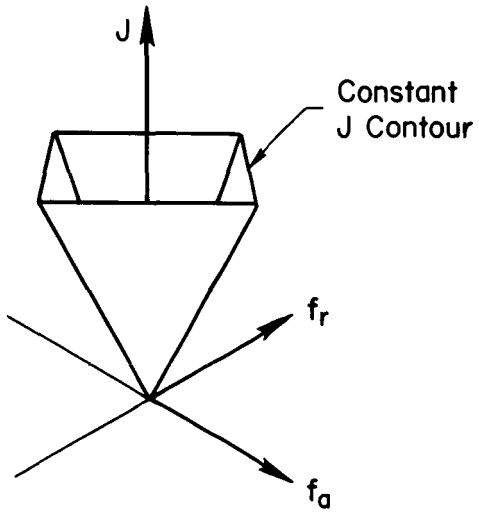

Criterion Surface

An additional relationship is:

$$J = -A_{\dot{\phi}}^2 \operatorname{sgn} \Delta K_{\dot{\phi}}^2 \operatorname{sgn}(\dot{\phi}_c - \dot{\phi})^2$$
$$-A_y^2 \operatorname{sgn} \Delta K_y^2 \operatorname{sgn}(a_{c_c} - a_c)^2 \qquad (53)$$

This shows that J is either always decreasing at a finite rate towards its lower bound, zero, or that J is zero. Thus if $\Delta K_{\dot{\phi}}$ and ΔK_y are finite, J will reach zero in a finite time interval. Since f_a and f_r vanish when J = 0, and the errors e_a and e_r vanish with f_a and f_r we are assured that the errors are asymptotically stable and that they will converge to zero values.

When controlled element mismatch and/or disturbance inputs are acting, the stability analysis for this simplified system is considerably complicated. This is even more so than in the case treated in Section II. Further conclusions with respect to the stability of this simplified system must be obtained experimentally.

The above discussion treats the exact behavior of derivatives of the sgn(·) function when (·) = 0 rather cavalierly. This detail is unimportant as a practical matter, however, because the sgn(·) function we have used is hardly an accurate model of an actual electronic switch or relay in the close vicinity of zeros of the switching function in any case. What is important is that the above equations do accurately describe the physical realization of the gain adjustment law outside the region of non-ideal equipment effects.

Some other observations are in order. It seems clear that the adaptive gains may tend to have a limit cycle about point $\Delta K_{\dot{\phi}} = \Delta K_y = 0$, and may tend to chatter about the lines $\Delta K_{\dot{\phi}} = 0$ and $\Delta K_y = 0$. The frequency and amplitude would be expected to be respectively infinite and zero,in theory. Actually, small lags introduced by non-ideal effects in equipment, the filters necessary in realization, and imperfect knowledge of the controlled element equations may produce a high but finite frequency limit cycle or chatter mode of low amplitude. This mode of behavior may or may not be unacceptable if it appears. It did not appear prominently in the simulation records to be discussed next.

SIMULATION RESULTS

The digital adjustment law was implemented in the aileron channel only,for the purpose of demonstrating its capabilities. A number of experiments were carried out and the key results will follow some brief prefatory remarks.

Unfortunately, the simulation did not correspond precisely with the theoretical development just given because we did not have enough

analog equipment available. Our objective was to show the feasibility of the concept rather than to evolve a final form for its implementation, and, with this in mind, certain shortcuts were taken.

First of all Eq 44 was used as the mechanizational basis rather than Eq 47 which provides the practical simplification of the system. So the multiplication, which is the function to be supplanted by the scheme, actually remained in the simulation. The output of the multiplier, $e_a(\partial e_a/\partial K_\phi)$, was processed by a three state relay to yield the pot rate signal $\dot{K}_\phi$. The sketch below shows the form of the simulation setup for the comparison between the analog adjustment logic and digital adjustment logic.

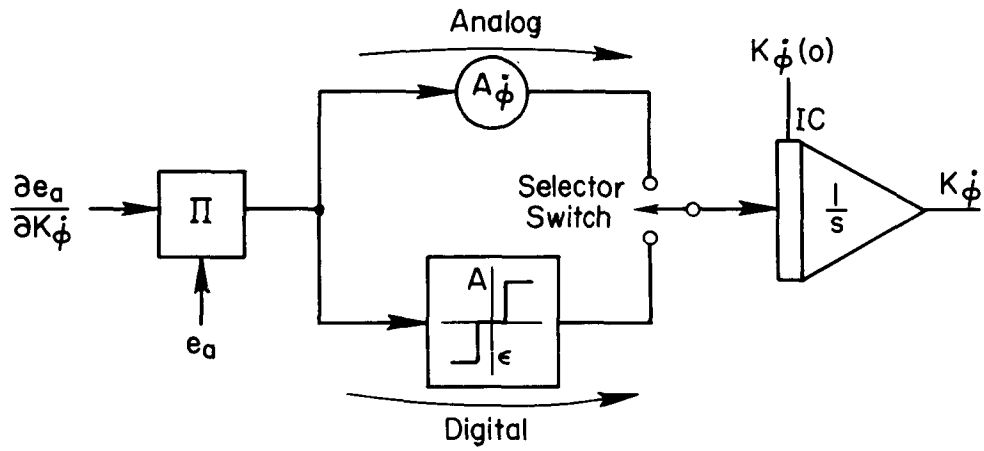

The analog scheme appears the simpler one here only because of the mechanization shortcut just described.

The three state relay used to approximate the signum function had deadzone width 2ϵ and amplitude levels $\pm A$. These parameters were set to values for which the behavior of the two adjustment laws is comparable. There may be more optimum values but for our purposes this was the approach adopted. It turned out that performance was not at all sensitive to ϵ and A over a large range of values. This somewhat surprising result was a fortuitous one. It should be pointed out as an aside, that, although only a symmetrical relay function was

considered, there may well be practical advantages to a non-symmetrical one in an actual application.

Figure 13 shows a comparison between the two mechanizations at flight condition 810 when a square wave roll command forces the system. The rudder path gain, K_y, is constant at its correct value. In part A of the figure the analog adaptive scheme is employed and in part B the digital adaptive logic scheme is used. The initial offsets are the same in each case. Notice that when the square wave first changes sign the system receives a double amplitude step and a large $K_{\dot{\phi}}$ adjustment is made by the analog adjustment logic. The digital adaptive logic at this same point only adjusts the gain the same amount that it did when the input started, impressing a single amplitude step upon the system. Thus the gain adjustment is sensitive to command level for the analog scheme and is insensitive for the digital logic scheme. This bears out our expectations in the light of Eq 43 and 47.

In both cases shown in Fig. 13, adjustment is satisfactory. While convergence may appear to be slow the adaptive gains are appropriate for the real time execution of the mission. The gain might, of course, be made much higher at this flight condition in agreement with the analytical proof of stability.

Figure 14 shows the behavior of the system with the digital adjustment logic during 170 seconds of the mission. The approximately Gaussian roll angle command is used here. The rudder loop gain is being set by the analog adjustment scheme as it was previously. Overplotted on the $K_{\dot{\phi}}$ trace is a dotted curve which represents, according to the surveys (Appendix A), the optimum handling qualities gain trajectory. The actual gain is even closer to the ideal gain than it was in the original scheme (see Fig. 9). The error, e_a, is also smaller. So, it turns out, the digital adjustment scheme is not only simpler but it seems to give better overall performance, at least in this ideal case of no disturbance input. The simple digital gain

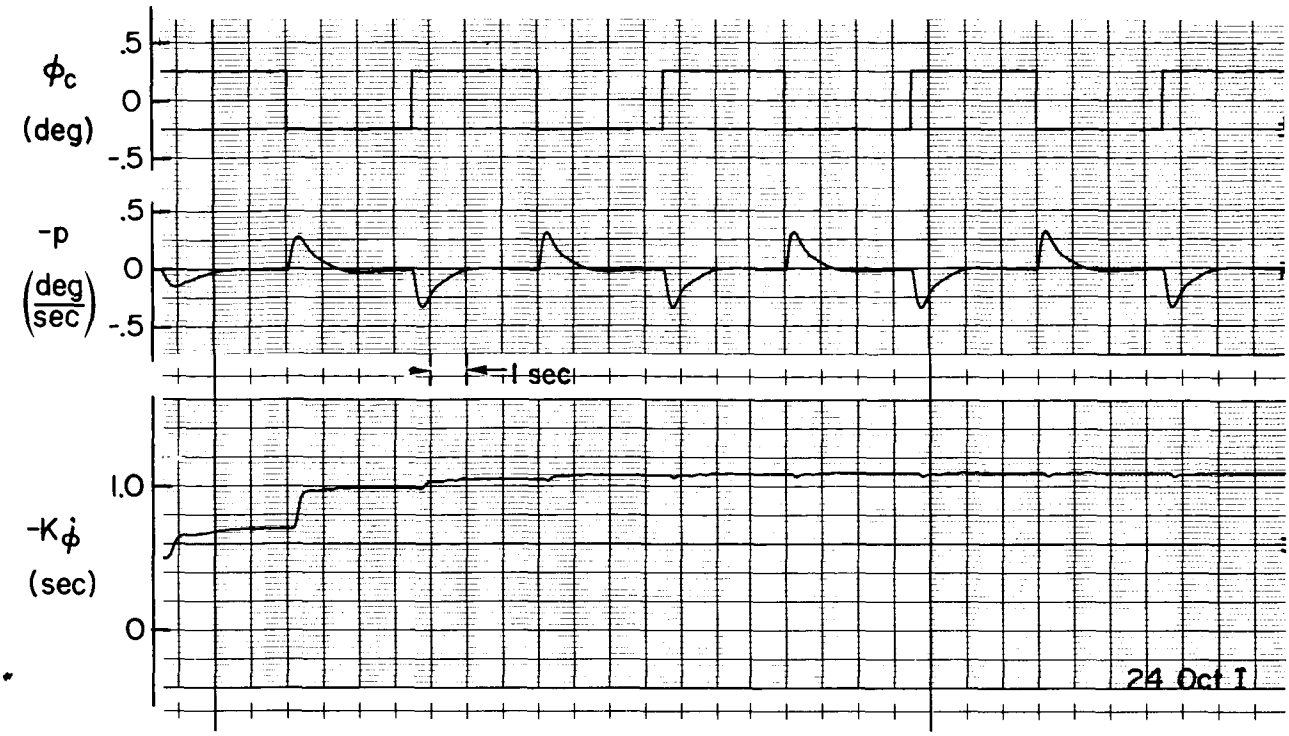

a) Analog Adaptive Logic

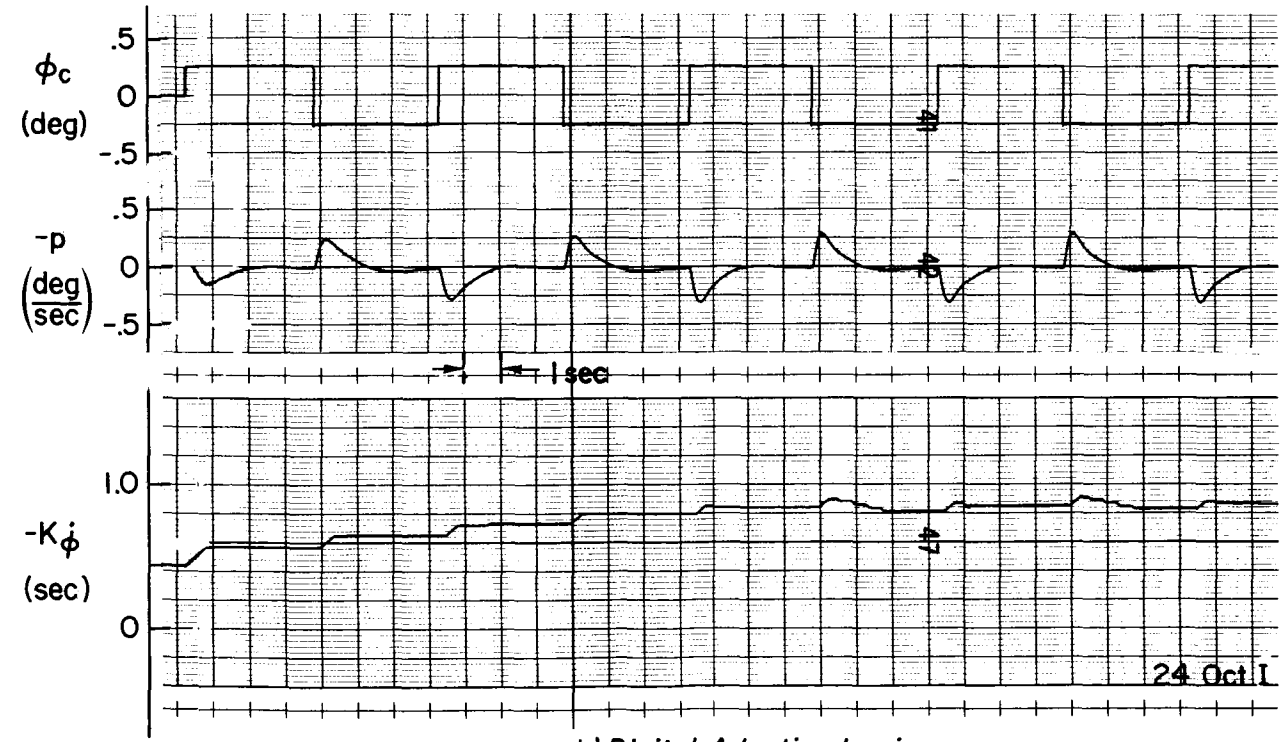

b) Digital Adaptive Logic

Figure 13. Comparison of Gain Adjustment Laws

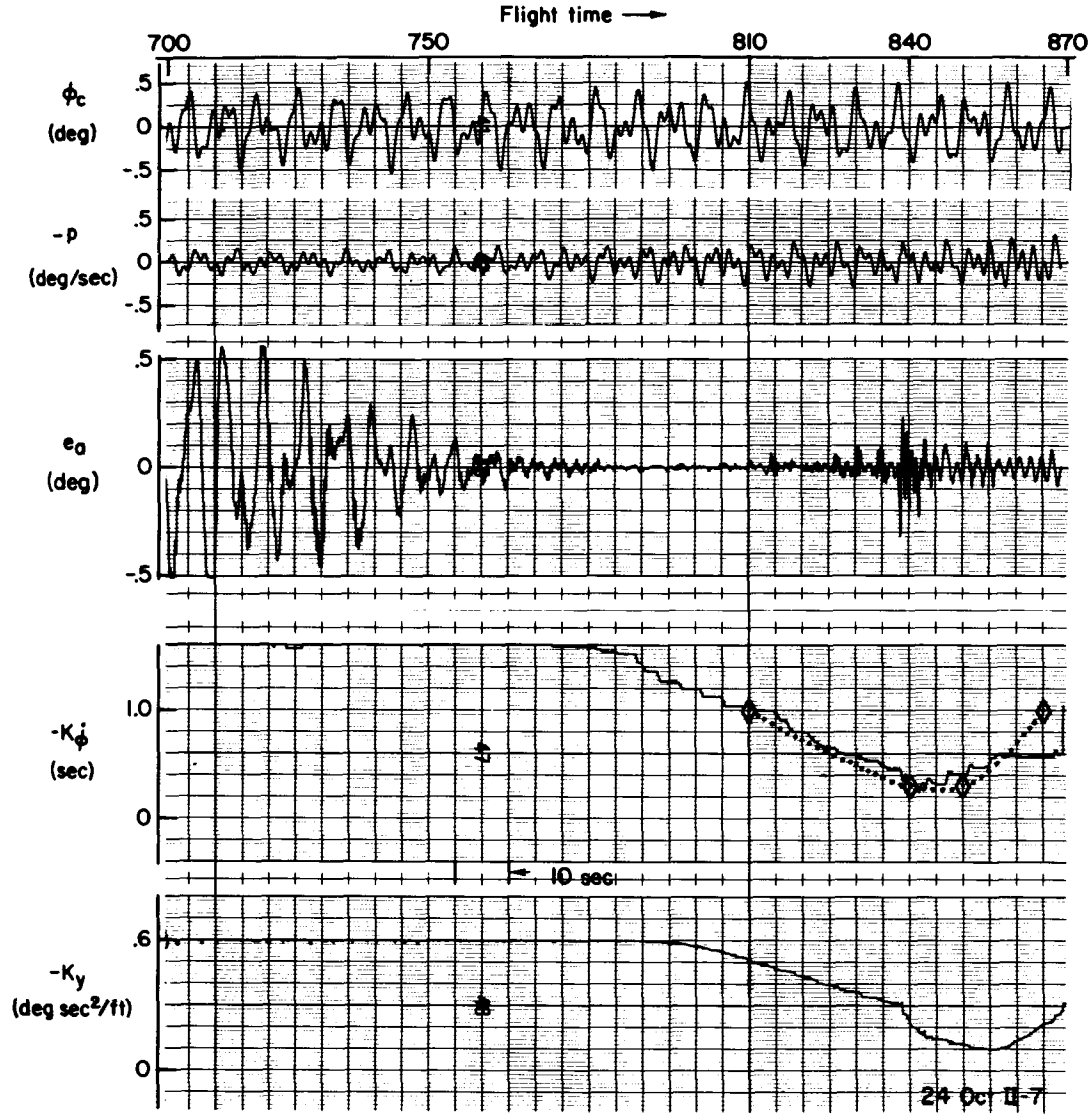

Figure 14. Real Time with Digital Adjustment Logic Setting $K_{\dot{\varphi}}$

adjustment logic is indeed an attractive way to mechanize the adaptive control function technique.

In summary, the following items have been discussed in this section.

- An attractively simple mechanization is possible.
- It is flexible as well as simple.
- Desirable stability properties exist in the ideal case.
- Simulation shows that overall performance may well be enhanced by digital gain adjustment logic.

SECTION V

CONCLUSIONS AND RECOMMENDATIONS

The research reported herein has led to a general procedure for constructing adaptive control systems appropriate for linear, multi-control point controlled elements. The adaptive control function technique, as it is called, can be mechanized with a very modest amount of equipment. The system is especially remarkable in this respect when applied to multi-control point problems. We have shown how modifications, necessary for mechanizing the system with real physical devices, should be incorporated into the design. Aspects of these modifications which allow us to further reduce system complexity have been discussed. An alternative adaptive gain adjustment law has been developed which renders the adaptive gain adjustments independent of the input level, and to some extent, further simplifies the system mechanization. The adaptive gain adjustment responses have been proven to be stable under certain ideal conditions.

Simulation of an adaptive lateral stability augmentation system for a hypothetical manned, lifting-body,entry vehicle has demonstrated application of the adaptive control function technique to a difficult flight control problem. The adaptive control function system was shown to be capable of providing a speed of adaptation well in excess of that required for this application. The system was also shown to operate properly in the face of disturbance inputs.

Two recommendations for further research and application are as follows. Additional theoretical research on the stability of adaptive control function systems might succeed in treating "non-ideal" cases wherein there is controlled element-controlled element model mismatch and/or there are disturbance inputs acting. This possibility should be pursued. The second recommendation is that the adaptive

control function technique be put to an actual flight test. In view of the modest equipment requirement for these adaptive systems, it appears feasible to perform such a test at low cost by utilizing an existing variable stability aircraft having general purpose analog computation equipment aboard.

REFERENCES

1. Lang, G., J. M. Ham, "Conditional Feedback Systems,—A New Approach to Feedback Controls," AIEE Trans., Vol. 74, July 1955.

2. Whitaker, H. P., J. Yamron, A. Kezer, Design of Model-Reference Adaptive Control Systems for Aircraft, Report R-164, Massachusetts Institute of Technology, Instrumentation Laboratory, September 1958.

3. Osburn, P. V., H. P. Whitaker, A. Kezer, New Developments in the Design of Model Reference Adaptive Control Systems, IAS Paper No. 61-39, presented at the IAS 29th Annual Meeting, New York, New York, January 23-25, 1961.

4. Graupe, K. K., "The Analog Solution of Some Functional Analysis Problems," Trans. AIEE Communications and Electronics, pp. 793-799, January 1961.

5. Potts, T. F., G. N. Ornstein, A. B. Clymer, The Automatic Determination of Human and Other System Parameters, presented at the Western Joint Computer Conference, Los Angeles, 1961.

6. Miller, B. J., A General Method of Computing System Parameters with an Application to Adaptive Control, AIEE Winter General Meeting, New York, New York, January 28-February 2, 1962.

7. Hofmann, L. G., P. M. Lion, J. J. Best, Theoretical and Experimental Research on Parameter Tracking Systems, NASA CR-452, April 1966.

8. Rucker, R. A., Real Time System Identification in the Presence of Noise, Western Electronic Show and Convention, 1963.

9. McRuer, D. T., I. L. Ashkenas, H. R. Pass, Analysis of Multiloop Vehicular Control Systems, ASD-TDR-62-1014, March 1964.

10. Shipley, P. P., A. G. Engel, Jr., J. W. Hung, Self-Adaptive Flight Control by Multivariable Parameter Identification, AFFDL-TR-65-90, August 1965.

11. Ashkenas, I. L., D. T. McRuer, "Optimization of the Flight Control Airframe System," J. Aerospace Sci., Vol. 27, no. 3, March 1960.

12. Ashkenas, I. L., D. T. McRuer, "A Theory of Handling Qualities Derived from Pilot-Vehicle System Considerations," Aerospace Eng. Rev., Vol. 21, no. 2, February 1962.

13. Kezer, A., L. G. Hofmann, A. G. Engel, Jr., Applications of Model-Reference Adaptive Control Techniques to Provide Improved Bending Response of Large Flexible Missiles, Massachusetts Institute of Technology, Instrumentation Laboratory, E-1042, June 1961.

14. Whitaker, H. P., "Massachusetts Institute of Technology Presentation," Proceedings of the Self Adaptive Flight Control Systems Symposium, WADC-TR-59-49, 13-14 January 1959, pp. 58-78.

15. Anderson, G. W., R. N. Buland, G. R. Cooper, "The Aeronutronic Self-Optimizing Automatic Control System," Proceedings of the Self Adaptive Flight Control Systems Symposium, WADC-59-49, 13-14 January 1959, pp. 349-408.

16. Hofmann, L. G., J. J. Best, Lateral SAS Surveys for a Manned Lifting Entry Vehicle, Systems Technology, Inc., WP-172-1, 7 March 1967.

17. Ashkenas, I. L., D. T. McRuer, Competing Flight Control Systems for Entry Glider Lateral Control, ASD-TDR-62-699, February 1964.

18. Letter to Mr. Lee Gregor Hofmann, Systems Technology, Inc., from Mr. Floyd L. Thompson, NASA/Langley Research Center, 14 December 1966.

19. Stapleford, R. L., J. A. Tennant, Lateral-Phugoid Mode Effects on Airplane Handling Qualities, Section III, AFFDL-TR-67-2, June 1967.

20. Ashkenas, I. L., D. T. McRuer, Determination of Lateral Handling Quality Requirements from Airframe-Human Pilot System Studies, WADC-TR-59-135, June 1959.

21. Ashkenas, I. L., D. T. McRuer, Approximate Airframe Transfer Functions and Application to Single Sensor Control Systems, WADC-TR-58-82, June 1958.

22. Stapleford, R. L., D. E. Johnston, G. L. Teper, and D. H. Weir, Development of Satisfactory Lateral-Directional Handling Qualities in the Landing Approach, NASA CR-239, July 1965.

23. McRuer, D., D. Graham, E. Krendel, and W. Reisener, Jr., Human Pilot Dynamics in Compensatory Systems, Theory, Models, and Experiments with Controlled Element and Forcing Function Variations, AFFDL-TR 65-15, July 1965.

APPENDIX A

HYPOTHETICAL, MANNED, LIFTING-BODY ENTRY VEHICLE; BASIC DATA AND SYSTEMS SURVEYS

In this Appendix, we summarize the basic vehicle data, for lateral handling qualities considerations, at six flight conditions which encompass the critical phase of the entry trajectory. Next, a handling qualities assessment is made to identify the particular problems characteristic of the unaugmented vehicle. This leads in a natural way to the evolution of a stability augmentation system (SAS). Before delving into the details of the SAS, however, a review of the multiloop analysis procedure, necessary for analyzing this problem efficiently, is accomplished. Following this, a basic SAS configuration is evolved by considering, on a competitive basis, the various ways in which the handling qualities problems may be eliminated by SAS design. Finally, the problem constraints which require that certain SAS parameters be adaptive will be stated.

BASIC DATA

The lateral transfer functions used herein are based on the following Laplace transformed aircraft equations of motion for body-fixed axes,

$$\begin{bmatrix} s - Y_v & \dfrac{-sW_o - g\cos\theta_o}{V_{T_o}} & \dfrac{sU_o - g\sin\theta_o}{V_{T_o}} \\ L'_\beta & s(s - L'_p) & -L'_r \\ -N'_\beta & -sN'_p & (s - N'_r) \end{bmatrix} \begin{Bmatrix} \beta \\ \dfrac{p}{s} \\ r \end{Bmatrix} = \begin{Bmatrix} Y^*_\delta \\ L'_\delta \\ N'_\delta \end{Bmatrix} \delta \quad \text{(A-1)}$$

where δ can be either δ_a or δ_r.

Additional variables are given by:

$$\dot{\Phi} = p + r \tan \theta_o \tag{A-2}$$

$$\dot{\Psi} = \frac{r}{\cos \theta_o} \tag{A-3}$$

$$a_y = V_{T_o}(Y_v\beta + Y_\delta^*\delta) = V_{T_o}\dot{\beta} - W_o p + U_o r - g \cos \theta_o \varphi \tag{A-4}$$

$$a_y' = a_y + l_x \dot{r} - l_z \dot{p} \tag{A-5}$$

Numerical values of reference dimensions, inertias, dimensionless stability derivatives and transfer function factors for all flight conditions considered in the system surveys are summarized in the following tables.

TABLE A-1

REFERENCE DIMENSIONS AND INERTIAS

(Ref. 18)

Parameter	Units	Flight Condition (Time in seconds)					
		630	725	810	840	850	865
S	ft^2	150.	same				
b	ft	15.	same				
U_o	ft/sec	6070	3250	1750	1150	940	687
W_o	ft/sec	3500	2320	419	331	342	134
m	slugs	200	same				
I_x	10^3 slug-ft^2	1.0	same				
I_z	10^3 slug-ft^2	5.0	same				
I_{xz}	10^3 slug-ft^2	0.3	same				
θ_o	deg	34	33	-8	-12	-7	-17
α_o	deg	30	35.5	13.5	16	20	11

TABLE A-2

DIMENSIONLESS STABILITY DERIVATIVES

(Ref.18)

Parameter	Flight Condition (Time in seconds)					
	630	725	810	840	850	865
C_{y_β}	-0.6	-0.8	-0.8	-1.1	-1.2	-0.9
C_{y_p}	0.0	same				
C_{y_r}	0.0	same				
$C_{y_{\delta_a}}$	0.0	same				
$C_{y_{\delta_r}}$	0.0	0.0	0.04	0.04	0.04	0.04
C_{l_β}	-0.07	-0.09	-0.04	-0.17	-0.20	-0.20
C_{l_p}	-0.07	-0.09	-0.12	-0.20	-0.20	-0.20
C_{l_r}	0.2	same				
$C_{l_{\delta_a}}$	-0.008	-0.008	-0.012	-0.023	-0.030	-0.034
$C_{l_{\delta_r}}$	0.0	0.0	0.007	0.008	-0.02	-0.03
C_{n_β}	0.04	0.04	-0.02	0.12	0.18	0.22
C_{n_p}	0.1	same				
C_{n_r}	-0.2	-0.2	-0.3	-0.5	-0.6	-0.6
$C_{n_{\delta_a}}$	0.0	0.0	-0.002	0.002	-0.002	-0.022
$C_{n_{\delta_r}}$	0.0	0.0	-0.019	-0.020	-0.04	-0.06

TABLE A-3

DIMENSIONAL STABILITY DERIVATIVES

Parameter	Units	Flight Condition (Time in seconds)					
		630	725	810	840	850	865
Y_v	sec^{-1}	- .00546	- .0187	- .0615	- .168	- .189	- .111
$Y^*_{\delta_a}$	sec^{-1}	0	0	0	0	0	0
$Y^*_{\delta_r}$	sec^{-1}	-7.80×10^{-6}	-4.68×10^{-6}	.00308	.00610	.00630	.00493
L'_β	sec^{-2}	-13.2	-25.0	-17.4	-90.8	-91.1	-49.3
L'_p	sec^{-1}	- .0134	- .0450	- .201	- .678	- .700	- .548
L'_r	sec^{-1}	.0392	.101	.321	.594	.592	.464
L'_{δ_a}	sec^{-2}	- 1.56	- 2.28	- 5.13	-12.8	-14.5	- 9.32
L'_{δ_r}	sec^{-2}	- .00188	- .00625	2.48	3.79	-10.8	- 8.86
N'_β	sec^{-2}	.741	.742	- 2.71	7.70	11.6	8.44
N'_p	sec^{-1}	.00330	.00782	.0226	.0280	.0289	.0226
N'_r	sec^{-1}	- .00584	- .0150	- .0846	- .308	- .390	- .305
N'_{δ_a}	sec^{-2}	- .0935	- .137	- .474	- .547	- 1.06	- 1.70
N'_{δ_r}	sec^{-2}	.000105	.000185	- 1.43	- 1.96	- 4.43	- 3.64

TABLE A-4

EXACT TRANSFER FUNCTION FACTORS:
CHARACTERISTIC AND AILERON NUMERATOR

Parameter	Flight Condition (Time in seconds)					
	630	725	810	840	850	865
	$\Delta = \underbrace{(s + 1/T_s)\ (s + 1/T_R)}\ (s^2 + 2\zeta_d\omega_d s + \omega_d^2)$ or $s^2 + 2\zeta_1\omega_1 s + \omega_1^2$					
$1/T_s$ (ζ_1)	(.49)	(.51)	(-.16)	.0679	.0611	.0843
$1/T_R$ (ω_1)	(.0061)	(.0135)	(.165)	.285	.365	.360
ζ_d	.0035	.0084	.17	.070	.066	.062
ω_d	2.69	3.89	1.20	5.71	6.49	4.21
	$N^{\varphi}_{\delta_a} = A\varphi\ \underbrace{(s^2 + 2\zeta_\varphi\omega_\varphi s + \omega_\varphi^2)}$ or $(s + 1/T_{\varphi_1})\ (s + 1/T_{\varphi_2})$					
$A\varphi$	-1.62	-2.37	5.06	-12.6	-14.4	-8.80
ζ_φ $(1/T_{\varphi_1})$	.006	.014	(-.936)	.076	.076	.059
W_φ $(1/T_{\varphi_2})$	1.33	1.60	(1.11)	3.26	4.07	4.13
	$N^{r}_{\delta_a} = A_r\ (s + 1/T_{r_1})\ \underbrace{(s^2 + 2\zeta_r\omega_r s + \omega_r^2)}$ or $(s + 1/T_{r_1})\ (s + 1/T_{r_2})$					
A_r	-.0935	-.137	-.474	-.547	-1.06	-1.70
$1/T_{r_1}$	.00763	.0116	.076	.0950	.0933	.230
ζ_r $(1/T_{r_2})$	.0093	.02	(-1.46)	.081	.064	.065
ω_r $(1/T_{r_3})$	3.57	4.66	(1.89)	8.66	9.24	4.27

TABLE A-4 (Continued)

RUDDER NUMERATOR FACTORS

Parameter	Flight Condition (Time in seconds)					
	630	725	810	840	850	865
	$N^{r}_{\delta_r} = A_r \left(s + 1/T_r\right) \left(s^2 + 2\zeta_r\omega_r s + \omega_r^2\right)$					
A_r	0	0	-1.43	-1.96	-4.43	-3.64
$1/T_r$			.0761	.0950	.0933	.231
ζ_r			.034	.073	.067	.065
ω_r			2.27	4.59	6.39	3.65
	$N^{a_{y'}}_{\delta_r} = A_{ay'} \left(s + 1/T_{y'_1}\right) \left(s + 1/T_{y'_2}\right) \left(s^2 + 2\zeta_{y'}\omega_{y'}s + \omega_{y'}^2\right)$					
$A_{ay'}$	0	0	-.00891	-.315	-10.9	-10.7
$1/T_{y'_1}$			-.0206	-.0162	-.242	-.117
$1/T_{y'_2}$			.131	.388	.350	.455
$\zeta_{y'}$			-.11	-.058	.054	.031
$\omega_{y'}$			164.	40.3	6.96	5.06
	$N^{a_{y''}}_{\delta_r} = A_{ay''} \left(s + 1/T_{y''_1}\right) \left(s + 1/T_{y''_2}\right) \underbrace{\left(s^2 + 2\zeta_{y''}\omega_{y''}s + \omega_{y''}^2\right)}$ or $\left(s + 1/T_{y''_3}\right) \left(s + 1/T_{y''_4}\right)$					
$A_{ay''}$	0	0	.705	.665	-8.68	-8.88
$1/T_{y''_1}$			-.0208	-.0163	-.269	-.124
$1/T_{y''_2}$			.132	.400	.380	.472
$\zeta_{y''}\left(1/T_{y''_3}\right)$			(-18.0)	(-25.8)	.051	.028
$\omega_{y''}\left(1/T_{y''_4}\right)$			(18.6)	(28.6)	7.10	5.30

TABLE A-4 (Concluded)

RUDDER NUMERATOR AND COUPLING NUMERATOR FACTORS

Parameter	Flight Conditions (Time in seconds)					
	630	725	810	840	850	865
	$N^{\varphi}_{\delta_r} = A_\varphi \underbrace{(s^2 + 2\zeta_\varphi\omega_\varphi s + \omega_\varphi^2)}$ or $(s + 1/T_{\varphi_1})(s + 1/T_{\varphi_2})$					
A_φ	0	0	2.68	4.21	-10.2	-7.75
ζ_φ $(1/T_{\varphi_1})$			(-3.35)	(-5.61)	.064	.057
ω_φ $(1/T_{\varphi_2})$			(3.31)	(5.70)	6.81	5.51
	$N^{\varphi a_y'}_{\delta_a \delta_r} = B (s^2 + 2\zeta_B\omega_B s + \omega_B^2)$					
B	0	0	4.97	12.9	114.	42.8
ζ_B			-.0073	-.035	-.0035	-.017
ω_B			13.6	17.5	8.08	4.42
	$N^{\varphi a_y''}_{\delta_a \delta_r} = D \underbrace{(s^2 + 2\zeta_D\omega_D s + \omega_D^2)}$ or $(s + 1/T_{D_1})(s + 1/T_{D_2})$					
D	0	0	.721	-.645	87.6	33.3
ζ_D $(1/T_{D_1})$			-.024	(-65.8)	-.0065	-.021
ω_D $(1/T_{D_2})$			35.7	(93.1)	9.22	5.01
	$N^{\varphi\ r}_{\delta_a \delta_r} = C (s + 1/T_C)$					
C	0	0	8.5	27.1	52.8	18.9
$1/T_C$			.0636	.135	.158	.0685

LATERAL HANDLING QUALITIES DEFICIENCIES

In this subsection, we examine critically the lateral handling qualities of the unaugmented vehicle. This is a necessary prelude to intelligent design of the SAS.

Roll Damping

The low frequency roots of the characteristic equation couple, resulting in the so called "lateral phugoid"* at flight condictions 630, 725 and 810. See Table A-4. The lateral phugoid is the result of low roll damping and large effective dihedral. Because of its low frequency this mode is not considered to be particularly troublesome. It is effectively the same as two roots at the origin insofar as its effect in the crossover region on the closed-loop control of the vehicle is concerned.

At flight conditions 840, 850 and 865 the low frequency roots are typical for stable spiral and roll subsidence modes. However, the roll damping is quite low.

A roll damper will clearly be a necessary part of the SAS. For this purpose we will use a $\dot{\phi}$ to δ_a feedback. The convention for this reads $\dot{\phi} \longrightarrow \delta_a$. $\dot{\phi}$ will be assumed obtainable from a vertical gyro operating in the free mode during entry. Derived rate will be used.

ω_ϕ/ω_d Effects

$(\omega_\phi/\omega_d)^2$ is summarized in the following table.

*The handling qualities implications of the lateral phugoid mode effects are treated in Ref. 19.

TABLE A-5

ω_φ/ω_d EFFECTS—UNAUGMENTED AIRCRAFT

FLT. COND.	$(\omega_\varphi/\omega_d)^2$	COMMENTS
630	0.245	Too small
725	0.169	Very small
810	-0.840	N.G., Roll reversal
840	0.325	Too small
850	0.394	Too small
865	0.940	Okay

When the dutch roll is very lightly damped, as here, Ref. 17 indicates as desirable $1.0 > (\omega_\varphi/\omega_d)^2 > 0.5$ in order to avoid roll rate reversals. Only the 865 flight condition meets this criterion. Even at 865 the situation is not entirely acceptable because the combination of very low dutch roll damping and very small ω_φ—ω_d separation will mean that a roll damping closure will not produce sufficient dutch roll damping. This is acceptable for aileron inputs because of the small dutch roll modal response coefficients for the dutch roll mode but will probably not be adequate for gust (β_g) because the modal response coefficients for the dutch roll mode then tend to be larger.

An additional means for increasing dutch roll damping must be found. This might be crossfeed, or feedback of yaw rate, sideslip, or lateral acceleration to the rudder. Of the other flight conditions, only in the case of 810, 840 and 850 can ω_φ/ω_d be changed by means other than the roll damper, e.g., by feeding back sideslip angle to rudder, because there is no rudder effectiveness at flight conditions 630 and 725.

Other ω_φ/ω_d related problems also exist. Notice that the dutch roll frequency or stiffness is low at flight condition 810. See Table A-4. This results from negative yawing moment due to sideslip.

For good handling qualities, the dutch roll frequency should be 3.0 to 5.0 rad/sec. The requirement to stiffen the dutch roll practically can only be met by feedback to rudder.

Still another problem exists at flight condition 810. This is the so-called roll reversal indicated by the negative $(\omega_\varphi/\omega_d)^2$ ratio in Table A-5. This too, is the result of negative yawing moment due to sideslip. Possible fixes for this problem are aileron-to-rudder crossfeed or feedback of lateral acceleration or sideslip to rudder.

MULTILOOP ANALYSIS

Lateral aircraft dynamics pose a two control point problem, i.e., both rudder and aileron control inputs are possible. To develop maximum insight to this moderately complex control problem we must use the most efficient analytical tools available. In this case, the multiloop analysis technique reported in Ref. 9 is particularly appropriate. Without resorting to proofs or consideration of the general problem, results which are useful for the problem at hand are summarized below and related to the aircraft equations of motion.

Our objective is to analyze the dynamic characteristics of the closed-loop lateral control system in Fig. A-1. The inputs to the unagumented aircraft, A/C, are denoted by δ_a (<u>actual</u> aileron surface deflection) and δ_r (<u>actual</u> rudder surface deflection). The outputs which concern us are the roll angle, φ, and some other motion quantity such as yaw rate, r, or lateral acceleration, a_y', which we shall denote in general by q.

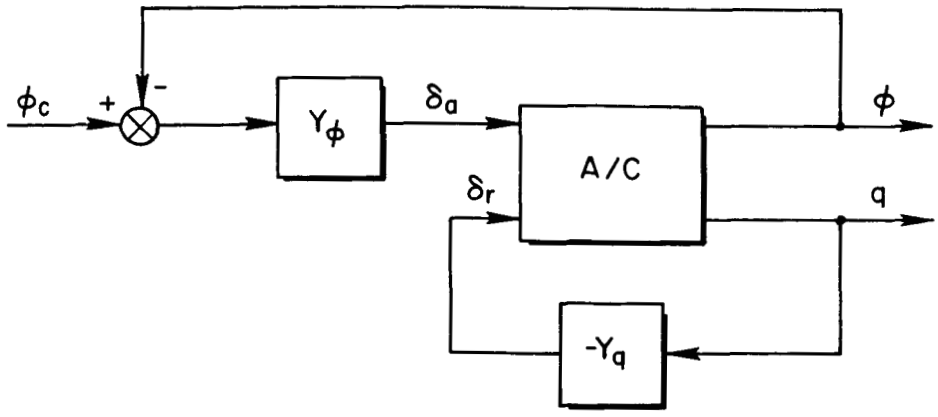

Figure A-1. Lateral Aircraft Closed-Loop Control System

The controllers, G_φ and G_q, include the servo transfer functions and compensation. The controllers include the human pilot as well as electromechanical functions of the SAS.

The first step is to develop the open-loop transfer function from $\delta_a \rightarrow \varphi$, with the $q \rightarrow \delta_r$ loop closed, from first principles of servo-analysis. In Fig. A-2, Δ is the characteristic polynomial of the Laplace

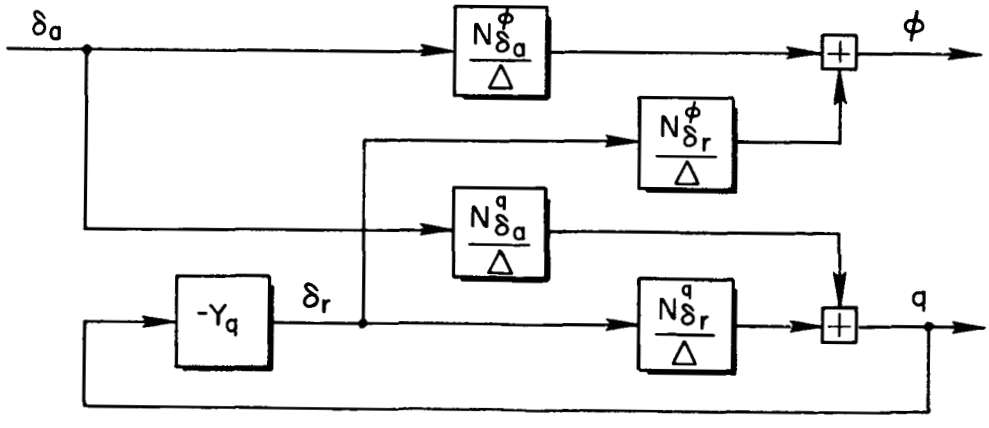

Figure A-2. Effect of Inner Loop Closure on Aircraft Dynamics

transformed aircraft equations of motion. $N^{\varphi}_{\delta_a}$, for example, is a numerator polynomial which, together with Δ in $N^{\varphi}_{\delta_a}/\Delta$ forms the transfer function for the unaugmented aircraft from δ_a to φ. $N^{\varphi}_{\delta_a}$ can be obtained from the Laplace transformed aircraft equations of motion, say, by Cramer's rule.

The transfer function for $\delta_a \rightarrow \varphi$ with the $q \rightarrow \delta_r$ loop closed is:

$$\left(\frac{\varphi}{\delta_a}\right)_{q\rightarrow\delta_r} \triangleq \frac{N^{\varphi'}_{\delta_a}}{\Delta} = \frac{N^{\varphi}_{\delta_a}}{\Delta} + \frac{N^{q}_{\delta_a}}{\Delta}\,\frac{-G_q\Delta}{\Delta + G_q N^{q}_{\delta_r}}\,\frac{N^{\varphi}_{\delta_r}}{\Delta}$$

$$= \frac{N^{\varphi}_{\delta_a} + G_q(N^{\varphi}_{\delta_a}N^{q}_{\delta_r} - N^{q}_{\delta_a}N^{\varphi}_{\delta_r})/\Delta}{\Delta + G_q N^{q}_{\delta_r}} \qquad \text{(A-6)}$$

At this point let us introduce the coupling numerator:

$$N^{\varphi\ q}_{\delta_a\delta_r} \triangleq (N^{\varphi}_{\delta_a}N^{q}_{\delta_r} - N^{q}_{\delta_a}N^{\varphi}_{\delta_r})/\Delta \qquad \text{(A-7)}$$

Δ is always an exact factor of the numerator polynomial on the LHS of Eq A-7. Therefore $N^{\varphi\ q}_{\delta_a\delta_r}$ is a polynomial, and is very often of lower order than any of its constituent numerators. It can be shown that the coupling numerators can also be obtained by a method analogous to Cramer's rule. That is, $N^{\varphi\ q}_{\delta_a\delta_r}$ can be obtained from the Laplace transformed aircraft equations of motion by substituting the δ_a control effectiveness column into the φ column of the characteristic matrix and the δ_r control effectiveness column into the q column of the characteristic matrix, and then computing the determinant of the result. Several identities among coupling numerators are also of importance.

$$N_{\delta_i\delta_j}^{q_k q_l} = -N_{\delta_i\delta_j}^{q_l q_k} = -N_{\delta_j\delta_i}^{q_k q_l} = N_{\delta_j\delta_i}^{q_l q_k} \tag{A-8}$$

If $$q_l = \sum_p a_p(s)x_p,$$

then $$N_{\delta_i\delta_j}^{q_k q_l} = \sum_p a_p(s) N_{\delta_i\delta_j}^{q_k x_p} \tag{A-9}$$

also $$N_{\delta_i\delta_i}^{q_k q_l} = 0 \quad \text{and} \quad N_{\delta_i\delta_j}^{q_k q_k} = 0 \tag{A-10}$$

Consider the last two identities, Eq A-6 and A-7 and identify $N_{\delta_a}^{\varphi'}$ as:

$$N_{\delta_a}^{\varphi'} = N_{\delta_a}^{\varphi} + G_q N_{\delta_a\delta_r}^{\varphi\, q} \tag{A-11}$$

Clearly then, the <u>numerator</u>, $N_{\delta_a}^{\varphi}$, may be modified only by feeding some <u>other</u> motion quantity than φ back to some <u>other</u> control point than δ_a (because otherwise the coupling numerator will vanish). This statement is true in general and can be extended to the n-control point problem.

The closed-loop expression for the $\varphi_c \rightarrow \varphi$ transfer function is

$$\left(\frac{\varphi}{\varphi_c}\right)_{\substack{\varphi \rightarrow \delta_a \\ q \rightarrow \delta_r}} = \frac{G_\varphi \left[N_{\delta_a}^{\varphi} + Y_q N_{\delta_a\delta_r}^{\varphi\, q}\right]}{\Delta + G_q N_{\delta_r}^{q} + G_\varphi \left[N_{\delta_a}^{\varphi} + Y_q N_{\delta_a\delta_r}^{\varphi\, q}\right]} = \frac{G_\varphi N_{\delta_a}^{\varphi'}}{\Delta' + G_\varphi N_{\delta_a}^{\varphi'}} \tag{A-12}$$

where $$\Delta' = \Delta + G_q N_{\delta_r}^{q} \tag{A-13}$$

The numerators of the aircraft as experienced by the pilot (i.e., with respect to control <u>stick</u> and <u>pedal</u> deflections in distinction to

control surface deflection) may be modified by control crossfeed. Aileron-to-rudder crossfeed effects are summarized below. Pedal deflections are denoted by δ_r'. Stick deflections and aileron deflections are equivalent, assuming servodynamics are negligible.

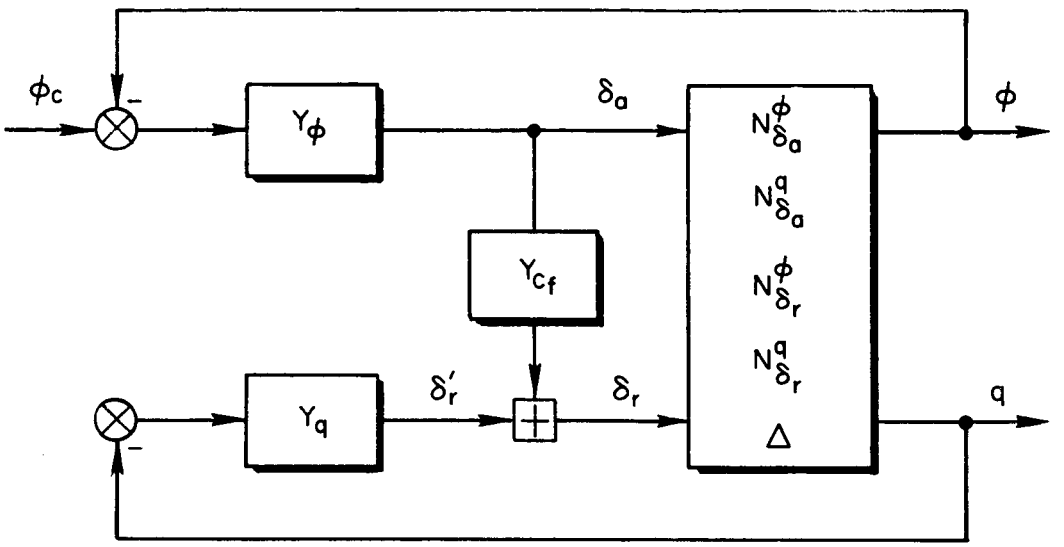

Figure A-3. Effect of Aileron-to-Rudder Crossfeed

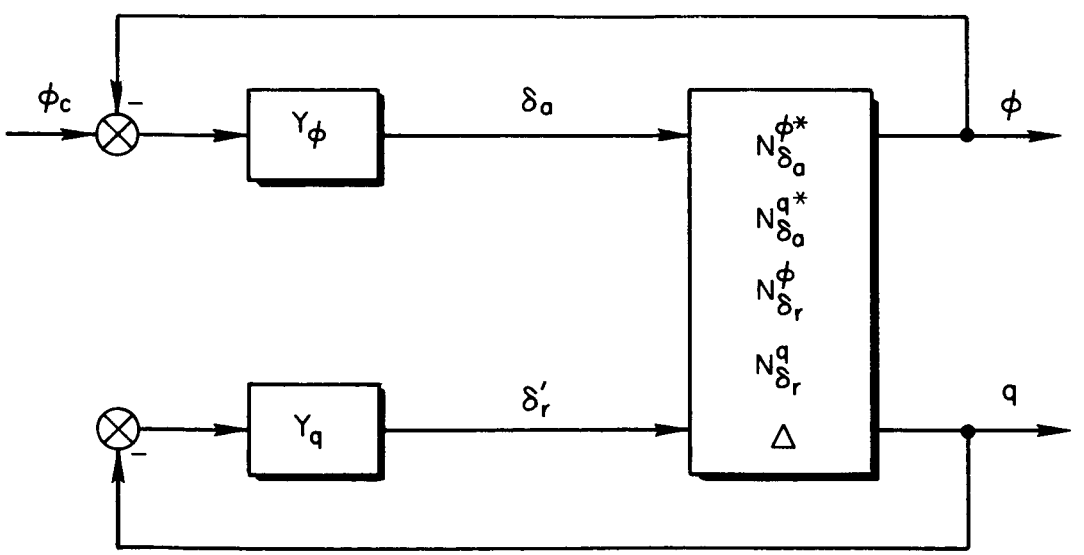

Figure A-4. Equivalent System to Figure A-3

The modified numerators are

$$N_{\delta_a}^{(\ )*} = N_{\delta_a}^{(\ )} + Y_{cf}N_{\delta_r}^{(\ )} \tag{A-14}$$

so that, for example

$$\left.\frac{\varphi}{\delta_a}\right|_{\substack{\varphi \to \delta_a \\ q \to \delta_r}} = \frac{N_{\delta_a}^{\varphi^{*'}}}{\Delta''} = \frac{(N_{\delta_a}^{\varphi^*} + G_q N_{\delta_a \delta_r}^{\varphi\ q})}{\Delta + G_q N_{\delta_r}^{q} + G_\varphi (N_{\delta_a}^{\varphi^*} + G_q N_{\delta_a \delta_r}^{\varphi\ q})} \tag{A-15}$$

Note that a single crossfeed does not affect the coupling numerator:

$$N_{\delta_a \delta_r}^{\varphi\ q^*} \equiv N_{\delta_a \delta_r}^{\varphi\ q} \tag{A-16}$$

The above development illustrates the fact that the effects of aileron to rudder crossfeed may be included in the previous analytical framework merely by replacing the unstarred δ_a numerators by starred numerators and choosing Y_{cf} appropriate to the crossfeed and the rudder servodynamics.

For compactness it is helpful to use a notation that will avoid the repeated use of the Laplace variable, s. For this purpose, we <u>define</u>:

$$(1/T) = (s + 1/T)$$

$$\begin{bmatrix} \zeta \\ \omega \end{bmatrix} = \left[s^2 + 2(\zeta)\omega s + \omega^2 \right]$$

$$\{\kappa\} = \text{Root locus gain}$$

Superscripts of primes and/or asterisks denote the number of loop closures which have modified the 1/T, ζ or ω of the system transfer function factors.

SYSTEMS SURVEYS

Effect of Roll Damper at Flight Conditions 630 and 725

Because of the large ω_φ—ω_d separation, it is an easy matter to obtain good dutch roll damping. However, most likely, roll rate reversals and fair sized (but <u>not</u> lightly damped) sideslip motions will <u>have</u> to be tolerated because of limited aileron control effectiveness available and the absence of rudder control effectiveness.

TABLE A-6

ω_φ/ω_d EFFECTS—WITH ROLL DAMPER

FLT. COND.	ω_φ/ω_d'*	$(\omega_\varphi/\omega_d')^2$	ω_d'
630	0.688	0.473	1.92
725	0.492	0.242	3.25

*Prime denotes one loop closed, in this case $\varphi \xrightarrow[SAS]{} \delta_a$

This will be especially true at flight condition 725 because of the very large ω_φ—ω_d' separation (see preceding table). While still larger gains could be used to advantage theoretically, they may well cause control saturation and/or tend to cause larger sideslip angles because of reduction in dutch roll stiffness that must accompany higher gains.

The pilot can close a $\varphi \rightarrow \delta_a$ loop to achieve approximately 1.0 rad/sec bandwidth using only a modest amount of lead, i.e., $(s + 1/T_L) = (s + 2.0)$. Lead is not required to stabilize the system. Additional pilot lead (T_L max = 5.0) can be used to obtain increased system bandwidth.

It seems clear that under emergency conditions with the roll damper failed, the pilot's lead, i.e., $(s + 0.2)$ is sufficient to obtain in excess of 1.0 rad/sec bandwidth. This calculation was not performed, however.

Competing SAS Systems for Flight Conditions 810, 840, 850 and 865

In this subsection, the objective is to evaluate candidate SAS configurations on a competitive basis. Root locus sketches will be utilized for evaluating the suitability of each candidate at the flight conditions where it is most likely to be a poor choice. This technique enables us to rapidly reduce the list of candidates to the one or two configurations that will most likely work out well.

The root locus sketches can be constructed using very simple approximations for the SAS transfer functions. Here, servodynamics and pilot reaction time delay effects will be neglected. For example, G_φ in Figure 1 consists of two parts. One represents the $\varphi \rightarrow \delta_a$ loop closure by the pilot and the other, the $\dot{\varphi} \rightarrow \delta_a$ SAS roll damper closure.

$$G_\varphi = \frac{\delta_a}{\varphi} = Y_\varphi + Y_{\dot{\varphi}}\, s \qquad \text{(A-17)}$$

The pilot describing function is taken to have the form:

$$Y_\varphi = \frac{\delta_a}{\varphi} = \{K_p\}\ (1/T_L) \qquad \text{(A-18)}$$

The roll damper form is:

$$Y_{\dot{\varphi}} = \frac{\delta_a}{\dot{\varphi}} = \{K_{\dot{\varphi}}\} \qquad \text{(A-19)}$$

For G_q (q is some motion quantity such as yaw rate, r), the only loop closures are those of the SAS so that:

$$G_q = Y_q \qquad \text{(A-20)}$$

We are now ready to consider the candidates.

Consider the effect of the closure of $\varphi \rightarrow \delta_a$ by the pilot with or without a roll damper. The critical situation occurs at flight condition 810 because of the so-called roll reversal, i.e., ω_φ^2 is negative. The root locus sketch below shows a rapidly divergent closed-loop root which will always result for reasonable values of gain of either sign.

Pilot + Roll Damper Closure at Flight Condition 810

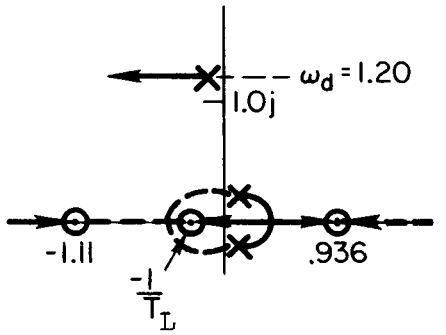

Aircraft

$$\frac{N_{\delta_a}^{\varphi}}{\Delta} = \frac{(-5.06)(-0.936)(1.11)}{\begin{bmatrix}-0.16\\0.165\end{bmatrix}\begin{bmatrix}0.17\\1.20\end{bmatrix}}$$

Pilot + Roll Damper

$$G_\varphi = \frac{\delta_a}{\varphi} = \{K_\phi\}(1/T_L)$$

Crossfeed can be used to remedy the roll reversal problem. Since the δ_a numerator is the one to change, the crossfeed must be $\delta_a \rightarrow \delta_r$.

$$N_{\delta_a}^{\varphi^*} = N_{\delta_a}^{\varphi} + Y_{cf} N_{\delta_r}^{\varphi} \qquad \text{(A-21)}$$

Effect of Crossfeed at Flight Condition 810

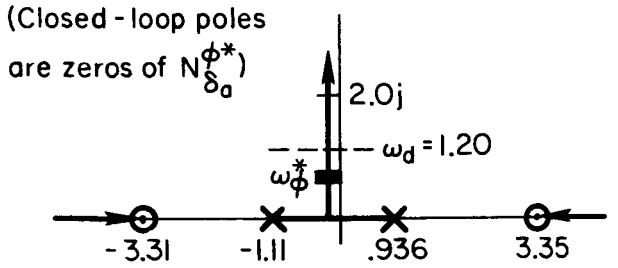

Open-Loop Function

$$= Y_{cf} \frac{N_{\delta_r}^{\varphi}}{N_{\delta_a}^{\varphi}}$$

Crossfeed

$$Y_{cf} = \{K_{cf}\}$$

While the crossfeed fixes up the roll reversal, it does not provide any stiffening of the dutch roll which is definitely required. To appreciate this, consider what happens when the roll damper loop is closed. $(\omega_\varphi^*/\omega_d)^2$ must be enough less than unity so that adequate damping is achieved, but should be greater than 0.5. This leads to the situation sketched below.

Effect of Roll Damper at Flight Condition 810
with $\delta_a \rightarrow \delta_r$ Crossfeed Acting

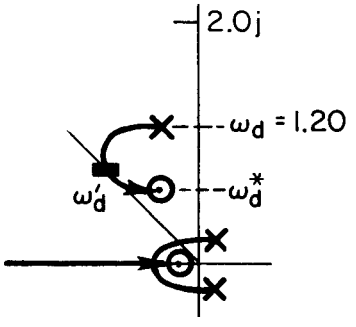

Aircraft ($\delta_a \rightarrow \delta_r$ Acting)

$$\frac{\dot{\varphi}^*}{\frac{N}{\Delta}\delta_a} = \frac{\{A_\varphi^*\}(0)\begin{bmatrix}\zeta_\varphi^* \\ \omega_\varphi^*\end{bmatrix}}{\begin{bmatrix}-0.16 \\ 0.165\end{bmatrix}\begin{bmatrix}0.17 \\ 1.20\end{bmatrix}}$$

Roll Damper

$$Y_{\dot{\varphi}} = \frac{\delta_a}{\dot{\varphi}} = \{K_{\dot{\varphi}}\}$$

On the other hand, $(\omega_\varphi^*/\omega_d)^2$ might be more nearly equal to unity eliminating the stiffness problem to some extent, but at the expense of damping.

Consideration must also be given to another potential problem created by this fix. At flight condition 865 $(\omega_\varphi/\omega_d)^2$ is nearly unity. This means that if a constant gain crossfeed is used an <u>unfavorable</u> $\omega_\varphi^*/\omega_d$ would result. (A closed-loop root is in the RHP.) The alternative is to have an adaptive crossfeed gain supplied electromechanically or by the pilot. Neither solution is really attractive in view of the marginal performance improvement at flight condition 810. Root locus sketches illustrating this aspect of the problem (when constant crossfeed gain is used) are shown below.

Effect of Crossfeed at Flight Condition 865

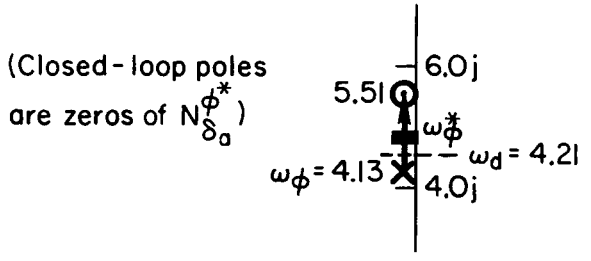

Open-Loop Function

$$= Y_{cf} \frac{N^{\varphi}_{\delta_r}}{N^{\varphi}_{\delta_a}}$$

Crossfeed

$$Y_{cf} = \{K_{cf}\}$$

Effect of Roll Damper at Flight Condition 865
with $\delta_a \rightarrow \delta_r$ Crossfeed Acting

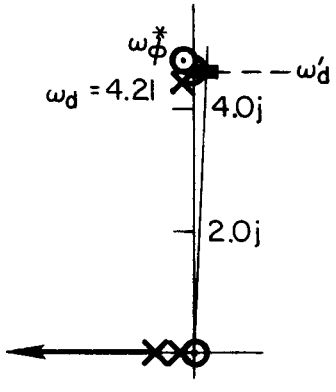

Aircraft ($\delta_a \rightarrow \delta_r$ Acting)

$$\frac{N^{\dot{\varphi}^*}_{\delta_a}}{\Delta} = \frac{\{A^*_{\dot{\varphi}}\}(0) \begin{bmatrix} \zeta^*_{\varphi} \\ \omega^*_{\varphi} \end{bmatrix}}{(0.0843)(0.360) \begin{bmatrix} 0.062 \\ 4.21 \end{bmatrix}}$$

Roll Damper

$$Y_{\dot{\varphi}} = \{K_{\dot{\varphi}}\}$$

The next candidate fix is to tilt the spin axis of the vertical reference forward through angle Θ_T. This means that the roll damper loop feeds back a new motion quantity, η, where assuming $r \doteq \dot{\psi}$

$$\eta \doteq \dot{\phi} \cos \Theta_T + r \sin \Theta_T \qquad \text{(A-22)}$$

$$N^{\eta}_{\delta_a} = \cos \Theta_T N^{\dot{\phi}}_{\delta_a} + \sin \Theta_T N^{r}_{\delta_a} \qquad \text{(A-23)}$$

If we develop this numerator at flight condition 810 it is clear that this fix, too, solves the roll reversal problem.

Effect of Sensor Tilt on $N^{\eta}_{\delta_a}$ at Flight Condition 810

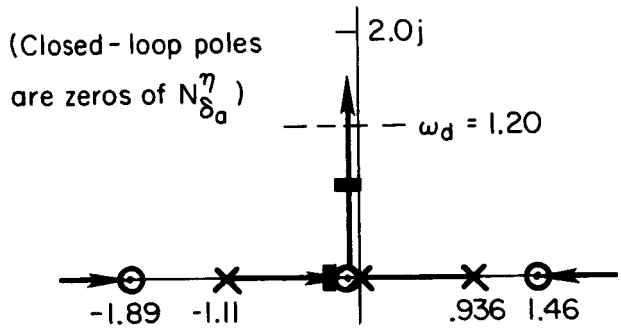

Open-Loop Function

$$= \frac{\sin \Theta_T \, N^{r}_{\delta_a}}{\cos \Theta_T \, N^{\dot{\phi}}_{\delta_a}}$$

However, this fix also fails to stiffen the dutch roll. See the roll damper closure below.

Effect of Roll Damper at Flight Condition 810
with Tilted Sensor

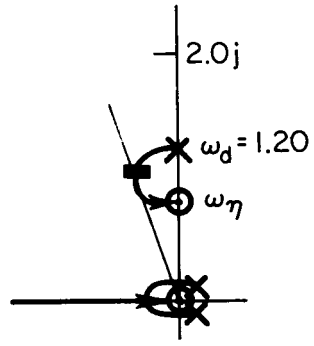

Aircraft

$$\frac{N^{\eta}_{\delta_a}}{\Delta} = \frac{\{A_\eta\}(0)\begin{bmatrix}\zeta_\eta \\ \omega_\eta\end{bmatrix}}{\begin{bmatrix}-0.16 \\ 0.165\end{bmatrix}\begin{bmatrix}0.17 \\ 1.20\end{bmatrix}}$$

Roll Damper

$$Y_\eta = \frac{\delta_a}{\eta} = \{K_\eta\}$$

Traditionally, feedback of lateral acceleration to rudder has been the appropriate way to achieve dutch roll stiffening. It turns out that this aircraft is amenable to this approach. But before getting to the final surveys which have been done in some detail, we must consider yaw rate feedback to rudder as a candidate inner-loop closure for completeness.

It is most desirable to use washed-out yaw rate to eliminate the need for a yaw rate command in order to execute turns. In the typical case for which this is useful, ω_r/ω_d is less than unity so that dutch roll damping is increased by the $r \rightarrow \delta_r$ feedback. At flight condition 810 the entry glider does not conform in either respect to the above situation. ω_r/ω_d is greater than one, and the zeros of $N^{\varphi}_{\delta_a}$ are on the positive and negative portions of the real axis. The resulting closures are unsatisfactory because a low frequency divergence remains.

This is developed in the following sketches.

Effect of $r \rightarrow \delta_r$ Closure
on Δ' at Flight Condition 810

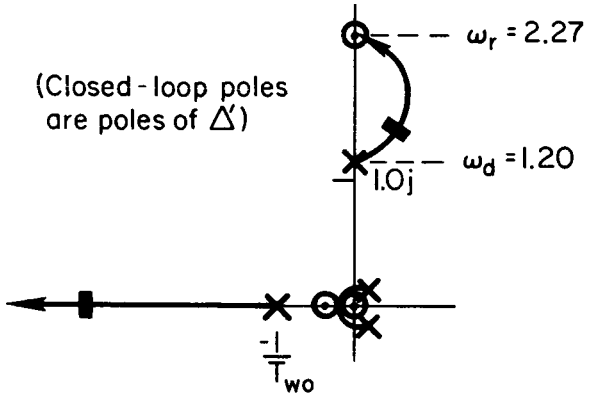

$$\Delta' = \Delta + Y_r N^{r}_{\delta_r}$$

Open-Loop Function

$$Y_r \frac{N^{r}_{\delta_r}}{\Delta} = Y_r \frac{\{-1.43\}(0.0761)\begin{vmatrix}0.034\\2.27\end{vmatrix}}{\begin{vmatrix}-0.16\\0.165\end{vmatrix}\ \begin{vmatrix}0.17\\1.20\end{vmatrix}}$$

Yaw Damper with Washout

$$Y_r = \frac{\delta_r}{r} = \{K_r\}\ \frac{(0)}{(1/T_{WO})}$$

Effect of $r \rightarrow \delta_r$ Closure
on $N^{\varphi'}_{\delta_a}$ at Flight Condition 810

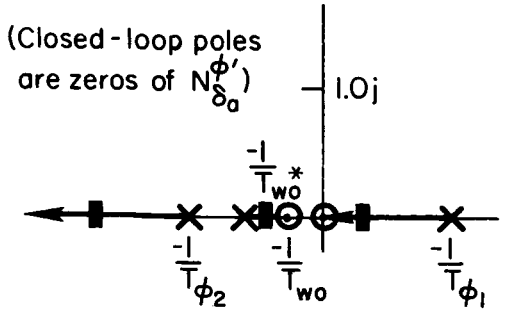

$$N^{\varphi'}_{\delta_a} = N^{\varphi}_{\delta_a} + Y_r N^{\varphi}_{\delta_a \delta_r}$$

Open-Loop Function

$$Y_r \frac{N^{\varphi}_{\delta_a \delta_r}}{N^{\varphi}_{\delta_a}} = Y_r \frac{\{8.5\}(0.0636)}{\{-5.06\}(-0.936)(1.11)}$$

Yaw Damper with Washout

$$Y_r = \{K_r\}\ \frac{(0)}{(1/T_{WO})}$$

Effect of Roll Damper at Flight Condition 810
with Washed-Out $r \rightarrow \delta_r$ Acting

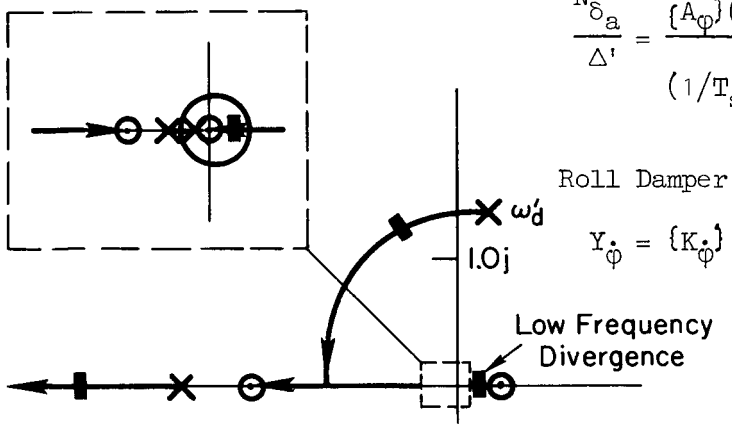

Augmented Aircraft

$$\frac{N^{\dot{\varphi}'}_{\delta_a}}{\Delta'} = \frac{\{A_{\dot{\varphi}}\}(0)(1/T_{W0}^{+})(1/T'_{\varphi_1})(1/T'_{\varphi_2})}{(1/T'_S)(1/T'_R)(1/T'_{W0})\begin{bmatrix}\zeta'_d \\ \omega'_d\end{bmatrix}}$$

Roll Damper

$$Y_{\dot{\varphi}} = \{K_{\dot{\varphi}}\}$$

If yaw rate feedback is to be useful here, it must be lag/lead compensated. (Yaw rate commands will be necessary with this compensation.)

Effect of $r \rightarrow \delta_r$ Closure on $N^{\varphi'}_{\delta_a}$ at Flight Condition 810
(With Lag/Lead Compensation)

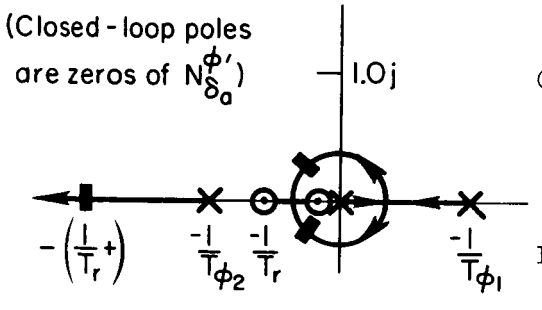

$$N^{\varphi'}_{\delta_a} = N^{\varphi}_{\delta_a} + Y_r N^{\varphi\ r}_{\delta_a \delta_r}$$

Open-Loop Function

$$Y_r \frac{N^{\varphi\ r}_{\delta_a \delta_r}}{N^{\varphi}_{\delta_a}} = Y_r \frac{\{8.5\}(0.0636)}{\{-5.06\}(-0.936)(1.11)}$$

Lag/Lead Compensated Yaw Damper

$$Y_r = \{K_r\} \frac{(1/T_r)}{(0)}$$

Effect of $r \rightarrow \delta_r$ Closure on Δ' at Flight Condition 810
(With Lag/Lead Compensation)

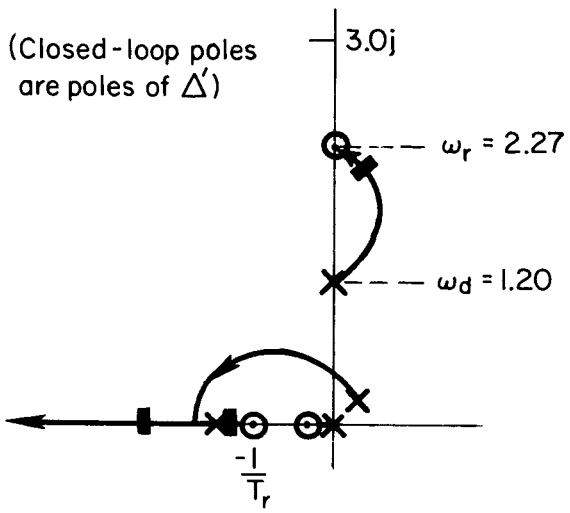

$$\Delta' = \Delta + Y_r N^r_{\delta_r}$$

Open-Loop Function

$$Y_r \frac{N^r_{\delta_r}}{\Delta} = Y_r \frac{\{-1.43\}(0.0761)\begin{bmatrix}0.034\\2.27\end{bmatrix}}{\begin{bmatrix}-0.16\\0.165\end{bmatrix}\begin{bmatrix}0.17\\1.20\end{bmatrix}}$$

Lag/Lead Compensated Yaw Damper

$$Y_r = \{K_r\}\frac{(1/T_r)}{(0)}$$

Effect of Roll Damper at Flight Condition 810
(With Lag/Lead $r \rightarrow \delta_r$ Acting)

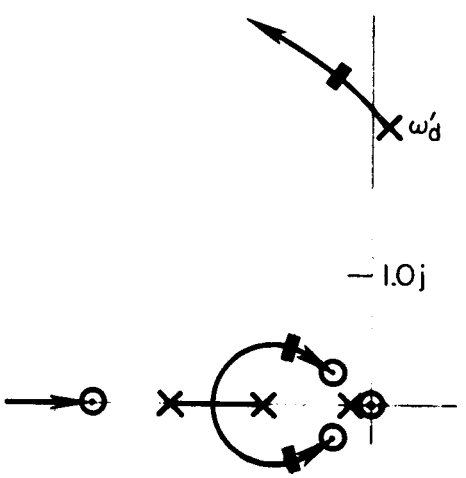

Augmented Aircraft

$$\frac{N^{\dot{\varphi}'}_{\delta_a}}{\Delta'} = \frac{\{A_\varphi\}(0)(1/T_r)\begin{bmatrix}\zeta'_\varphi\\ \omega'_\varphi\end{bmatrix}}{(1/T'_r)(1/T'_s)(1/T'_R)\begin{bmatrix}\zeta'_d\\ \omega'_d\end{bmatrix}}$$

Roll Damper

$$Y_{\dot{\varphi}} = \{K_{\dot{\varphi}}\}$$

It turns out that the system can be stabilized and the actual dutch roll can be stiffened. However, the lag of the compensation in combination with the roll subsidence root presents a low frequency apparent dutch roll mode to the pilot while the apparent roll subsidence root is at infinity. A high gain $\varphi \rightarrow \delta_a$ pilot closure is needed to suppress the apparent dutch roll mode adequately. This loop cannot be closed at high gain because the actual dutch roll mode will tend to become unstable due to the pilot reaction time delay effect.

Finally, we come to consider feedback of lateral acceleration to rudder. First we must choose a location for the accelerometer. If the location is chosen to be the center of percussion with respect to the rudder, then the accelerometer instantaneously senses a quantity proportional to sideslip angle. Sideslip angle is the desired feedback quantity for stiffening the dutch roll, of course. It also turns out that this feedback fixes up the roll reversal problem. The center of percussion is a distance l_{x_o}(forward) of the center of gravity. Reference 21 gives l_{x_o} as:

$$l_{x_o} = -U_o \frac{Y^*_{\delta_r}}{N'_{\delta_r}} \qquad \text{(A-24)}$$

The lateral acceleration measured at the center of percussion location at flight condition 810 is denoted by a'_y. At flight condition 810, $l_{x_o} \doteq 3.88$ ft. However, at flight condition 865, $l_{x_o} \doteq 0.95$ ft which means that the accelerometer is considerably forward of the center of percussion at that condition, and the quantity sensed no longer closely approximates sideslip angle. This is not necessarily a major concern because at flight condition 865 dutch roll stiffening is adequate. The real problem at flight condition 865 is lack of $\omega_\varphi - \omega_d$ separation and/or dutch roll damping. To remedy this we need only perturb the accelerometer location slightly to obtain adequate $\omega_\varphi - \omega_d$ separation at flight condition 865 and adequate dutch roll stiffening

at flight condition 810. A location, l_x = 3.38 ft forward of the center of gravity, is suitable. The lateral acceleration at this new location is a''_y.

To more keenly appreciate the results of changed accelerometer location on the various dutch roll related factors of the transfer functions, we have constructed Table A-7 below. When interpreting the entries in this table we must keep their involvement in the expressions for $N^{\varphi}_{\delta_a}$ and Δ' in mind in order to assess the effects of the $a_y^{(\ )} \rightarrow \delta_r$ feedback.

$$N^{\varphi'}_{\delta_a} = N^{\varphi}_{\delta_{\delta_a}} + Y_{a_y}(\ ) N^{\varphi\ a_y(\ )}_{\delta_a \delta_r} \tag{A-25}$$

$$\Delta' = \Delta + Y_{a_y}(\ ) N^{a_y(\ )}_{\delta_r} \tag{A-26}$$

TABLE A-7

SUMMARY OF ACCELEROMETER LOCATION EFFECTS UPON DUTCH ROLL RELATED TRANSFER FUNCTION FACTORS AT FLIGHT CONDITIONS 810 AND 865

FLT. COND.	$N^{\varphi}_{\delta_a}$	$N^{\varphi\ a''_y}_{\delta_a \delta_r}$	$N^{\varphi\ a'_y}_{\delta_a \delta_r}$	Δ	$N^{a''_y}_{\delta_r}$	$N^{a'_y}_{\delta_r}$
810	$\begin{matrix}(-0.936)\\(\ 1.11\ )\end{matrix}$	$\begin{bmatrix}-0.024\\35.7\end{bmatrix}$	$\begin{bmatrix}-0.0073\\13.6\end{bmatrix}$	$\begin{bmatrix}0.17\\1.20\end{bmatrix}$	$\begin{matrix}(-18.0)\\(\ 18.6)\end{matrix}$	$\begin{bmatrix}-0.11\\164.\end{bmatrix}$
865	$\begin{bmatrix}0.059\\4.13\end{bmatrix}$	$\begin{bmatrix}0.021\\5.01\end{bmatrix}$	$\begin{bmatrix}-0.017\\4.42\end{bmatrix}$	$\begin{bmatrix}0.062\\4.21\end{bmatrix}$	$\begin{bmatrix}0.028\\5.30\end{bmatrix}$	$\begin{bmatrix}0.031\\5.06\end{bmatrix}$

The numbers show that

- The $a_y^{(\ )} \rightarrow \delta_r$ feedback can fix the reversal. (The roots of $N^{\varphi'}_{\delta_a}$ tend toward those of $N^{\varphi\ a_y(\ )}_{\delta_a \delta_r}$ as $K_{a_y(\ )}$ is increased.)

- Greater ω_φ—ω_d separation at flight condition 865 is possible. (Same reason as above plus roots of Δ' tend toward those of $N_{\delta_r}^{a_y''}$ as $K_{a_y''}$ is increased.)

- The new accelerometer location does not compromise the dutch roll stiffening at flight condition 810.

In order to also augment dutch roll damping (particularly at flight condition 865) we will use lead/lag compensation in the $a_y'' \rightarrow \delta_r$ path. The following sketches show the development of $N_{\delta_a}^{\varphi'}$ and Δ' at flight conditions 810 and 865 using this feedback.

The sketches show that, indeed, the reversal, stiffness and dutch roll damping problems are solved for the critical flight conditions by the compensated $a_y'' \rightarrow \delta_r$ feedback. Closures of the roll damping loop and ultimately, of the $\varphi \rightarrow \delta_a$ loop through the pilot bear this out.

Development of $N_{\delta_a}^{\varphi'}$ and Δ' at Flight Condition 865

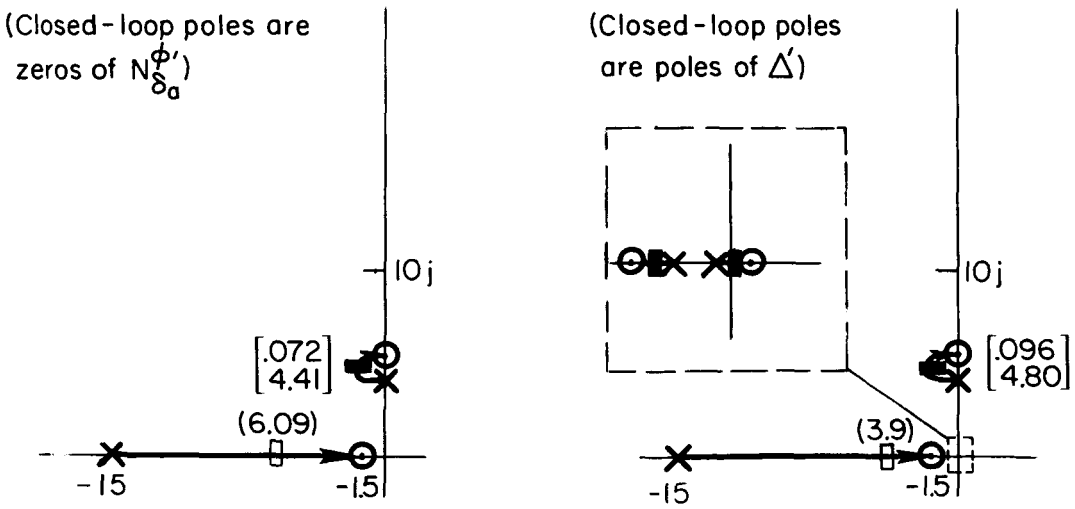

Development of $N_{\delta_a}^{\varphi'}$ and Δ' at Flight Condition 810

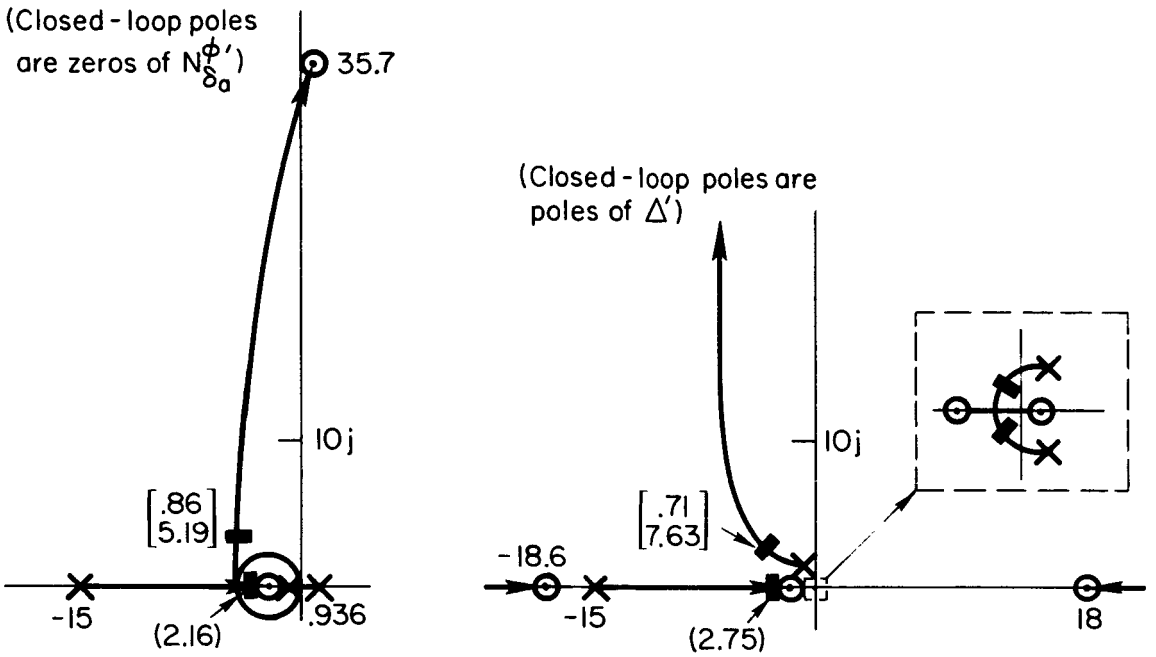

The open-loop functions in each of the above sketches are,

Open-Loop Function for $N_{\delta_a}^{\varphi'}$

$$= Y_{a_y}'' \frac{N_{\delta_a}^{\varphi} N_{\delta_r}^{a_y''}}{N_{\delta_a}^{\varphi}}$$

Open-Loop Function for Δ'

$$= Y_{a_y}'' \frac{N_{\delta_r}^{a_y''}}{\Delta}$$

The compensation for the lateral acceleration loop in each of the above sketches is $(s + 1.5)/(s + 15.0)$. The loop gain, $(-K_{a_y}'')_{dB}$, is -10.0.

Considerations of Controllability After a Single Failure

Consider pilot controllability at flight conditions 630 and 725 following a roll damper failure. The pilot will be able to control the double integrator-like vehicle in emergency operation, but will <u>not</u> have a high opinion of the handling qualities.

Much the same will be true at flight conditions 810 through 865 in the event of a roll damper failure. However, the dutch roll will be better damped by the $a''_y \rightarrow \delta_r$ inner loop and the roll subsidence frequency will have increased somewhat (but by no means enough). Both these factors will improve the handling qualities relative to situation above.

$a''_y \rightarrow \delta_r$ failure. At flight condition 810 this failure poses a critical pilot controllability problem when the roll damper is engaged because (you will recall) $a''_y \rightarrow \delta_r$ is required for stability. The question is: can the pilot provide a substitute for the failed loop?

Likely candidates are:

- $\delta_a \xrightarrow[\text{pilot}]{} \delta_r$ crossfeed. This is easily accomplished for emergency operation.
- $a_y \xrightarrow[\text{pilot}]{} \delta_r$ (a_{y_p} = lateral acceleration at the pilot's head). The pilot's head was estimated to be 5.88 ft forward of the c.g.

The first remedial action is easily within the pilot's capability, but, as we have seen previously, aileron-to-rudder crossfeed is not too effective a fix at flight condition 810 because the dutch roll frequency is low and requires stiffening which is not supplied by this fix. It is shown in Ref. 16 that the second remedial action is ineffective for stabilizing the dutch roll because of the combined effects of the pilot reaction time delay and lack of $\omega''_\varphi - \omega''_d$ separation. Also, the fairly rapid divergence ($-0.808 > 1/T > 0.936$) that results when $a''_y \rightarrow \delta_r$ fails does not allow the pilot sufficient time to assess the problem

and then adapt. This indicates that the $a_y'' \rightarrow \delta_r$ inner loop should most likely be fail operational (triply reduntant). Dual redundancy (with hardover monitors) might be sufficient if the pilot switched systems in an emergency without first trying to assess the source of the failure.

The roll damping loop need only be a single loop because the pilot can serve as an adequate backup.

Reliability and Equipment Count Considerations

$\dot{\varphi} \rightarrow \delta_a$, $r \rightarrow \delta_r$ and $a_y'' \rightarrow \delta_r$ can produce a system that will always be controllable after a single failure (rudder servo must be redundant). However, system dynamic performance after a $a_y'' \rightarrow \delta_r$ failure would be inferior to the system using fail operational $a_y'' \rightarrow \delta_r$ in place of $r \rightarrow \delta_r$ and $a_y'' \rightarrow \delta_r$ single loops. Equipment counts are nearly the same (see Appendix F of Ref. 22).

Dual redundant $a_y'' \rightarrow \delta_r$ shows an equipment count advantage, but probably requires too much of the pilot. The requirements to achieve system dynamic performance objectives for this vehicle provide nearly all the design constraints; therefore, the reliability/cost tradeoff does not enter the picture.

Detailed Analysis of Selected System

Detailed numerical analysis of the lead/lag compensated $a_y'' \xrightarrow[SAS]{} \delta_r$, $\dot{\varphi} \xrightarrow[SAS]{} \delta_a$, $\varphi \xrightarrow[pilot]{} \delta_a$ system has been carried out. In addition to the compensation considered in the above surveys, we have included aileron and rudder servodynamics

$$Y_{as} = Y_{rs} = \frac{(25)}{(25)} \qquad \text{(A-27)}$$

and a conservative estimate of the pilot's reaction time delay, $\tau_e = 0.36$ sec, when no pilot lead is required and $\tau_e = 0.51$ sec when

near maximum pilot lead is required. See Ref. 23. The form of the pilot describing function used in analysis is

$$Y_p = -K_p \frac{(s - 2/\tau_e)}{(s + 2/\tau_e)} (s + 1/T_L) \qquad \text{(A-28)}$$

The time delay here is approximated by a first-order over first-order Padé representation. The constituent transfer functions of G_φ and $G_{a_y''}$ become

$$G_\varphi = Y_p Y_{as} + Y_{\dot{\varphi}} Y_{as}\, s \qquad \text{(A-29)}$$

$$G_{a_y''} = Y_{a_y''}\, Y_{rs} \qquad \text{(A-30)}$$

The results of the closed-loop analyses are contained in the following series of tables.

Dynamic performance at all flight conditions is as expected from the preceding surveys.

TABLE A-8

CONTROLLER FORMS

$G_{a_y''}$	$sY_{\dot{\varphi}}Y_{as}$	Y_pY_{as}
$\frac{\{25\ K_{a_y''}\}(1.5)}{(25)(15)}$	$\frac{\{25\ K_{\dot{\varphi}}\}(0.0)}{(25)}$	$\frac{\{25\ K_p\}(-2/\tau_\varphi)(1/T_L)}{(2/\tau_e)(25)}$

$\tau_e = 0.36$ sec

TABLE A-9

CONTROLLER GAINS

FLT. COND.	$-K_{a_y''}\big\|_{dB}$	$-K_{\dot{\phi}}\big\|_{dB}$	$K_p\big\|_{dB}$	$1/T_L$	$K_p/T_L\big\|_{dB}$
630	N.A.	7.0	5.0	2.0	11.0
725	N.A.	7.0	5.0	2.0	11.0
810	-10	0.0	-20.0	25.0	8.0
840	-20	-10.0	-30.0	25.0	-2.0
850	-20	-10.0	-30.0	25.0	-2.0
865	-10	0	-25.0	25.0	3.0

TABLE A-10

SUMMARY OF CLOSED-LOOP DYNAMICS

FLT. COND.	$\left(\frac{\varphi}{\delta_a}\right)_{a_y'' \to \delta_r} = \frac{N_{\delta_a}^{\varphi'}}{\Delta'}$	$-K_{a_y''_{dB}}$
630	$\frac{\{-1.62\}\begin{bmatrix}.0060\\1.33\end{bmatrix}}{\begin{bmatrix}.490\\.00610\end{bmatrix}\begin{bmatrix}.0035\\2.69\end{bmatrix}}$	arb.
725	$\frac{\{-2.37\}\begin{bmatrix}.014\\1.60\end{bmatrix}}{\begin{bmatrix}.51\\.0135\end{bmatrix}\begin{bmatrix}.0084\\3.89\end{bmatrix}}$	arb.

TABLE A-10-Concluded

SUMMARY OF CLOSED-LOOP DYNAMICS

FLT. COND.	$\frac{\varphi}{\delta_a}_{a_y'' \rightarrow \delta_r} = \frac{N_{\delta_a}^{\varphi'}}{\Delta'}$	$-K_{a_y''}\Big\|_{dB}$
810	$\frac{\{-5.06\}(2.16)(30.2)\left[\begin{smallmatrix}.86\\5.19\end{smallmatrix}\right]}{(2.75)(21.1)\left[\begin{smallmatrix}.91\\.0456\end{smallmatrix}\right]\left[\begin{smallmatrix}.71\\7.63\end{smallmatrix}\right]}$	-10
840	$\frac{\{-12.65\}(10.7)(27.2)\left[\begin{smallmatrix}.29\\4.22\end{smallmatrix}\right]}{(.0528)(.308)(9.99)(25.8)\left[\begin{smallmatrix}.23\\7.40\end{smallmatrix}\right]}$	-20
850	$\frac{\{-14.4\}(6.01)(47.5)\left[\begin{smallmatrix}.22\\5.34\end{smallmatrix}\right]}{(.0292)(.367)(7.12)(54.4)\left[\begin{smallmatrix}.077\\6.66\end{smallmatrix}\right]}$	-20
865	$\frac{\{-8.8\}(6.09)(63.4)\left[\begin{smallmatrix}.072\\4.41\end{smallmatrix}\right]}{(.0074)(.401)(3.90)(106.)\left[\begin{smallmatrix}.096\\4.80\end{smallmatrix}\right]}$	-10

TABLE A-11

SUMMARY OF CLOSED-LOOP DYNAMICS

FLT. COND.	$\left(\frac{\varphi}{\delta_a}\right)_{\substack{a_y'' \to \delta_r \\ \dot{\varphi} \to \delta_a}} = \frac{N_{\delta_a}^{\varphi''}}{\Delta''}$	$-K_{\dot{\varphi}}\Big\vert_{dB}$
630	$\frac{\{-1.62\}(25.0)\begin{bmatrix}.0060\\1.33\end{bmatrix}}{(0)(2.11)(20.7)\begin{bmatrix}0.58\\1.92\end{bmatrix}}$	7.0
725	$\frac{\{-2.37\}(25.0)\begin{bmatrix}.014\\1.60\end{bmatrix}}{(.0002)(1.82)(17.8)\begin{bmatrix}.83\\3.25\end{bmatrix}}$	7.0
810	$\frac{\{-5.06\}(2.16)(25.0)(30.2)\begin{bmatrix}.86\\5.19\end{bmatrix}}{(.0007)(1.53)(3.65)(8.20)(27.3)\begin{bmatrix}.71\\13.5\end{bmatrix}}$	0.0
840	$\frac{\{-12.65\}(3.62)(25.0)(30.1)\begin{bmatrix}.38\\8.40\end{bmatrix}}{(.0087)(1.97)(9.04)(19.4)(26.7)\begin{bmatrix}.44\\8.32\end{bmatrix}}$	-10.0
850	$\frac{\{-14.4\}(6.01)(25.0)(47.5)\begin{bmatrix}.22\\5.34\end{bmatrix}}{(.0042)(2.40)(8.44)(20.6)(53.9)\begin{bmatrix}.18\\6.97\end{bmatrix}}$	-10.0
865	$\frac{\{-8.80\}(6.09)(25.0)(63.4)\begin{bmatrix}.07\\4.41\end{bmatrix}}{(.0004)(20.2)(105.)\begin{bmatrix}.13\\4.54\end{bmatrix}\begin{bmatrix}.76\\6.32\end{bmatrix}}$	0

TABLE A-12

SUMMARY OF CLOSED-LOOP DYNAMICS

FLT. COND.	$\left(\frac{\varphi}{\delta_a}\right)_{\substack{a_y'' \to \delta_r \\ \phi \to \delta_a \\ \varphi \to \delta_a}} = \frac{Y_\varphi Y_{a_s} N'''_{\delta_a}}{\Delta'''}$	$K_p\Big\vert_{dB}$
630	$\frac{\{-40.5\ K_p\}(-5.55)(2.0)\begin{bmatrix}.0060\\1.33\end{bmatrix}}{(1.98)(25.5)\begin{bmatrix}.16\\1.01\end{bmatrix}\begin{bmatrix}0.26\\5.26\end{bmatrix}}$	5.0
730	$\frac{\{-59.3\ K_p\}(-5.55)(2.0)\begin{bmatrix}.014\\1.60\end{bmatrix}}{(2.02)(25.7)\begin{bmatrix}.21\\1.09\end{bmatrix}\begin{bmatrix}.17\\6.95\end{bmatrix}}$	5.0
810	$\frac{\{-126.\ K_p\}(-5.55)(2.16)(25.0)(30.2)\begin{bmatrix}.86\\5.19\end{bmatrix}}{(2.40)(27.3)\begin{bmatrix}.30\\2.29\end{bmatrix}\begin{bmatrix}.90\\6.62\end{bmatrix}\begin{bmatrix}.78\\14.4\end{bmatrix}}$	-20.0
840	$\frac{\{-317.K_p\}(-5.55)(3.62)(30.1)\begin{bmatrix}.38\\8.40\end{bmatrix}}{(19.1)(26.7)\begin{bmatrix}.19\\1.68\end{bmatrix}\begin{bmatrix}.36\\7.61\end{bmatrix}\begin{bmatrix}.97\\9.31\end{bmatrix}}$	-30.0
850	$\frac{\{-360.K_p\}(-5.55)(6.01)(25.0)(47.5)\begin{bmatrix}.22\\5.34\end{bmatrix}}{(5.84)(10.5)(20.4)(53.9)\begin{bmatrix}.23\\2.02\end{bmatrix}\begin{bmatrix}.13\\6.87\end{bmatrix}}$	-30.0
865	$\frac{\{-220.K_p\}(-5.55)(6.09)(63.4)\begin{bmatrix}.072\\4.41\end{bmatrix}}{(20.0)(105.)\begin{bmatrix}.52\\2.61\end{bmatrix}\begin{bmatrix}.14\\4.70\end{bmatrix}\begin{bmatrix}.97\\6.38\end{bmatrix}}$	-25.0

Selection of Adaptive Gains

Adaptive system gains will be $K_{a_y''}$, which must adjust to account for changes in combination of Δ, $N_{\delta_r}^{a_y''}$, $N_{\delta_a}^{\varphi}$, and $N_{\delta_a}^{\varphi}{}_{\delta_r}^{a_y''}$ with flight condition, and $K_{\dot{\varphi}}$, which can compensate to some extent for the widely varying control effectiveness in roll with flight condition.

The need for adaptive $K_{a_y''}$ is illustrated by the circumstances of flight condition 850. A value of $(-K_{a_y''})_{dB} = -10$ is suitable for all other flight conditions. To appreciate this need, let us compare the conflicting requirements for $(-K_{a_y''})$ at flight conditions 810 and 850.

TABLE A-13

EFFECT OF $K_{a_y''}$ AT FLIGHT CONDITIONS 810 AND 850

FLT. COND.	$(-K_{a_y})_{dB}$	ω_d'	ω_φ'	COMMENTS
810	0	16.8	10.52	DR* too stiff
	-10	7.63	5.19	
	-15	2.94	1.71	
	-20	2.16	0.943	DR not stiff enough
	-30	1.53		
850	0	7.00	8.37	$\omega_\varphi'/\omega_d'$ unfavorable
	-10	6.85	7.16	
	-15	6.70	6.26	$\omega_\varphi'/\omega_d \doteq 1.0$
	-20	6.66	5.34	$\omega_\varphi' - \omega_d'$ separation adequate to allow sufficient increase in DR damping
	-30	6.55	4.42	

*DR = Dutch Roll

Table A-13 shows that at flight condition 810 a gain in excess of -20.0 dB is required for adequate dutch roll stiffness while at flight condition 850 the gain must be -20.0 dB or less to permit a sufficient increase in dutch roll damping when the roll SAS closure is made. Inasmuch as these conflicting requirements are most probably a function of operating point rather than flight time, and because of the rich variety of possible entry flight plans, a good case can be made for an adaptive SAS.

APPENDIX B

DEVELOPMENT OF ADAPTIVE CONTROL FUNCTION SYSTEM EQUATIONS

Equations which describe the adaptive control function system for the vehicle in Section II are stated in a more general and compact way here. The effects of forcing because of mismatch and disturbance inputs are treated in greater detail than in Section II. Equations are written to show the modifications introduced by additional, outer loop closures around the adaptive system. The criterion implied under the assumption that the adaptive gain adjustment law is a steepest descent law is also given.

The equations are sufficiently general to enable the adaptive control function technique to be "applied" to many control situations merely by making appropriate specializations.

ADAPTIVE SYSTEM EQUATIONS WITHOUT OUTER LOOPS BUT WITH DISTURBANCE INPUTS AND ADAPTIVE FEEDBACK OF SECONDARY MOTION QUANTITIES

The controlled element is assumed to be constant coefficient and linear. Its transfer functions are given by

$$cu = (C/\Delta)fu + (D/\Delta)du \qquad \text{(B-1)}\dagger$$

$$mu = (M/\Delta)fu + (N/\Delta)du \qquad \text{(B-2)}$$

The u's are conformable vectors with unity elements. c is a diagonal matrix of variables to be controlled, that is, of primary motion

---

†Both time domain and Laplace transform domain equations will be used. Equations will be in terms of one or the other domains, but no distinction between domains will be drawn in the notation since the proper domain will be clear from the context.

quantities.† f is a diagonal matrix of control surface deflections, i.e., control functions. d is a diagonal matrix of disturbance inputs. m is a diagonal matrix of secondary motion quantities involved in the problem. The matrices, c and f, are of equal order.

The control law for the basis system is

$$fu = \left[r - c \,\middle|\, - Fm \right]_{\mathcal{L}^{-1}} k. \qquad \text{(B-3)}\dagger\dagger$$

r is a diagonal matrix of commands, that is, the reference values of c. The matrix F contains the feedback transfer functions. k is a vector of adaptively adjusted gains. Fixed gain control paths are assumed to be included in Eq B-1 and B-2. The basic system is illustrated in Fig. B-1.

An error vector is defined to be proportional to the difference between the commands, ru and calculated commands, $r_m u$. This calculation is performed by processing cu and mu by the mathematical inverse of a transfer function model for the system.

Choice of a system model is somewhat arbitrary. However, for our work here, we choose the form of the model to be the same as the basic system. The model controlled element transfer functions were taken to be approximately those of the actual controlled element at one particular operating point. The model gain vector, k_m, has elements corresponding with those of k. Its elements are chosen so that system model performance would be near "optimum" if it were excited by the commands, ru.

The error, a vector, is defined as

---

†Lower case letters are used for certain diagonal matrices because this distinction from the upper case for general matrices aids interpretation of the equations. For example, it follows that cu is a vector of variables to be controlled, etc. This cumbersome representation of vectors is necessary here in order to write all subsequent equations compactly.

††Subscripts of $\mathcal{L}$ and $\mathcal{L}^{-1}$ will be used on quantities to indicate respectively, the direct or inverse Laplace transform of a quantity.

$$e = \left[r - r_m \,\vdots\, 0 \right] k_m \tag{B-4}$$

The similarity of the model and the basic system enables us to write the model control law

$$\left[r_m \,\vdots\, 0 \right] k_m = f_m u + \left[c \,\vdots\, Fm \right]_{\mathcal{L}^{-1}} k_m \tag{B-5}$$

in consideration of Eq B-3. Disturbance inputs to the model are omitted since disturbance effects would be suppressed in an ideal system. Then, in consideration of Eq B-1, $f_m u$ can be obtained from

$$f_m u = \Delta_m C_m^{-1} cu \tag{B-6}$$

Equation B-4 can be rewritten using Eq B-5.

$$e = \left[r - c \,\vdots\, - Fm \right]_{\mathcal{L}^{-1}} k_m - f_m u \tag{B-7}$$

The error is mechanized in the adaptive system according to Eq B-7. The error mechanization is illustrated in Fig. B-1. Notice that the adaptive gains and their model counterparts are contained in matrices in this figure. The matrices, K and K_m, are related in a time invariant way to the gain vectors, k and k_m respectively, by alternate equations for the control function, $f_{(\cdot)}u$.

$$\left[r - c \,\vdots\, - Fm \right]_{\mathcal{L}^{-1}} k_{(\cdot)} = K_{(\cdot)} \left[r - c \,\vdots\, - Fm \right]_{\mathcal{L}^{-1}} u \tag{B-8}$$

This equation holds at every instant of time so there are always an equal number of unknowns and independent linear algebraic equations. Therefore, a unique relation between $K_{(\cdot)}$ and $k_{(\cdot)}$ always exists. Often, it is most readily obtained by inspection, however, rather than by solving the equations.

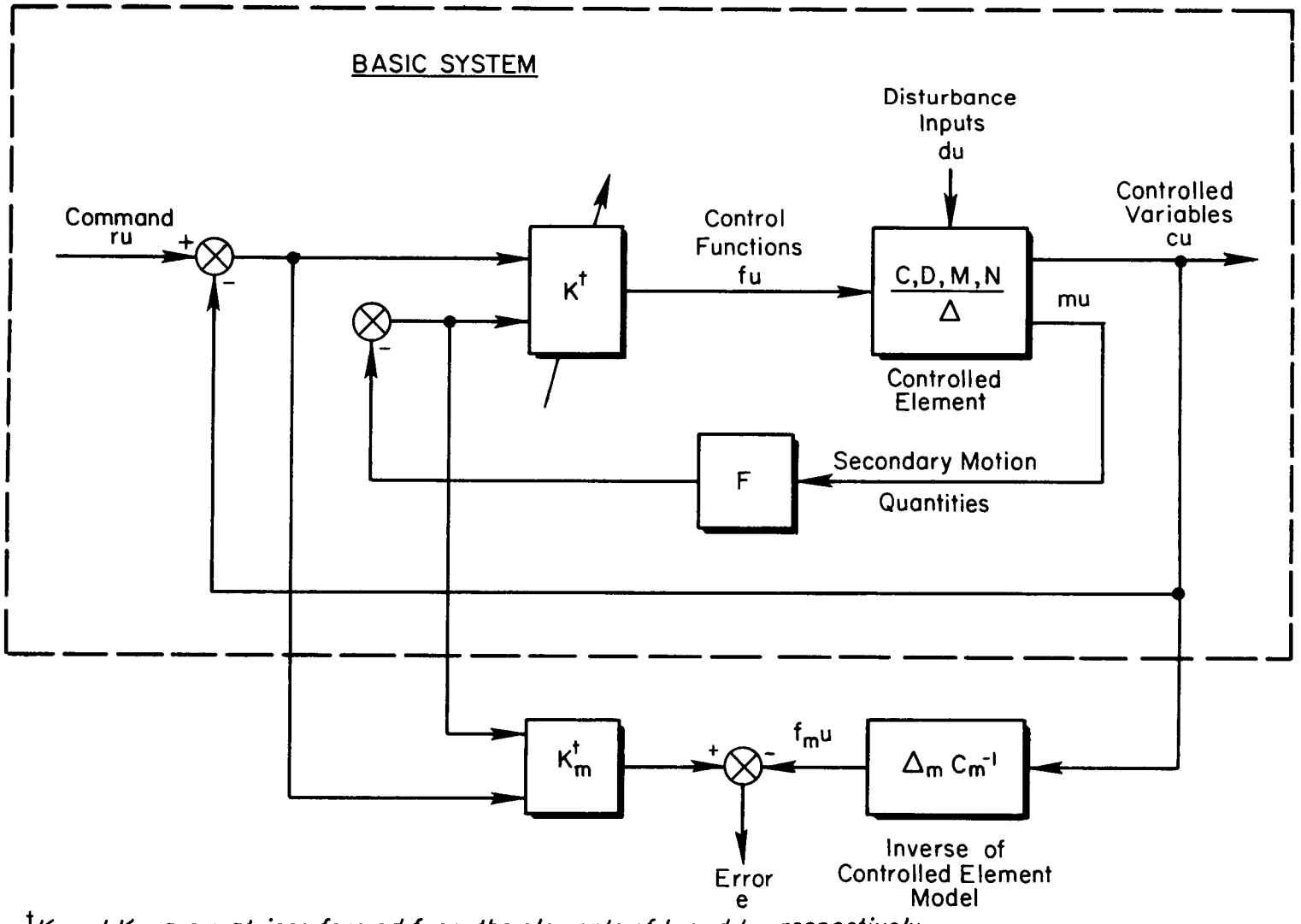

†*K and K_m are matrices formed from the elements of k and k_m respectively. See text and Eq. B-8 for details*

Figure B-1. Basic System and Mechanization of the Error

Let us adjust the gains of the adaptive system according to the following differential equation.

$$\dot{k} = A\left[r - c\,\frac{|}{|} - Fm\right]'_{\mathcal{L}^{-1}} e \qquad \text{(B-9)}$$

A is a diagonal matrix of adaptive loop gains. All diagonal elements of A are positive. Equation B-9 describes the mechanization of the adaptive system gains.

Stability and convergence of the adaptive system is studied in terms of the adaptive gain difference vector, Δk.

$$\Delta k \triangleq k_m - k \qquad \text{(B-10)}$$

Equations B-3, B-7 and B-10 can be used to express the error in terms of Δk.

$$e = \left[r - c\,\frac{|}{|} - Fm\right]_{\mathcal{L}^{-1}} \Delta k - \left[f_m - f\right]u \qquad \text{(B-11)}$$

Equations B-9, B-10 and B-11 can be used to obtain gain-difference differential equations.

$$\begin{aligned}\Delta\dot{k} = &-A\left[r - c\,\frac{|}{|} - Fm\right]'_{\mathcal{L}^{-1}} \left[r - c\,\frac{|}{|} - Fm\right]_{\mathcal{L}^{-1}} \Delta k \\ &+ A\left[r - c\,\frac{|}{|} - Fm\right]'_{\mathcal{L}^{-1}} \left[f_m - f\right]u\end{aligned} \qquad \text{(B-12)}$$

Equation B-12 is a vector-matrix expression comparable to Eq 22 and 23 in Section II.

When there is no signal mismatch between the system and its model in the sense that

$$f_m = f \qquad \text{(B-13)}$$

this implies that no disturbance inputs are acting, and no controlled element mismatch exists. Then, the last term on the RHS of Eq B-12 is zero, and the expression is an explicit function of all the linear algebraic dependencies on Δk. This is similar to the expression used in Section II to assess stability. When Eq B-13 is satisfied, Eq B-12 is stable because the coefficient matrix for Δk on the RHS of Eq B-12 is non-negative.

We are now interested in obtaining a similar description which holds when controlled element mismatch and disturbance inputs are present. This requires an expression for $\left[f_m - f\right]u$ in terms of $\left[r - c\,\vdots - Fm\right]$ and d. From Eq B-1, B-3, B-6 and B-10:

$$\left[f_m - f\right]u = \left[\Delta_m C_m^{-1} C/\Delta - I\right] \left\{\left[r - c\,\vdots - Fm\right]_{\mathcal{L}^{-1}}(k_m - \Delta k)\right\}_{\mathcal{L}} + \Delta_m C_m^{-1} D/\Delta\, du \tag{B-14}$$

Substitution of Eq B-14 into Eq B-12 assuming k_m is constant gives

$$\begin{aligned}\dot{\Delta k} = {} & -A\left[r - c\,\vdots - Fm\right]'_{\mathcal{L}^{-1}} \left[\left[\Delta_m C_m^{-1} C/\Delta\right] \left\{\left[r - c\,\vdots - Fm\right]_{\mathcal{L}^{-1}}\Delta k\right\}_{\mathcal{L}}\right]_{\mathcal{L}^{-1}} \\ & + A\left[r - c\,\vdots - Fm\right]'_{\mathcal{L}^{-1}} \left\{\left[\Delta_m C_m^{-1} C/\Delta - I\right]\left[r - c\,\vdots - Fm\right]k_m\right\}_{\mathcal{L}^{-1}} \\ & + A\left[r - c\,\vdots - Fm\right]'_{\mathcal{L}^{-1}} \left\{\Delta_m C_m^{-1} D/\Delta\, du\right\}_{\mathcal{L}^{-1}}\end{aligned} \tag{B-15}$$

The last two terms on the RHS of Eq B-15 are the forcing terms. Each may introduce a bias and a transient forcing effect. The second term on the RHS arises because of controlled element mismatch effects since it vanishes when

$$\Delta_m C_m^{-1} C/\Delta = I \tag{B-16}$$

This forcing is actually desirable because it tends to offset the effects of controlled element mismatch by calling for non-zero values

of Δk. The third term on the RHS of Eq B-15 arises because of the disturbance inputs. Whether this forcing is regarded as desirable or not is largely a point of view. Its effect is to suppress disturbance input components in $\left[r - r_m\right]u$, but this is often accomplished by calling for values of Δk which sacrifice a considerable amount of the basic system stability margin. This is especially true where the disturbance input power is large with respect to command power. Thus its desirability is somewhat controversial. It is possible to circumvent this "problem," however, if one is willing to measure the disturbance inputs.

The stability of the homogeneous part of Eq B-15 is the last point for discussion. In Eq B-12, the homogeneous solution is stable because the matrix

$$\left[r - c\,\middle|\,\middle|\,- Fm\right]'_{\mathcal{L}^{-1}} \left[r - c\,\middle|\,\middle|\,- Fm\right]_{\mathcal{L}^{-1}}$$

is non-negative. This is a <u>sufficient</u> condition for stability. If this matrix is also non-zero except at isolated instants, the homogeneous solution is asymptotically stable to $\Delta k = 0$. See Theorem 1 and pages 14 through 16 and pages 106 through 108 of Ref. 7 for detailed proof. What is more, under these circumstances, Eq B-13 holds so that $\Delta k = 0$ results in $e = 0$ because of Eq B-11. All these conclusions assume no mismatch of either kind. That is, Eq B-13 must be satisfied. Things are not so simple for the homogeneous solution to Eq B-15. This is because H in

$$H\Delta k = \left[r - c\,\middle|\,\middle|\,- Fm\right]'_{\mathcal{L}^{-1}} \left[\left[\Delta_m\, C_m^{-1}\, C/\Delta\right] \left\{\left[r - c\,\middle|\,\middle|\,- Fm\right]_{-1} \Delta k\right\}_{\mathcal{L}}\right]_{\mathcal{L}^{-1}} \quad \text{(B-17)}$$

is not necessarily a non-negative matrix. This fact denies use of the simple sufficiency condition for stability. A general, analytical treatment beyond this point does not seem warranted because it would pertain only to the homogeneous (unforced) solution.

A few qualitative remarks are in order, however. It seems evident

in view of Eq B-16, that small mismatches will still result in a non-negative matrix. This follows from the fact that the transfer functions matrix of $\Delta_m C_m^{-1} C/\Delta$ will have elements which are pole-zero dipoles when mismatch is small. If the power spectra of the elements of $\left[r - c \left| - Fm\right.\right]_{\mathcal{L}^{-1}}$ are at all broad, we can reasonably expect the H matrix to remain non-negative. So, while Eq B-15 is an exact expression, it is not useful for engineering analysis of the problem. It does, however, provide an intuitive feel for the effects of mismatch and disturbance inputs upon the gain-difference dynamic response.

The structure of this gain-difference dynamic system is illustrated in Fig. B-2. It shows that the elements of the closed loop are integrators, time-varying gains and transfer functions consisting of dipoles. When the transfer function matrix is unity, the closed loop is stable as noted previously. When the time-varying gains can be effectively approximated by constants, the system stability may be examined using root locus techniques.

INCLUSION OF OUTER LOOP CLOSURES

Outer loop closures may be represented by redefining r as

$$r = P(r_o - c) \qquad \text{(B-18)}\dagger$$

r_o is the diagonal matrix of outer loop commands. P is the matrix of outer loop compensation. This expression can be substituted in all equations for r. The results of the substitution into Eq B-15 are of particular interest because that equation determines the gain-difference dynamics.

---

†The matrix, c, could be replaced by a linear operation on the controlled element output matrix for greater generality, but this would not affect the observations which follow.

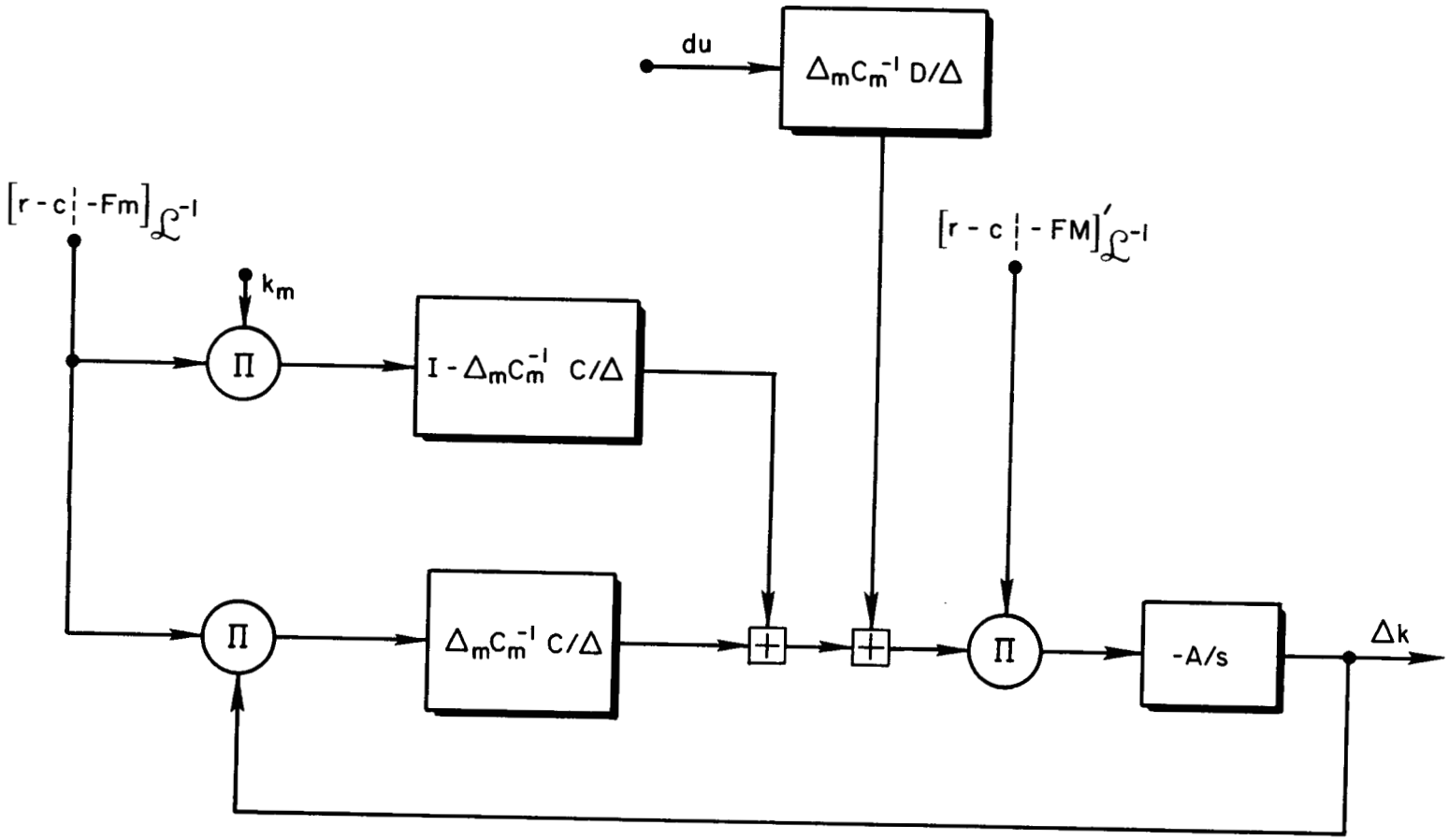

Figure B-2. Structure of Gain-Difference Dynamic System

$$\dot{\Delta k} = -A\left[Pr_o - (1+P)c\,\frac{1}{s} - Fm\right]'_{\mathcal{L}^{-1}}\left[\left[\Delta_m C_m^{-1} C/\Delta\right]\left\{\left[Pr_o - (1+P)c\,\frac{1}{s} - Fm\right]_{\mathcal{L}^{-1}}\Delta k\right\}_{\mathcal{L}}\right]_{\mathcal{L}^{-1}}$$
$$+ A\left[Pr_o - (1+P)c\,\frac{1}{s} - Fm\right]'_{\mathcal{L}^{-1}}\left[\left[\Delta_m C_m^{-1} C/\Delta - I\right]\left[Pr_o - (1+P)c\,\frac{1}{s} - Fm\right]k_m\right]_{\mathcal{L}^{-1}}$$
$$+ A\left[Pr_o - (1+P)c\,\frac{1}{s} - Fm\right]'_{\mathcal{L}^{-1}}\left\{\Delta_m C_m^{-1} D/\Delta\, du\right\}_{\mathcal{L}^{-1}} \qquad \text{(B-19)}$$

When the assumption is made that Eq B-16 is satisfied (no controlled element mismatch) the following results.

$$\dot{\Delta k} = -A\left[Pr_o - (1+P)c\,\frac{1}{s} - Fm\right]'_{\mathcal{L}^{-1}}\left[Pr_o - (1+P)c\,\frac{1}{s} - Fm\right]_{\mathcal{L}^{-1}}\Delta k$$
$$+ A\left[Pr_o - (1+P)c\,\frac{1}{s} - Fm\right]'_{\mathcal{L}^{-1}}\left\{\Delta_m C_m^{-1}\, D/\Delta\, du\right\}_{\mathcal{L}^{-1}} \qquad \text{(B-20)}$$

Equations B-19 and B-20 indicate that the outer loop closure effects are merely changes in the (time-varying) coefficients in the equations governing the parameter-difference dynamics. While these affect the level of the forcing resulting from disturbance inputs and controlled element mismatch, and the rate of convergence of the homogeneous solution, it does not seem likely that stability will be affected.

IMPLIED CRITERION

The gain adjustment law, Eq B-9, was selected because of the stability property that Δk displays when $f_m = f$. In other words, Eq B-9 was established for reasons of convenience. Now,it would be interesting to discover what criterion is being satisfied by Eq B-9, assuming it is a steepest descent law and that Eq B-13 is satisfied.

Steepest descent adjustment means that:

$$\dot{h} = -(\text{constant})\ \nabla_h J \qquad \text{(B-21)}$$

h is a gain vector, $\nabla_h(\cdot)$ denotes the gradient of $(\cdot)$ with respect to h, and J is the scalar criterion. We can arbitrarily take the constant

to be unity without loss of generality. The development on pages 21 through 23 of Ref. 7 shows that Eq B-21 is equivalent to

$$\dot{k} = -A \nabla_k J \qquad \text{(B-22)}$$

when

$$k = A^{1/2} h \qquad \text{(B-23)}$$

Recall that A is diagonal so that

$$A^{1/2} = \left[\sqrt{a_{ii}}\right]$$

In consideration of Eq B-10 and B-11, it is easy to see that

$$J = e' e/2 \qquad \text{(B-24)}$$

and that the gain adjustment law results in a steepest descent adjustment on the surface described by Eq B-24 in h coordinates. That is, when $e(\Delta k)$ is expressed as $e(A^{1/2}\Delta h)$.

APPENDIX C

SIMULATION CIRCUITS

The primary goal of this research program was to develop a control system capable of rapidly adapting to compensate for plant variations. What proved to be a particularly appropriate application was selected to demonstrate the principles of the adaptive system. The problem chosen was the lateral-directional stability augmentation of a representative, but hypothetical, manned, lifting-body, entry vehicle. A quantitative description of the dynamics of the vehicle is given in Appendix A. Certain aspects of the particular control problems posed by this vehicle have already been discussed in Section II.

Analog computation was chosen as the appropriate tool for system simulation. The EAI 680 computer system provided the complete real-time simulation. Preliminary studies were performed on the EAI TR-48, a considerably smaller computer system. This, it turned out, was highly advantageous in that the low cost TR-48 served well to show how to optimize the full scale simulation. The EAI 8400 digital computer provided some support, particularly in setting up function generators. All simulation work was accomplished at Electronic Associates, Inc. Princeton Computation Center, Princeton, New Jersey.

The details of the simulation follow.

The block diagram of the complete system is repeated here in Fig. C-1. References are made in Fig. C-1 to the appropriate detailed diagrams which comprise Fig. C-2 through C-12 of this Appendix.

THE VEHICLE

Pertinent trajectory (trim) characteristics are given in Fig. C-2. The sketch and definition list below identify the axis system and trim motion quantities.

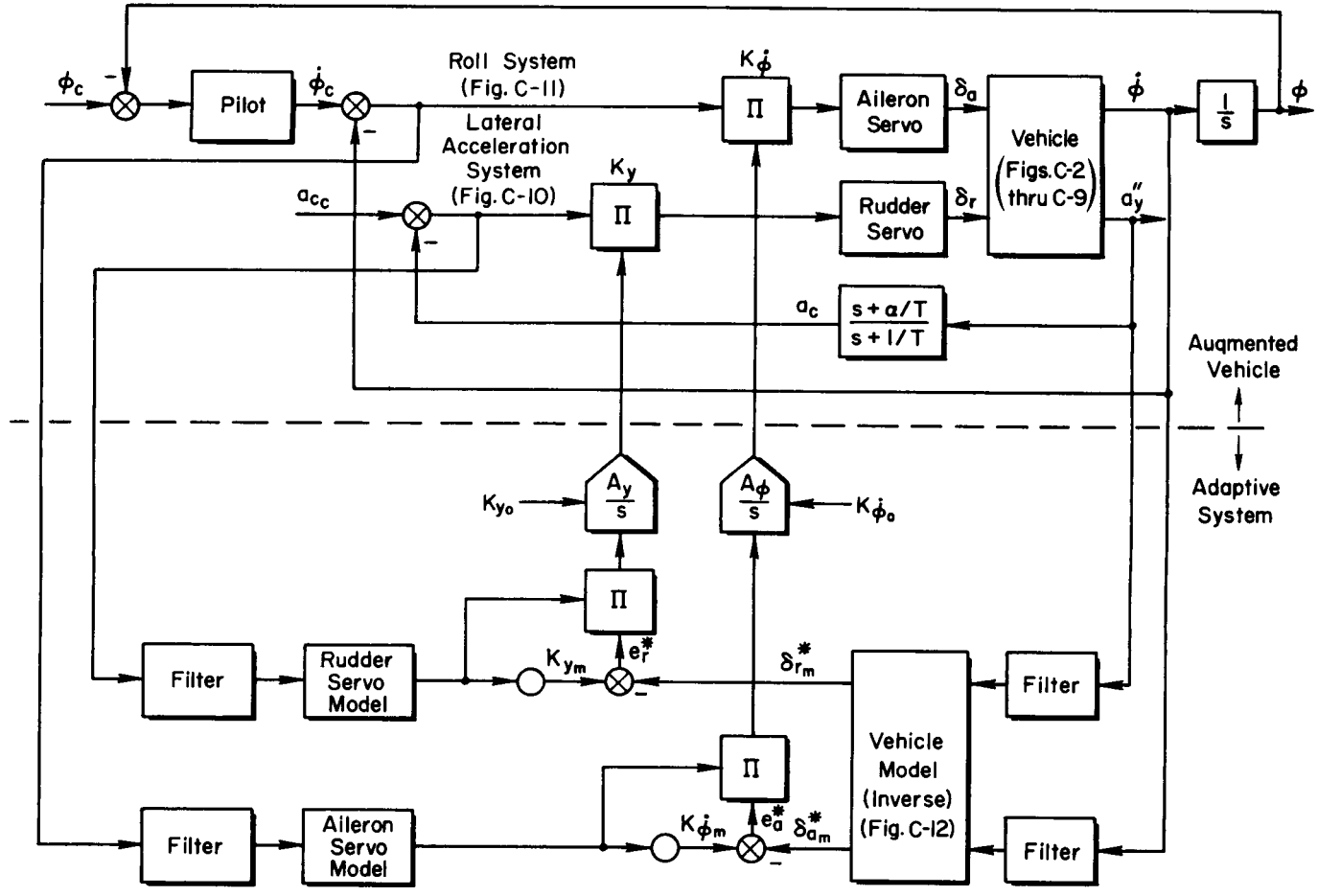

Figure C-1. Block Diagram of Complete System

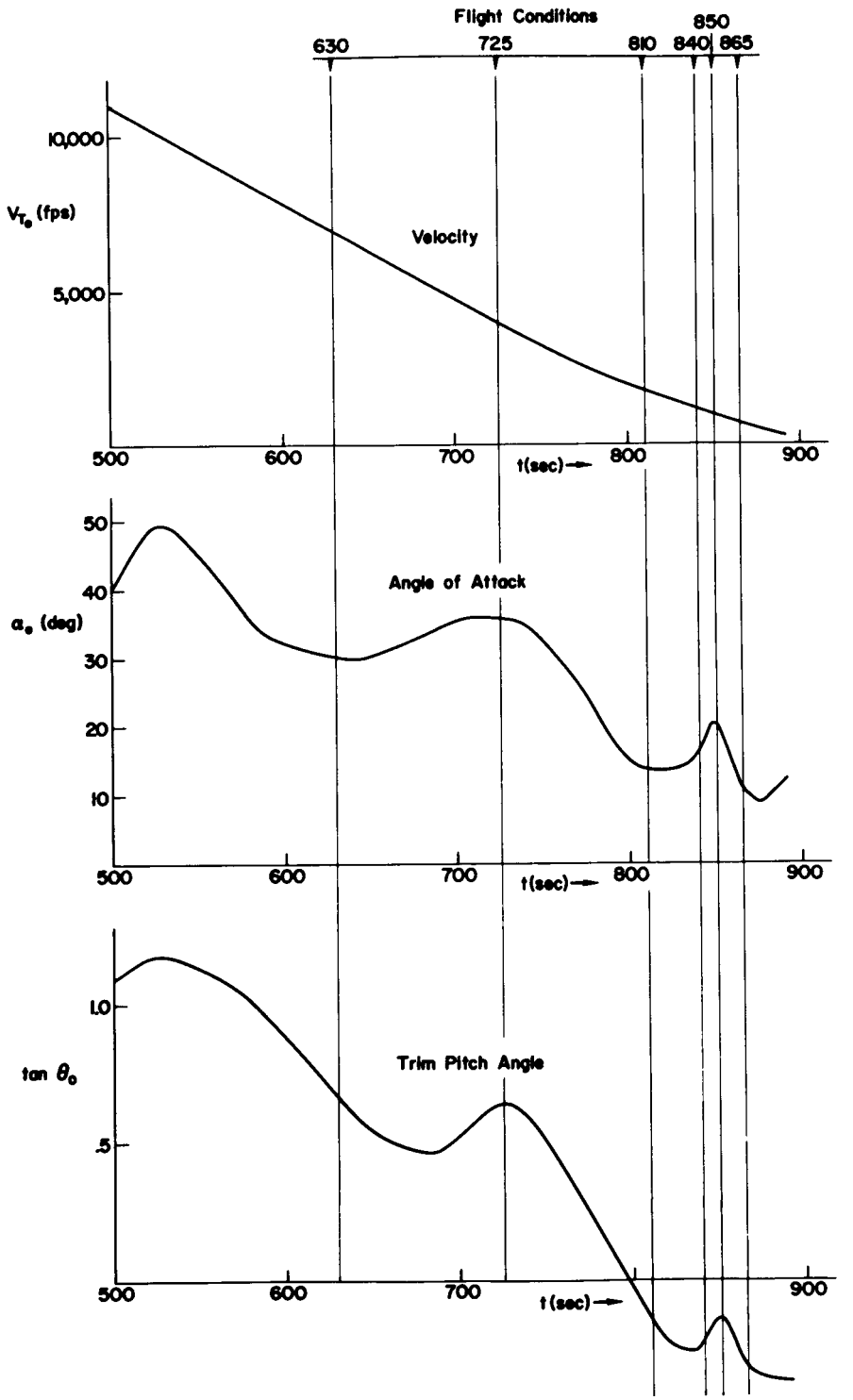

Figure C-2. Trajectory Characteristics

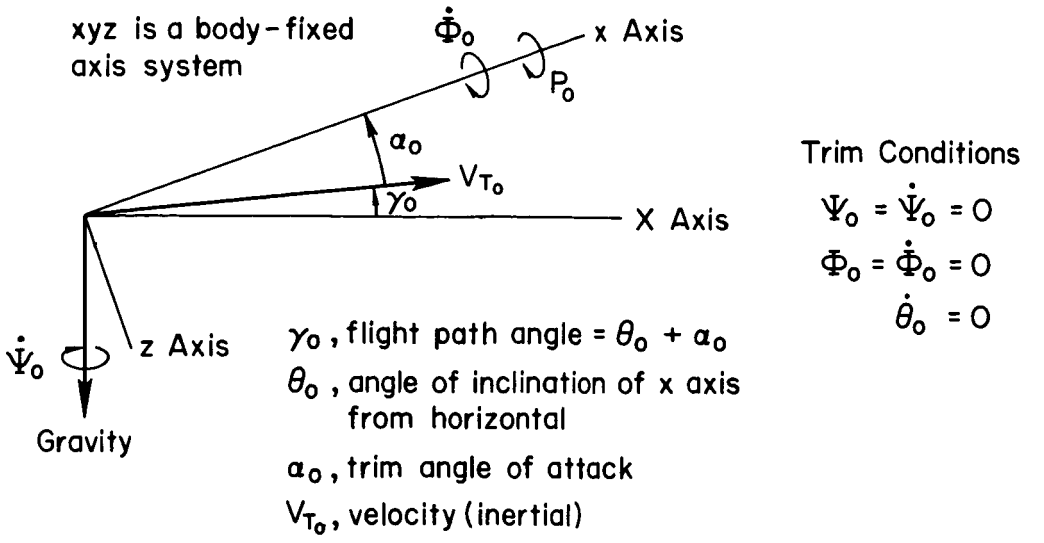

The segment of flight time selected encompasses the crucial conditions from the handling qualities viewpoint. In addition, the ranges through which the stability derivatives vary is extreme. The time varying stability derivatives are shown in Fig. C-3, C-4 and C-5. Stability derivatives not shown (L'_p, L'_r, N'_p, N'_r and others) are negligible for this vehicle and flight regime and are assumed zero. The time functions shown are the actual simulated functions. They were generated using diode function generators and some of the digital logic ("AND" gates) available in the 680 computer system.

The three vehicle equations of motion are shown in Fig. C-6, C-7 and C-8. The time varying stability derivative are generated by variable diode function generators (VDFG). Resolvers are used to produce the sine and cosine of angle of attack in the side force equation. Quarter square electronic multipliers are employed as shown.

The sensor equations are represented in Fig. C-9. φ is the bank angle of the vehicle and a_y is the lateral acceleration of a point on the vehicle l_x feet forward of the center of gravity. This distance is set into the accelerometer equation with a potentiometer and may be

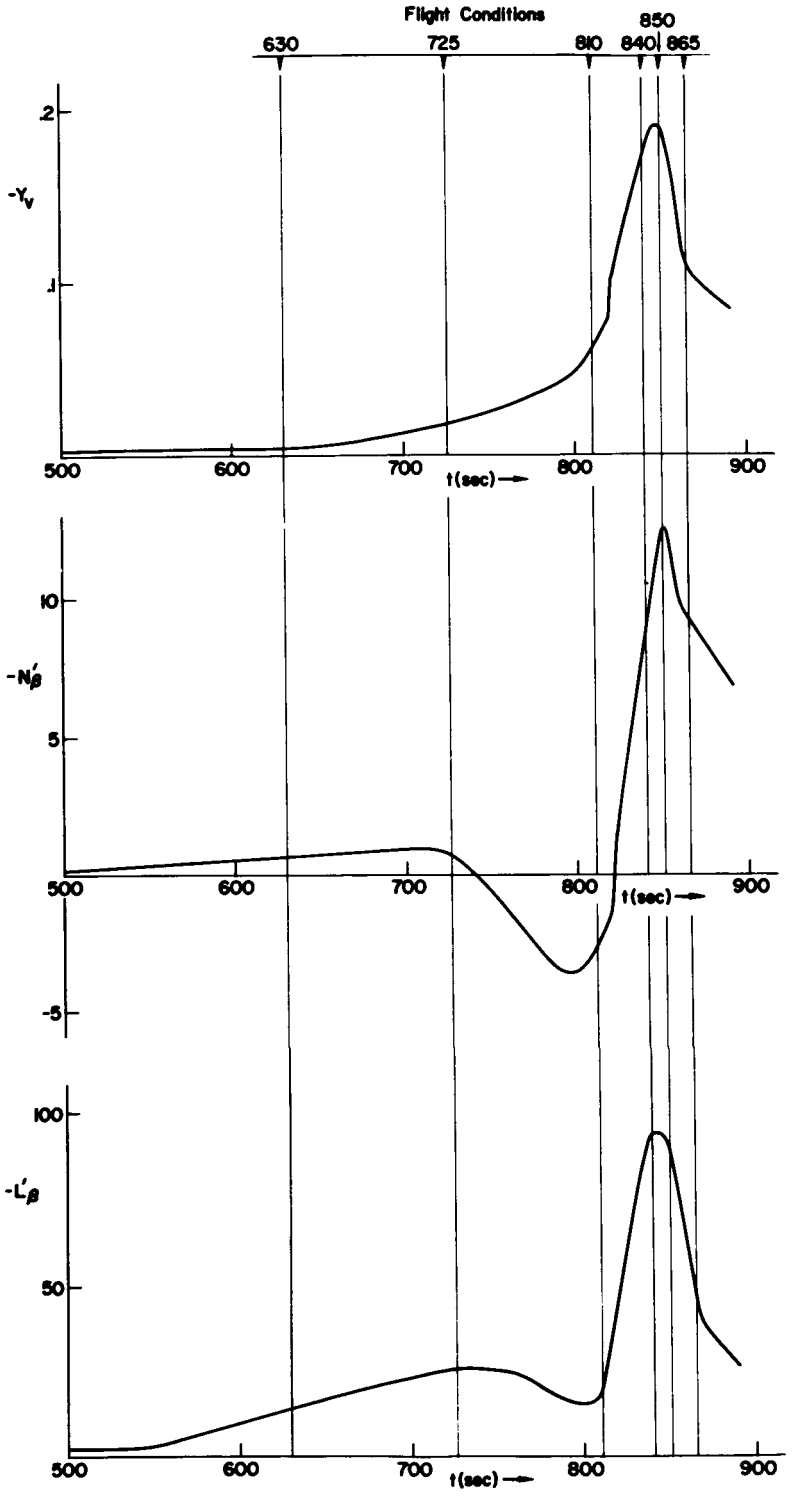

Figure C-3. Side-Slip Derivatives

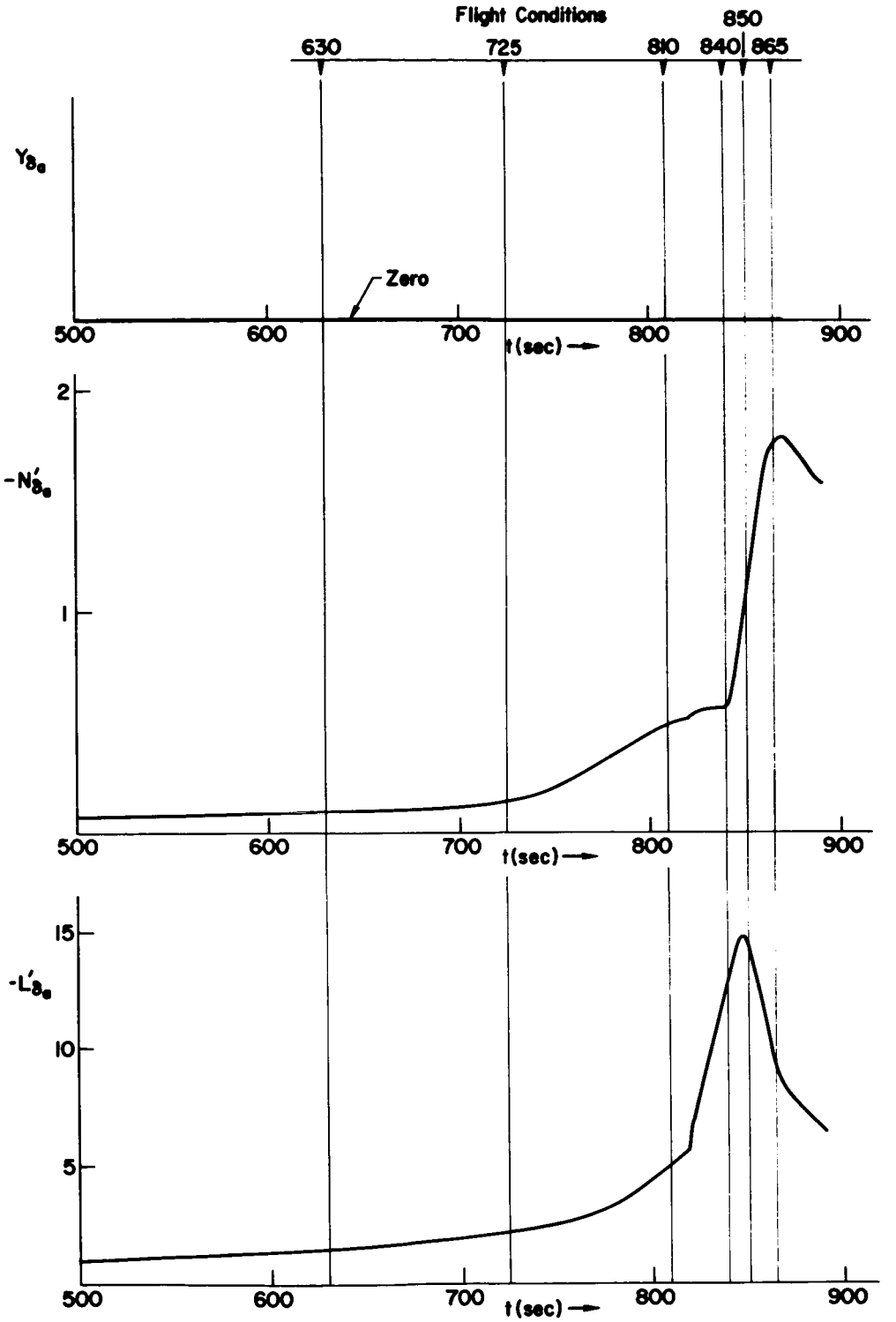

Figure C-4. Aileron Derivatives

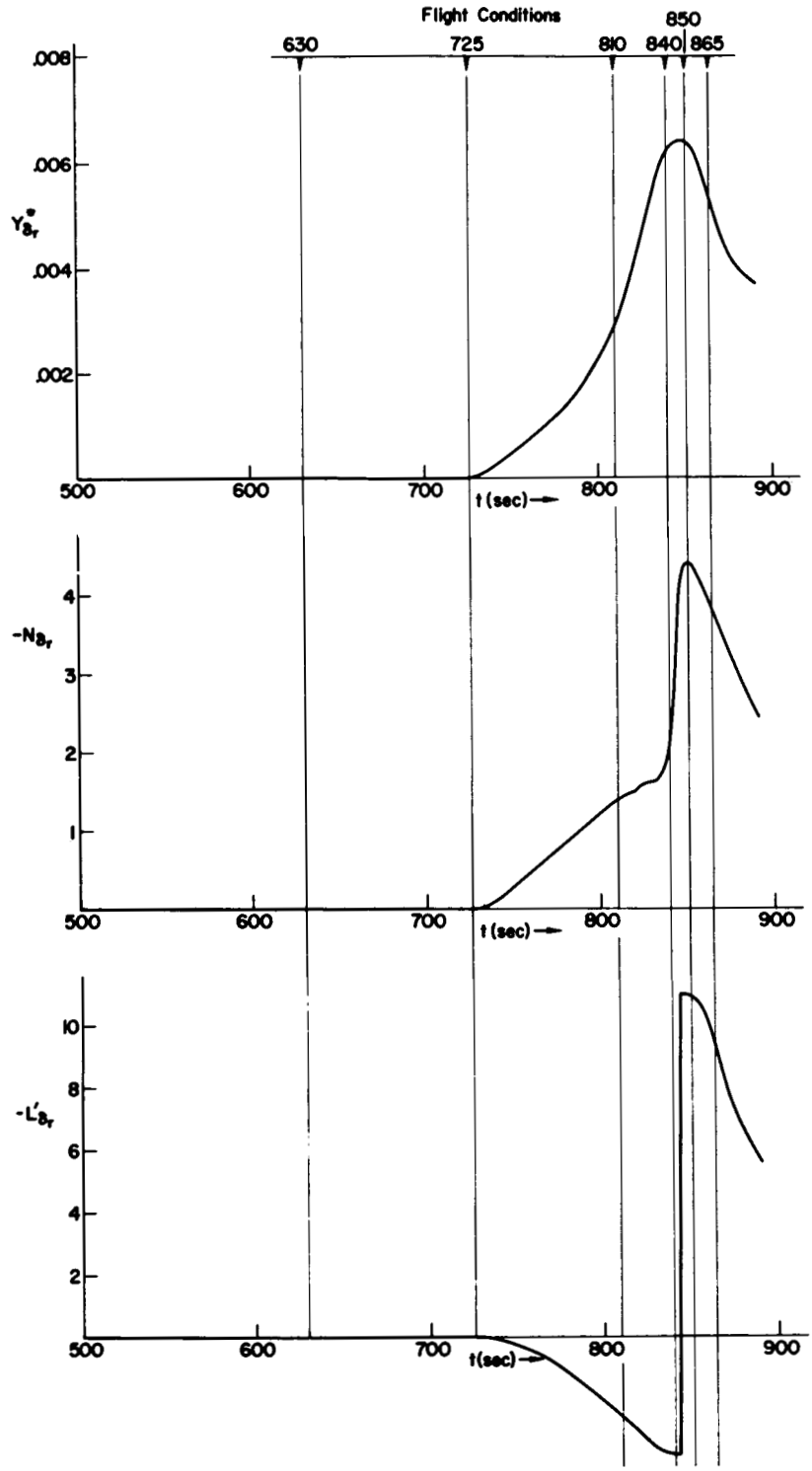

Figure C-5. Rudder Derivatives

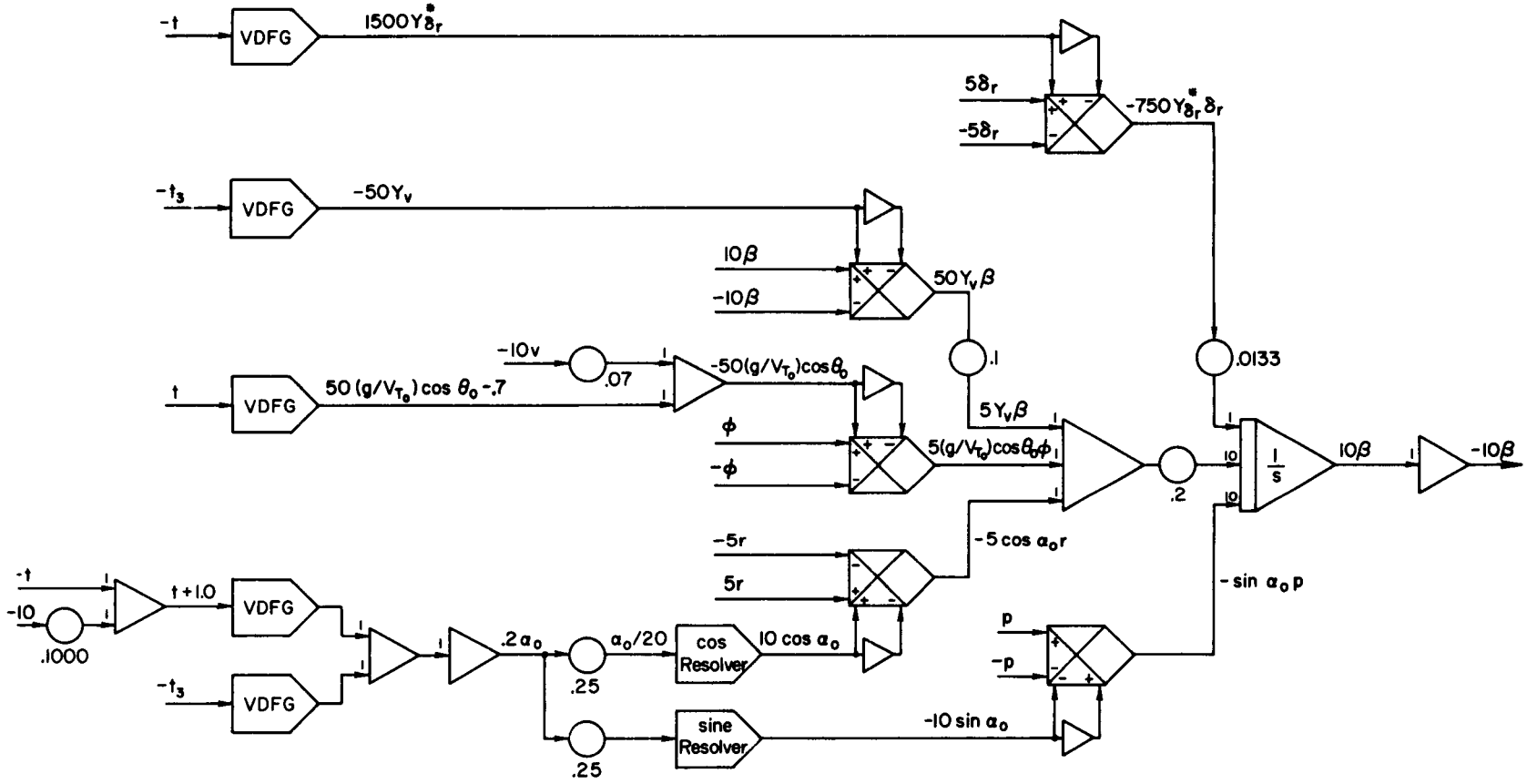

Figure C-6. Side Force Equation

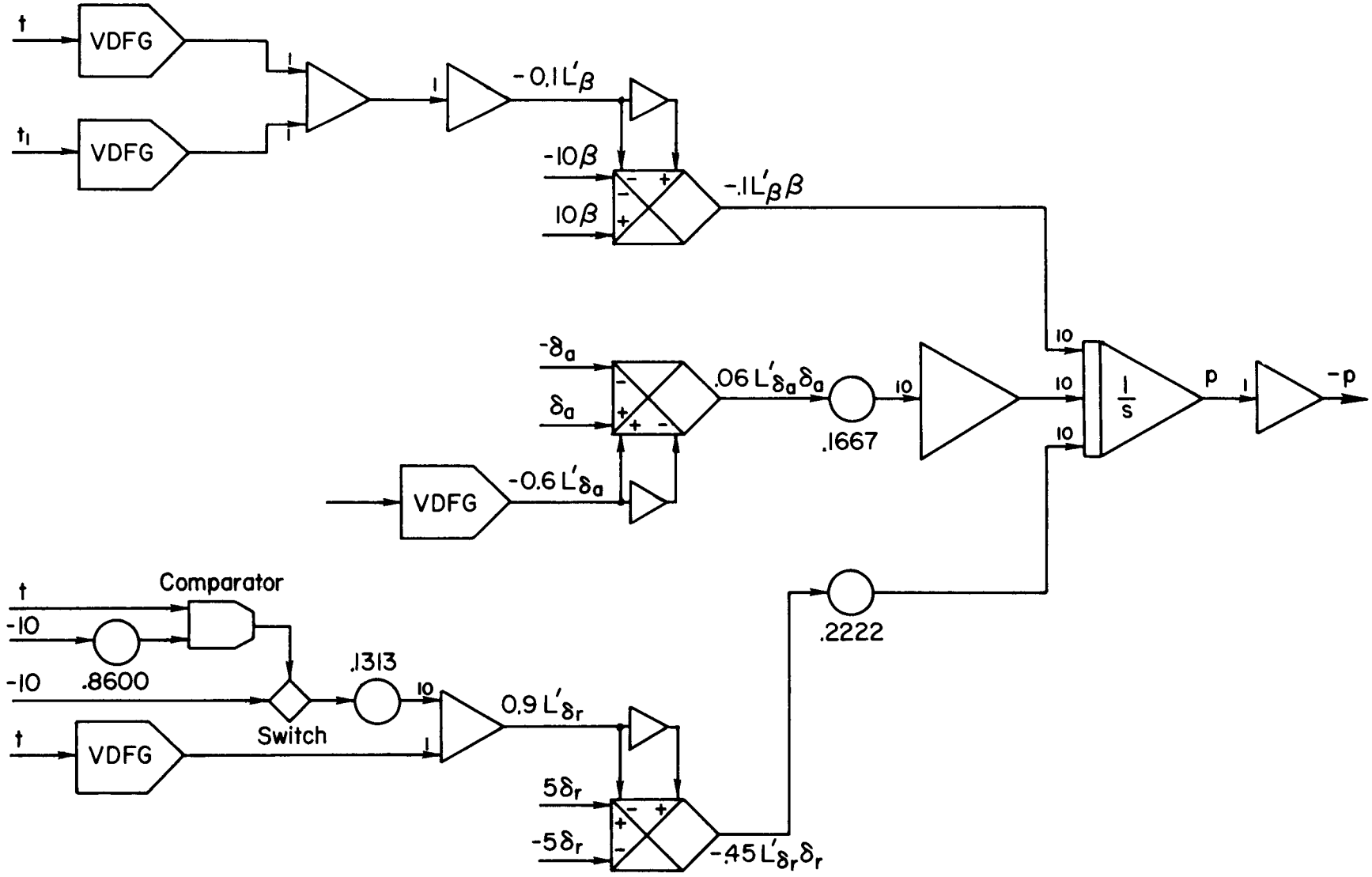

Figure C-7. Roll Moment Equation

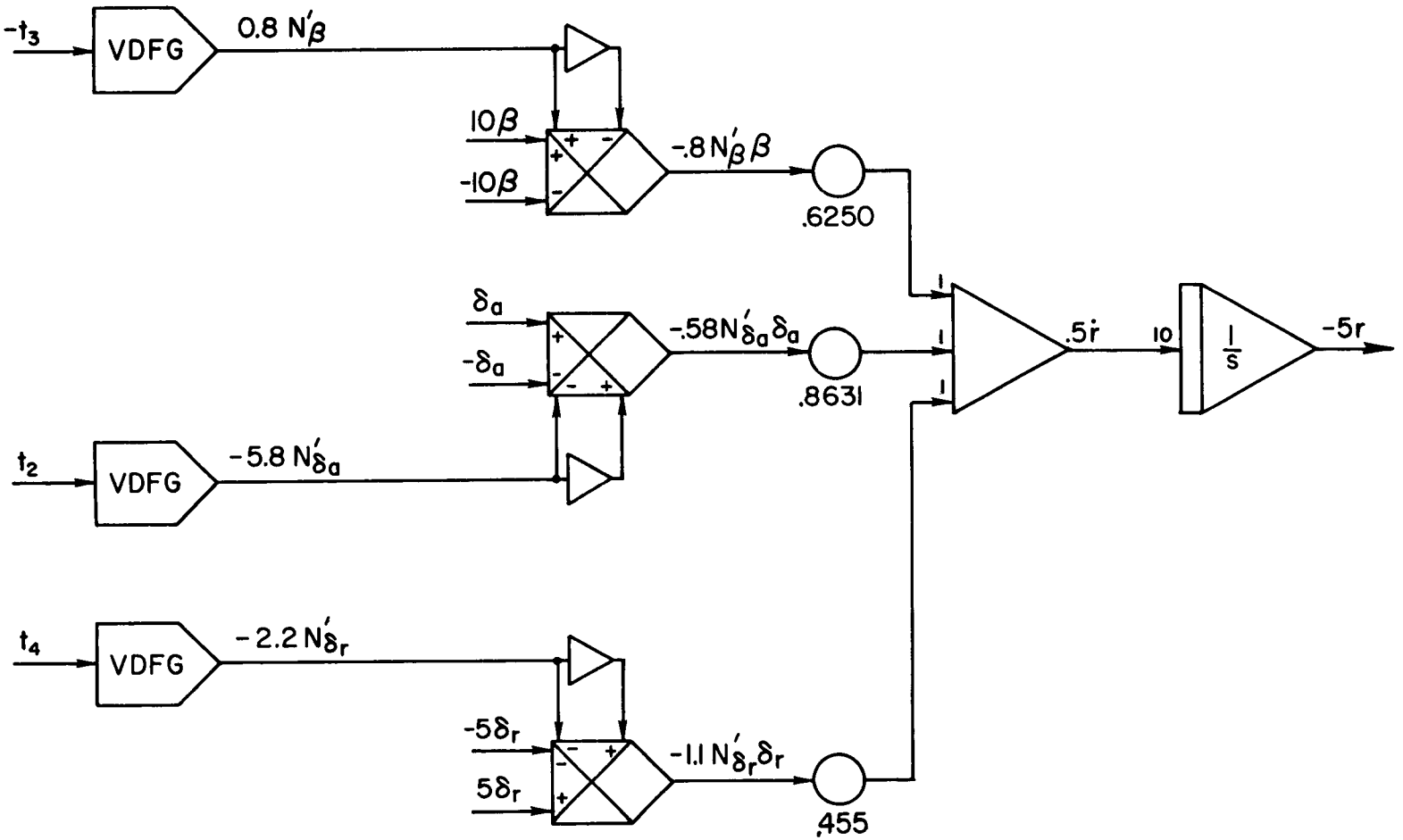

Figure C-8. Yaw Moment Equation

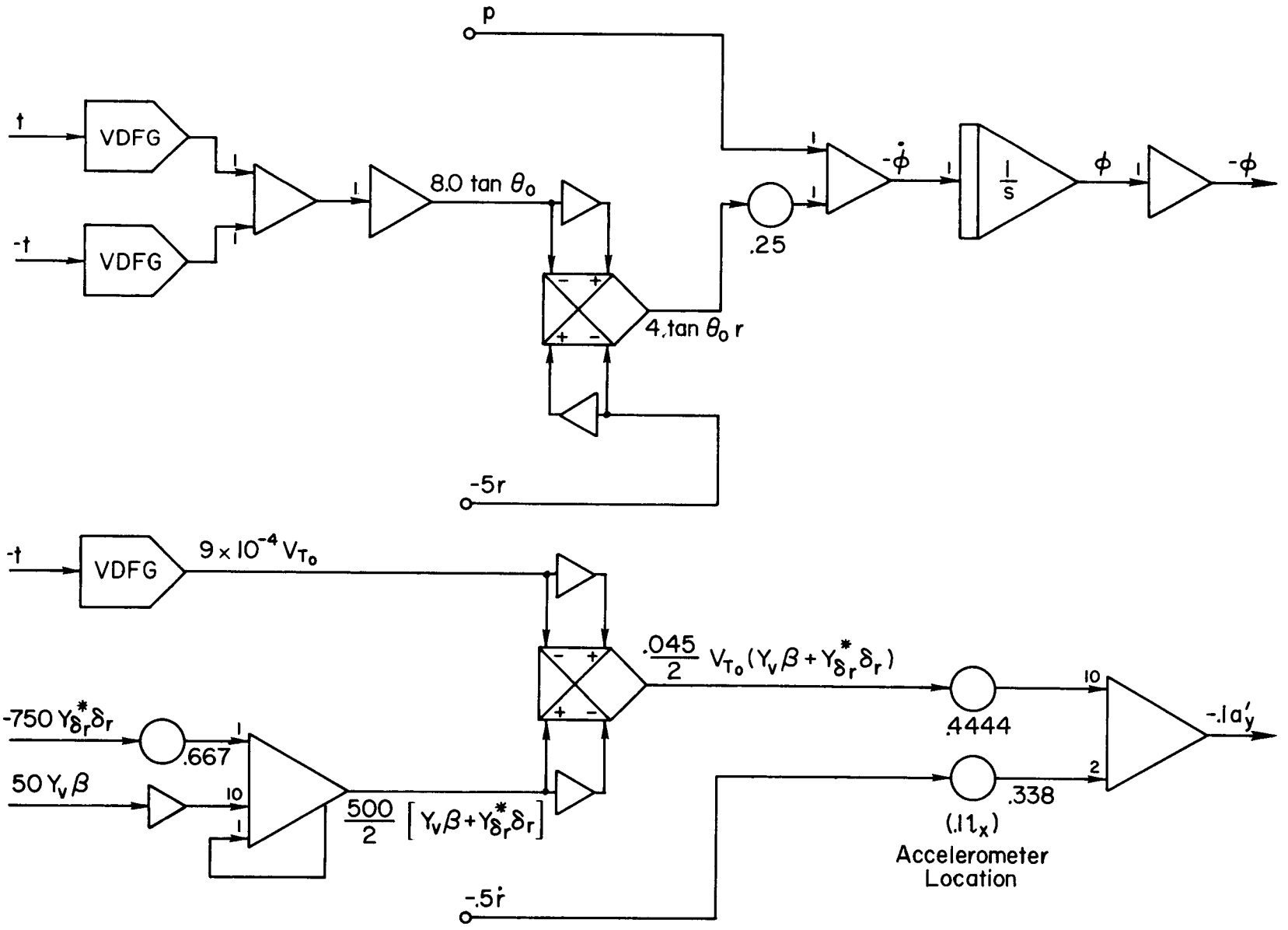

Figure C-9. Sensor Equations

varied over a wide range. For the experiments reported in Section III of this report l_x was 3.38 ft, the "optimum" value determined by the fixed flight time surveys.

Figure C-10 shows the lateral acceleration feedback loop of the stability augmentation system. a_y'' is equalized by a lead-lag circuit and feeds back to the acceleration command point. The command error, $a_{c_c} - a_c$, then goes through the gain K_y, and is the rudder servo command. Both the rudder and the aileron servos are represented by first order lags with break frequencies of 25 rad/sec.

The gain K_y is established by the adaptive loop. The command error $a_{c_c} - a_c$ is processed by a filter and a model of the servo (exact) to provide one component of the error signal e_r. The other component of e_r is the model output $\delta^*_{r_m}$. A multiplier weights the error to provide the rate of change of K_y. An integrator with initial condition K_{y_o} generates K_y for the augmenter loop.

Figure C-11 shows the roll rate feedback loop of the stability augmentation system. It is different from the lateral acceleration loop in only two ways. First, there is no equalization of the sensor output, the feedback signal. Secondly, the alternative scheme used to simulate the digital gain adjustment logic is shown. Section IV covers the analytical and experimental results obtained with this scheme.

Figure C-12 gives the diagram for the model of the inverse vehicle. The inputs are roll rate, $\dot{\phi}$, and filtered lateral acceleration, τ_{a_1}. τ is the filter time constant, and happens to appear as a scale factor on the signal a_1. Roll rate is processed by a filter with the same time constant, τ. The filter serves the dual purpose of pseudo-differentiation of roll rate and suppression of high frequency noise originating at the sensors. The outputs of the model are the desired rudder deflection, $\delta^*_{r_m}$, and the desired aileron deflection, $\delta^*_{a_m}$.

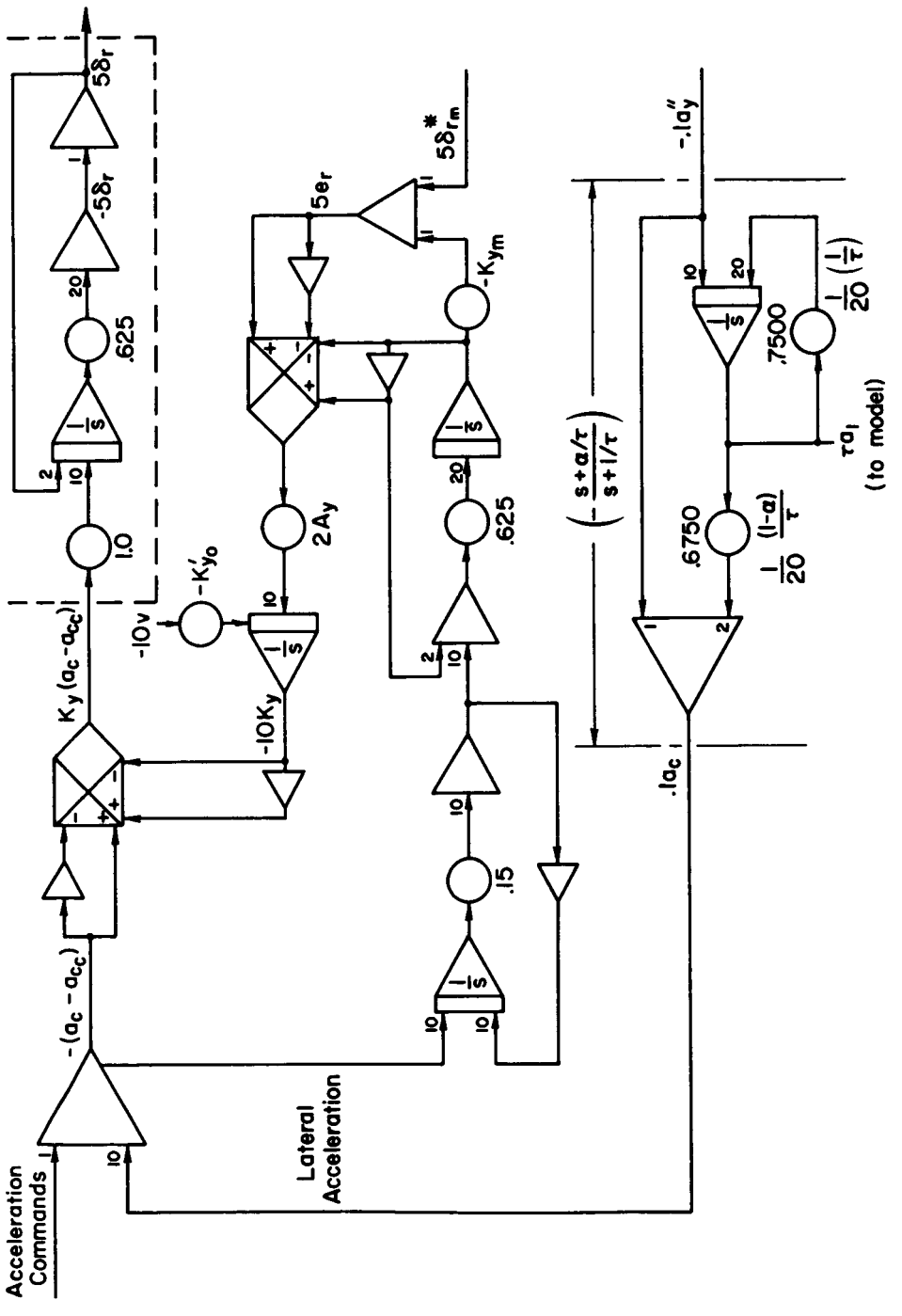

Figure C-10. Lateral Acceleration System

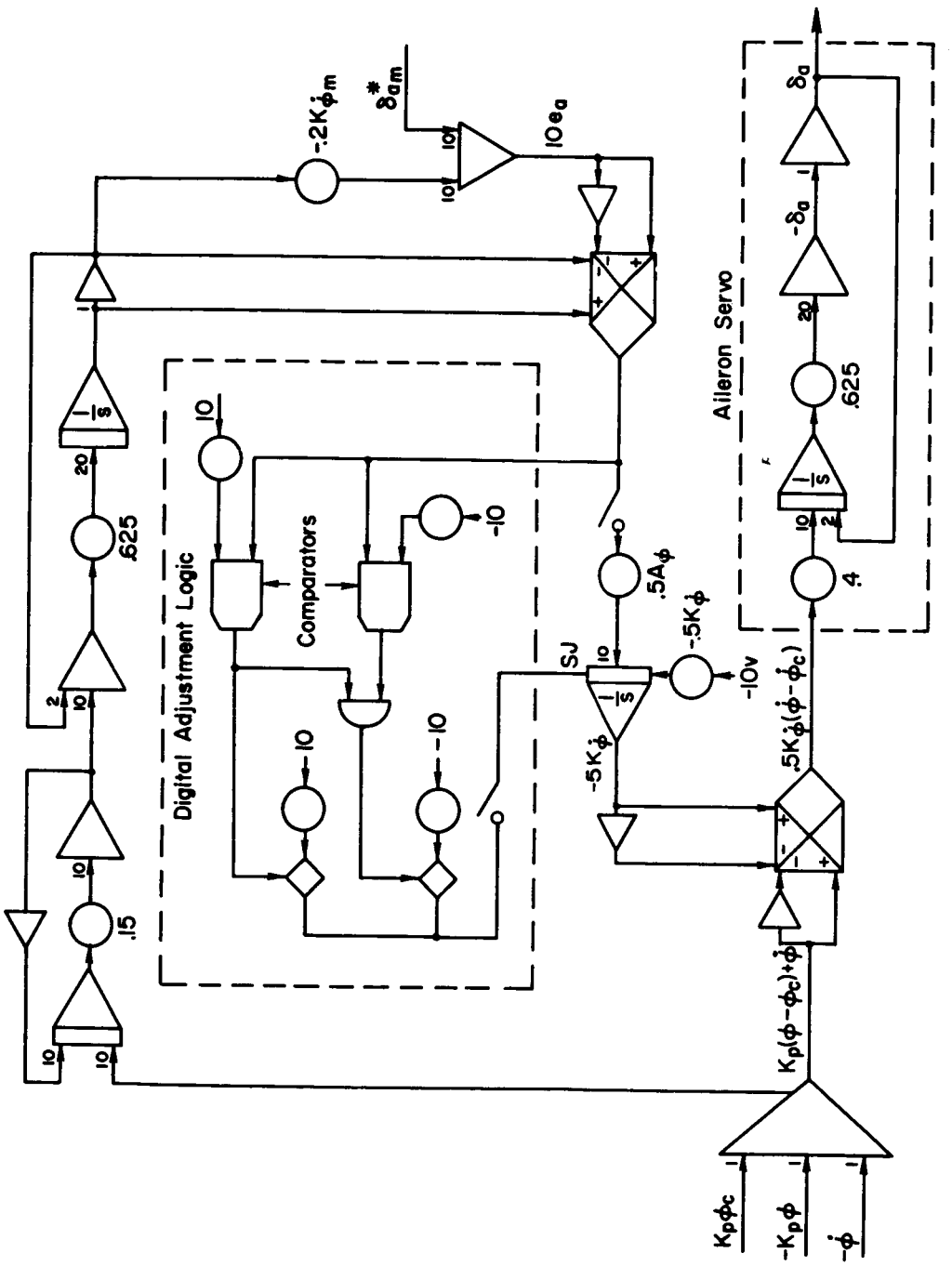

Figure C-11. Roll System

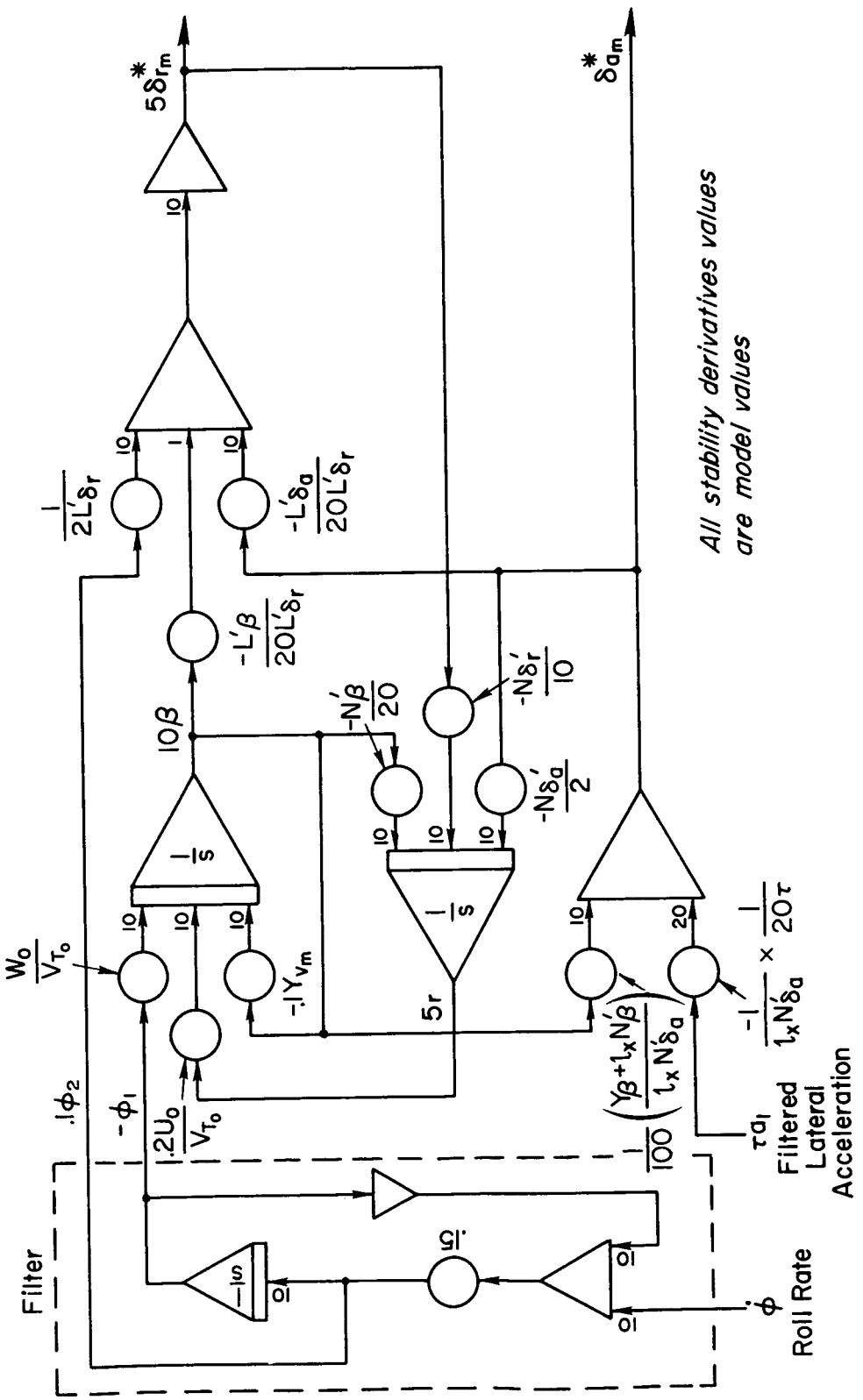

Figure C-12. Vehicle Model (Inverse)

Figure C-13 gives the details of the circuit used to generate the forcing functions for the system. Three oscillators, each of which is built from an integrator and a relay, are the important elements in the system. One oscillator, Osc.No. 1, supplies the square wave signal, and the three together are used to generate triangular waves which are summed and filtered to produce the approximately Gaussian, quasi-random, driving function. This quasi-random function "looks" random but it can be reproduced exactly at will. Naturally the spectrum can be adjusted to meet any requirement; the only limitation being that only three major frequency components are available, one for each oscillator. There are, of course, secondary frequency components (harmonics) present, and these are desirable in that they help mask the periodic nature of the signal.

Figures C-14 and C-15 show auxiliary circuits which are required to operate the simulation. Figure C-14 shows the various piecewise linear time ramps used to drive the diode function generators which provide the time varying stability derivatives. (See Fig. C-2 through C-5.) An integrator supplies a ramp function which is modified in several ways to supply signals with varying slopes. In this way maximum slopes of the VDFG's are artifically increased to suit the rapidly changing stability derivatives.

Figure C-15 shows the digital mode control logic required to secure valuable operational efficiency. Certain simplifications of these logic circuits are no doubt possible since they were partly implemented in the "heat of battle." The system shown, however, does work properly.

This concludes the presentation of the analog computer circuits. Overall, the simulation went very well—no unusual problems arose. In fact some of the anticipated difficulties (multiplier noise, VDFG drift, etc.) did not arise. We feel compelled to note that the EAI 680 computer system's performance exceeded our expectations.

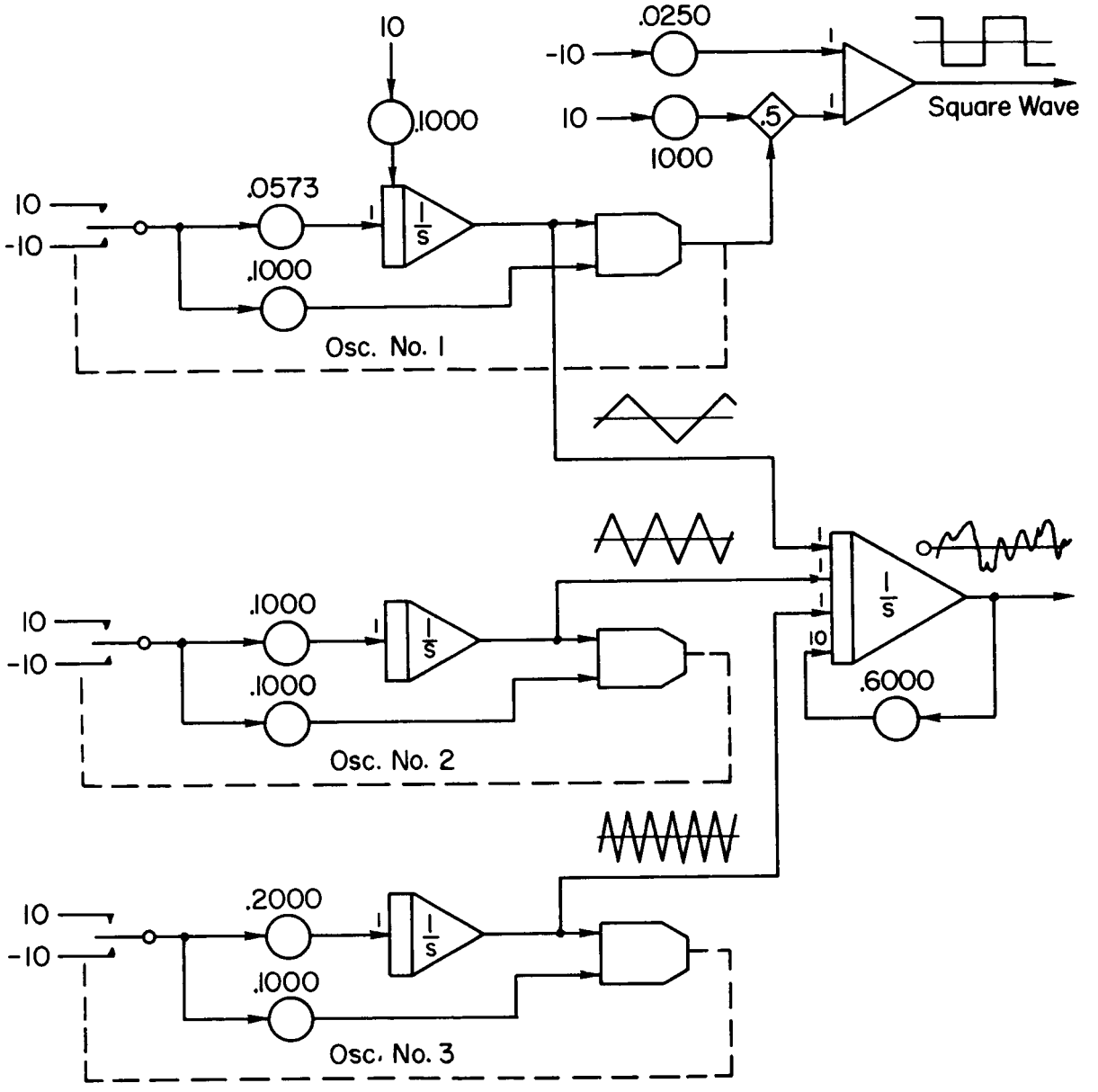

Figure C-13. Forcing Function Circuit

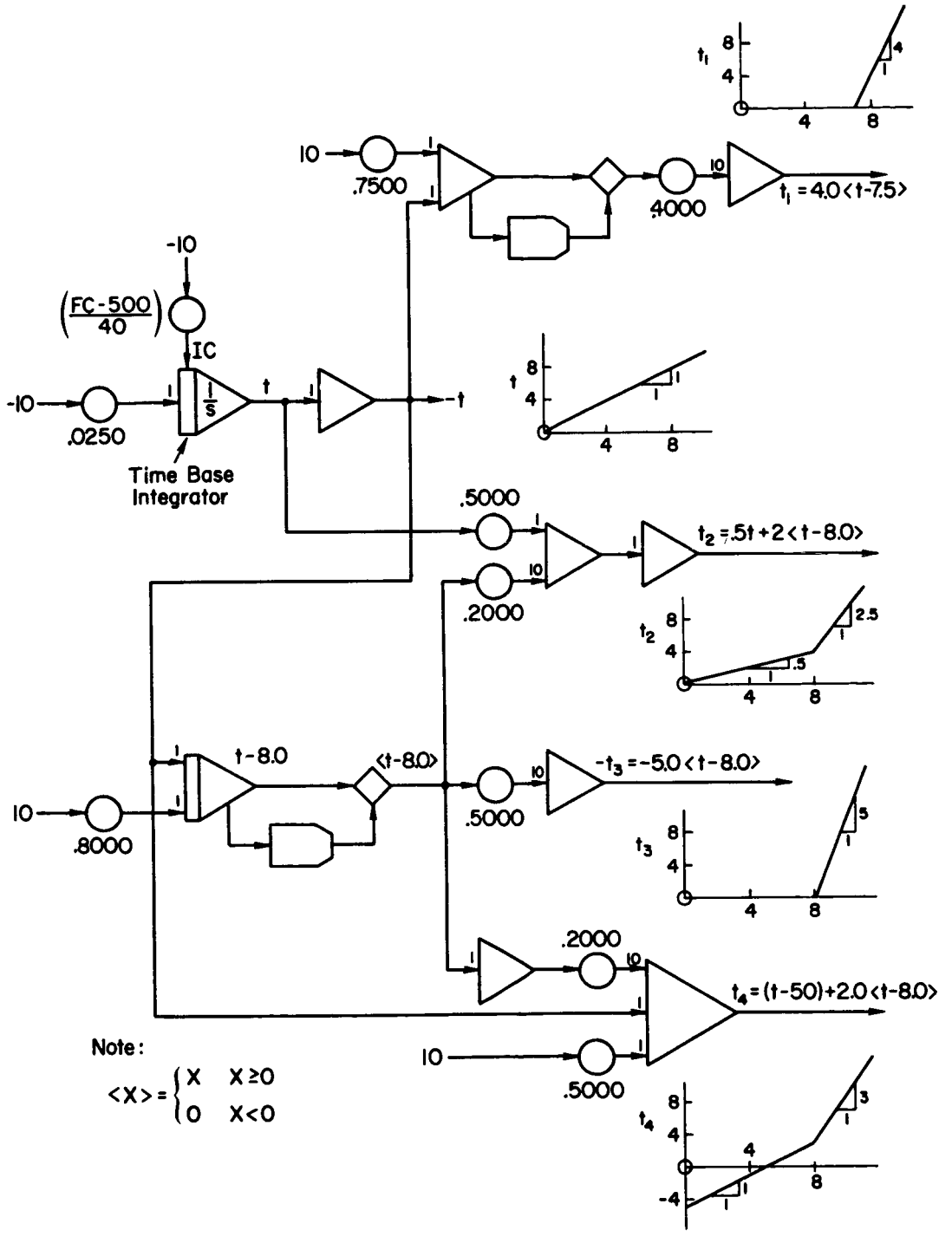

Figure C-14. Time Ramp VDFG Drives

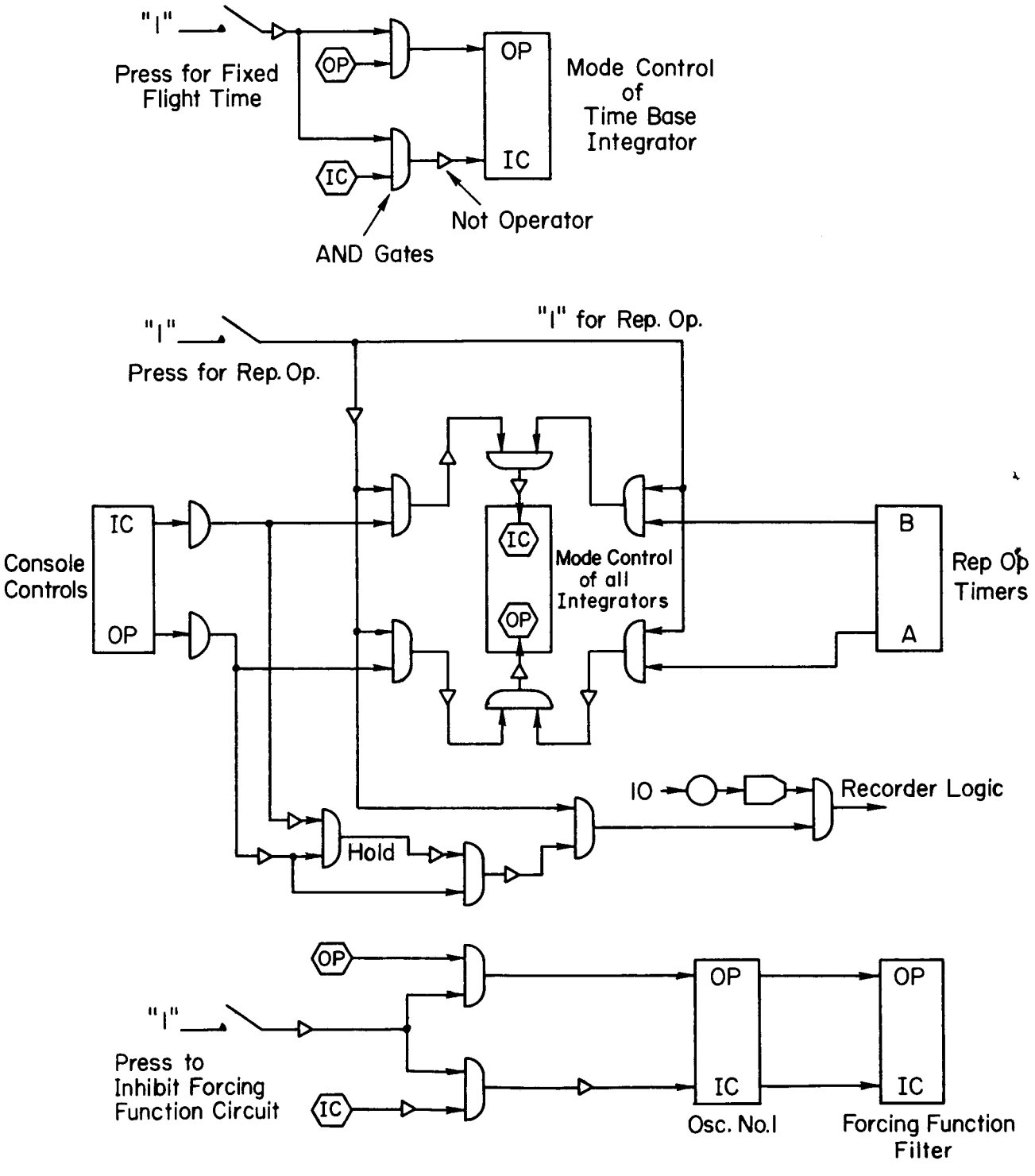

Figure C-15. Mode Control Logic